

FUNCTIONAL CHARACTERIZATION OF ALPHA-2  
ADRENERGIC INHIBITION OF AVP-STIMULATED  
SODIUM AND WATER TRANSPORT IN THE RAT  
CORTICAL COLLECTING DUCT

By

CONNIE ALLYN HÉBERT

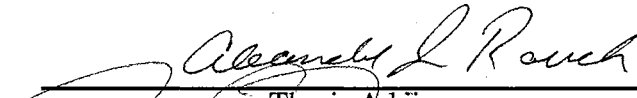
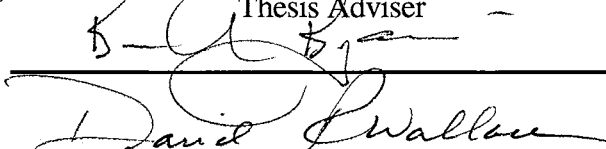
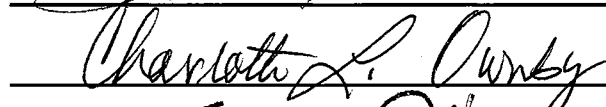
Sam Houston State University  
Huntsville, Texas  
1983

Master of Science  
University of Tulsa  
Tulsa, Oklahoma  
1995

Submitted to the Faculty of the  
Graduate College of the  
Oklahoma State University  
in partial fulfillment of  
the requirements for  
the Degree of  
DOCTOR OF PHILOSOPHY  
May, 2002

FUNCTIONAL CHARACTERIZATION OF ALPHA-2  
ADRENERGIC INHIBITION OF AVP-STIMULATED  
SODIUM AND WATER TRANSPORT IN THE RAT  
CORTICAL COLLECTING DUCT

Thesis Approved:

  
\_\_\_\_\_  
Thesis Adviser  
  
\_\_\_\_\_  
David Swallow  
  
\_\_\_\_\_  
Charlotte L. Ownby  
  
\_\_\_\_\_  
Dean of the Graduate College

## ACKNOWLEDGMENTS

This dissertation was long in coming and certainly could not have been accomplished without the support and patience of my advisor, committee members, and family. I thank Dr. Al Rouch for employing me in the lab and directing my studies. He is not only an excellent teacher, but a true friend. I will miss him if ever I go. I thank my committee members, Dr. Bruce Benjamin, Dr. Dave Wallace, Dr. Subbiah Sangiah, and Dr. Charlotte Ownby for their assistance and helpful advice. I also wish to acknowledge Dr. David John and Dr. Gary Watson, without whom this doctoral program would not exist.

I gratefully acknowledge Dr. Irene Von Cseh for her never-ending optimism and support. I thank her for inspiring me and motivating me. She opened my eyes to what is possible and showed me how to believe in myself.

Finally I thank Tom Hébert, my beloved husband, for enduring countless late dinners and financial debt without a whimper. Thank you for being “Mr. Mom” and taking care of the children. You did a great job.

I dedicate this manuscript to the memory of my mother, Christina Dakos Bradford, who once told me that I should become a Scientist.

## TABLE OF CONTENTS

Chapter	Page
I. INTRODUCTION.....	1
1.1 Background.....	1
1.2 Purpose of the Study.....	4
1.3 Specific Aims.....	5
II. REVIEW OF LITERATURE.....	6
2.1 Mammalian Nephron.....	6
2.2 Cortical Collecting Duct (CCD).....	8
2.3 Transporters and Ion Channels in the CCD.....	9
2.3.1 Water Channels.....	10
2.3.1 Sodium Channels.....	13
2.3.3 Potassium Channels.....	15
2.3.4 Chloride Channels.....	17
2.3.5 Sodium-Potassium ATPase.....	19
2.3.6 Sodium Transporters.....	20
2.4 Hormonal Control of Sodium and Water Transport in the CCD.....	22
2.4.1 Aldosterone.....	22
2.4.2 Vasopressin.....	23
2.4.3 Epinephrine and Norepinephrine.....	25
2.4.4 Dopamine.....	26
2.4.5 Serotonin.....	27
2.4.6 Atrial Natriuretic Peptide.....	28
2.4.7 Urodilatin.....	29
2.4.8 Endothelin.....	30
2.5 Membrane Receptors in the CCD.....	31
2.5.1 Vasopressin Receptors.....	32
2.5.2 Adrenergic Receptors.....	33
2.5.3 Imidazoline Receptors.....	34
2.5.4 Y Receptors.....	39
2.6 Signalling Pathways and Second Messengers in the CCD.....	41
2.6.1 G Proteins.....	42
2.6.2 Adenylyl Cyclase and cAMP.....	45
2.6.3 Protein Kinase A.....	45
2.6.4 Phosphatidylinositol Breakdown.....	46
2.6.5 Protein Kinase C.....	46
2.6.6 Prostaglandins.....	47
2.6.7 Calcium.....	48
III. RESEARCH DESIGN AND METHODS.....	50
3.1 Animals.....	50
3.2 Isolation and Perfusion of Renal Tubules.....	51
3.3 Solutions.....	52

3.4 Osmotic Water Permeability (Flux) Experiments.....	53
3.4.1 Determination of $P_f$ .....	53
3.4.2 Study Design for Flux Experiments.....	54
3.5 Electrophysiology Experiments.....	55
3.5.1 Determination of $V_t$ , $R_t$ , $V_{bl}$ , and $fR_{ap}$ .....	55
3.5.2 Study Design for Electrophysiology Experiments.....	58
3.6 Statistical Analysis.....	59
IV. SECOND MESSENGERS IN THE ALPHA-2 INHIBITION OF AVP-STIMULATED TRANSPORT IN THE RAT CCD.....	62
4.1 Introduction.....	62
4.2 Methods.....	63
4.3 Source of Biochemicals.....	65
4.4 Results.....	65
4.5 Discussion.....	72
V. EFFECT OF OXYMETAZOLINE, ARC-239, AND WB4101 ON SODIUM AND WATER TRANSPORT IN THE RAT CCD.....	79
5.1 Introduction.....	79
5.2 Methods.....	80
5.3 Source of Biochemicals.....	81
5.4 Results.....	81
5.4.1 Effect of Oxymetazoline on AVP-Stimulated $P_f$ .....	81
5.4.2 Effect of Oxymetazoline on $V_t$ , $R_t$ , $V_{bl}$ , and $fR_{ap}$ .....	82
5.4.3 Effect of ARC-230 on AVP-Stimulated $P_f$ .....	87
5.4.4 Effect of WB4101 on AVP-Stimulated $P_f$ .....	88
5.5 Discussion.....	88
VI. EFFECT OF IDAZOXAN AND AGMATINE ON WATER TRANSPORT IN THE RAT CCD.....	94
6.1 Introduction.....	94
6.2 Methods.....	96
6.3 Source of Biochemicals.....	97
6.4 Results.....	98
6.5 Discussion.....	100
VII. EFFECT OF PEPTIDE YY ON AVP-STIMULATED SODIUM AND WATER TRANSPORT IN THE RAT CCD.....	103
7.1 Introduction.....	103
7.2 Methods.....	104
7.3 Source of Biochemicals.....	104
7.4 Results.....	105
7.4.1 Effect of $PYY_{3-36}$ on AVP-Stimulated $P_f$ .....	105
7.4.2 Effect of $PYY_{3-36}$ on $V_t$ , $R_t$ , $V_{bl}$ , and $fR_{ap}$ .....	106
7.5 Discussion.....	108
VIII. SUMMARY.....	112
REFERENCES.....	116

APPENDICES.....	141
Appendix A - $\alpha$ -Adrenergic and Imidazoline Receptor Agonists and Antagonists.....	141
Appendix B - Experimental Drugs.....	142
Appendix C - Data Tables and Statistics .....	144
Appendix D - Stripchart Recordings from Electrophysiology Studies .....	183

## LIST OF TABLES

<b>Table</b>	<b>Page</b>
I. Hormonal Effects on Sodium and Water Reabsorption in the CCD.....	49
II. Composition of Solutions .....	52
III. Protocols to Investigate Second Messengers .....	63
IV. Electrophysiology Data for Oxymetazoline .....	83
V. Protocols to Investigate Idazoxan and Agmatine .....	97

## LIST OF DIAGRAMS

<b>Diagram</b>	<b>Page</b>
1. Receptors and Second Messengers.....	3
2. The Mammalian Nephron.....	7
3. V <sub>2</sub> Receptor in the Principal Cell.....	9
4. Membrane Topology of AQP-2.....	13
5. Membrane Topology of ENaC.....	15
6. Imidazoline Ring Structure.....	35
7. Biosynthesis of Agmatine.....	38
8. Topology of the G Protein-Coupled Receptor.....	43
9. Alpha-2 Receptor in the Principal Cell.....	44
10. Isolated Perfused Tubule Technique.....	51
11. Electrophysiological Measurements in the Principal Cell.....	55
12. Electrophysiology Experimental Setup.....	56

## LIST OF FIGURES

Figure	Page
1. AVP-stimulated $P_f$ under standard and low calcium conditions	
(A) AVP time-control study.....	67
(B) Low calcium bath does not affect AVP-stimulated $P_f$ .....	67
(C) Standard bath vs low calcium bath.....	67
2. Dexmedetomidine-induced inhibition of $P_f$ under standard and low calcium conditions	
(A) Dexmedetomidine inhibits AVP-stimulated $P_f$ .....	68
(B) Low calcium bath does not affect dexmedetomidine-induced inhibition of AVP-stimulated $P_f$ .....	68
(C) Standard bath vs low calcium bath.....	68
(D) Low calcium bath with Quin-2 AM.....	68
3. Effects of staurosporine and indomethacin	
(A) Staurosporine and indomethacin reverse dexmedetomidine-induced inhibition of AVP-stimulated $P_f$ .....	69
(B) Indomethacin does not affect $P_f$ .....	69
(C) Low dose staurosporine does not affect $P_f$ .....	69
(D) High dose staurosporine reverses dexmedetomidine-induced inhibition of AVP-stimulated $P_f$ .....	69
4. Electrophysiological effects of low calcium	
(A) Low calcium bath does not affect $V_t$ .....	70
(B) Low calcium bath does not affect $R_t$ .....	70
5. Electrophysiological effects of staurosporine and indomethacin	
(A) Staurosporine and indomethacin do not affect $V_t$ .....	71
(B) Staurosporine and indomethacin do not affect $R_t$ .....	71
6. Effect of administration order of PG and PKC inhibitors on dexmedetomidine-induced inhibition of $P_f$ .....	72
7. Effects of oxymetazoline on AVP- and cAMP-stimulated $P_f$	
(A) Oxymetazoline inhibits AVP-stimulated $P_f$ .....	84
(B) Oxymetazoline does not affect basal $P_f$ .....	84
(C) Oxymetazoline does not affect cAMP-stimulated $P_f$ .....	84
8. Electrophysiological effects of oxymetazoline	
(A) Oxymetazoline depolarizes $V_i$ in control rats.....	85
(B) Oxymetazoline increases $R_t$ in control rats.....	85
(C) Oxymetazoline depolarizes $V_i$ in low salt diet rats.....	85
(D) Oxymetazoline increases $R_t$ in low salt diet rats.....	85
(E) Oxymetazoline depolarizes $V_{bl}$ in low salt diet rats.....	86

(F) Oxymetazoline increases $fR_{tp}$ in low salt diet rats .....	86
(G) Oxymetazoline depolarizes $V_t$ in DOC-treated rats .....	86
(H) Oxymetazoline increases $R_t$ in DOC-treated rats.....	86
9. Effect of ARC-239 on dexmedetomidine-induced inhibition of $P_f$	
(A) ARC-239 reverses dexmedetomidine-induced inhibition of $P_f$ .....	87
(B) Effects of ARC-239 are reversible.....	87
10. Effect of WB4101 on dexmedetomidine-induced inhibition of $P_f$	
(A) WB4101 reverses dexmedetomidine-induced inhibition of $P_f$ .....	88
(B) Effects of WB4101 are reversible.....	88
11. Effect of idazoxan and agmatine on dexmedetomidine-induced inhibition of $P_f$	
(A) Idazoxan reverses dexmedetomidine-induced inhibition of $P_f$ .....	99
(B) Agmatine inhibits AVP-stimulated $P_f$ .....	99
(C) Yohimbine does not reverse agmatine-induced inhibition of $P_f$ .....	99
(D) Agmatine inhibits cAMP-stimulated $P_f$ and is not reversed with idazoxan.....	99
12. Effect of PYY <sub>3-36</sub> on AVP-stimulated $P_f$	
(A) 10 nM PYY <sub>3-36</sub> does not affect AVP-stimulated $P_f$ .....	106
(B) 100 nM PYY <sub>3-36</sub> inhibits AVP-stimulated $P_f$ .....	106
(C) Effects of PYY <sub>3-36</sub> are enhanced with yohimbine.....	106
13. Electrophysiological effects of PYY <sub>3-36</sub>	
(A) PYY <sub>3-36</sub> depolarizes $V_t$ .....	107
(B) PYY <sub>3-36</sub> increases $R_t$ .....	107

# Chapter I

## INTRODUCTION

### 1.1 Background

Two of the major functions of the kidney are to maintain the osmolality and volume of body fluids despite wide variations in daily intake of salt and water. The control of body fluid osmolality is important for normal cell function in all body tissues and control of body fluid volume is necessary for normal function of the cardiovascular system. The kidney accomplishes these tasks by regulating the excretion of water and salt. Although water and salt reabsorption occurs along the entire nephron, the final adjustments in the composition and volume of the urine are made in the collecting duct. The cortical collecting duct (CCD) is of special interest since it is primarily controlled by the hormones aldosterone and arginine vasopressin (AVP).

Aldosterone is a steroid hormone that stimulates salt reabsorption in the collecting duct by a mechanism involving increased protein synthesis and activation of sodium channels [1, 2]. AVP is a protein hormone that stimulates salt and water reabsorption in the collecting duct by activation of multiple signalling pathways and second messengers that lead to insertion of sodium channels and water channels into the plasma membrane [3, 4]. While the aldosterone effect may take an hour to occur, the AVP effect occurs within minutes, making AVP critical in maintaining constant plasma volume and osmolality [2, 5]. Inhibitors of AVP-stimulated salt and water reabsorption in the rat

CCD include alpha-2 ( $\alpha_2$ ) adrenergic agonists [6-8], atrial natriuretic peptide [9], prostaglandin E<sub>2</sub> [10], bradykinin [11], dopamine [12], peptide YY [13], and the neurotransmitter neuropeptide Y [14]. Imidazoline compounds also cause diuresis and natriuresis in the rat, but by a AVP-independent mechanism [15, 16].

The signalling pathways and second messengers indicated in AVP-stimulated transport and its inhibition are complex and do not function independently of each other. Some of the interactions between receptors and second messengers in the principal cell of the collecting duct are shown in diagram 1. The classic explanation of AVP-mediated salt and water reabsorption in the collecting duct consists of V<sub>2</sub> receptor stimulation by AVP which activates adenylyl cyclase (AC) leading to an increase in adenosine 3',5'-cyclic monophosphate (cAMP) within the cell [17, 18]. This action is inhibited by stimulation of  $\alpha_2$  receptors which inhibit AC and decrease cAMP accumulation within the cell [19, 20]. Some  $\alpha_2$  agonists are also imidazolines and can bind to an additional site separate from  $\alpha_2$  receptors, called imidazoline (I) receptors [21, 22]. Binding of imidazoline agents to I receptors in the rat induces diuresis and natriuresis that has been linked to the cAMP pathway [16, 23] and to the production of diacylglycerol [24]. More recently, Y receptors have been implicated in salt and water resorption in the kidney. Neuropeptide Y (NPY) and peptide YY (PYY), members of the family of pancreatic polypeptides, both bind to Y receptors which have also been found in the kidney [25]. NPY has been shown to inhibit AVP-stimulated water permeability in the CCD [26], while functional studies of PYY in the kidney have not yet been conducted.

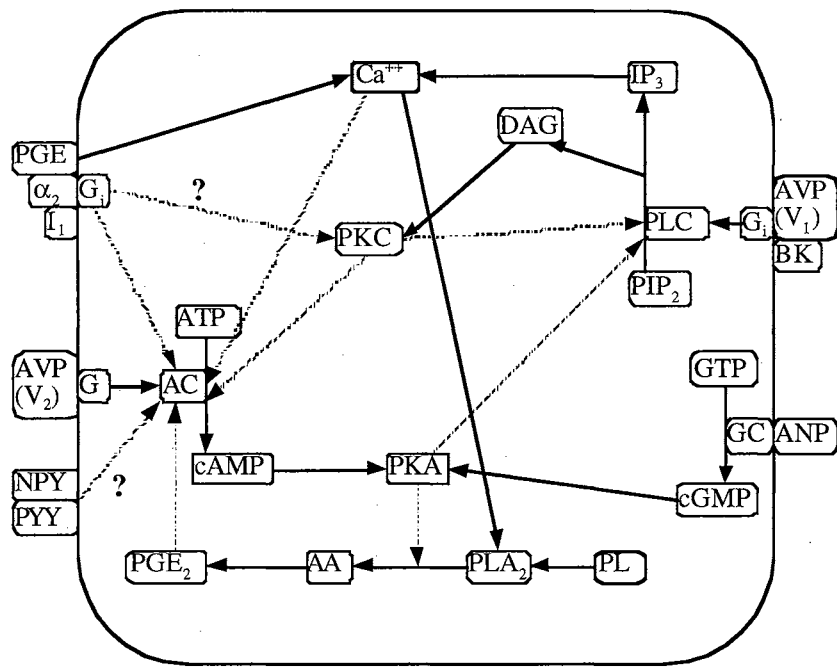


**Diagram 1.** Schematic representation of some of the receptors and signalling systems and their interactions in a cell. Solid lines represent stimulation or activation and broken lines represent inhibition. AVP, arginine vasopressin; ANP, atrial natriuretic peptide;  $\alpha_2$ , alpha-2 adrenergic receptor; PGE<sub>2</sub>, prostaglandin E<sub>2</sub>; NPY, neuropeptide Y; PYY, peptide YY; I, imidazoline receptor; D, dopamine; Ca<sup>++</sup>, calcium; PLC, phospholipase C; PKA and PKC, protein kinase A and C, respectively; PL, phospholipid; PLA<sub>2</sub>, phospholipase A<sub>2</sub>; AA, arachidonic acid; G<sub>i</sub>, inhibitory G protein; G<sub>s</sub>, stimulatory G protein; GC, guanylate cyclase; IP<sub>3</sub>, inositol 1,4,5-trisphosphate; PIP<sub>2</sub>, phosphatidyl inositol 4,5-bisphosphate; DAG, diacylglycerol; BK, bradykinin.

While binding of an  $\alpha_2$ , I, or Y agonist to the receptor is known to cause a decrease in salt and water reabsorption in the kidney, the exact mechanisms of these actions are still unclear. The V<sub>2</sub> receptor is coupled to a stimulatory G protein (G<sub>s</sub>) that stimulates salt and water permeability by AC activation, cAMP generation, and PKA activation [27]. The  $\alpha_2$  receptors are coupled to pertussis toxin (PTX)-sensitive inhibitory G proteins (G<sub>i</sub>) that inhibit AC activation and cAMP generation within the cell [19, 26, 28] (diagram

1). Additional evidence suggests, however, that other mechanisms independent of AC and cAMP inhibition are involved in the  $\alpha_2$  response. First,  $\alpha_2$  agonists inhibit AVP-stimulated salt and water permeability even in the presence of constant intracellular levels of cAMP [29]. Second, prostaglandin and PKC inhibitors reverse  $\alpha_2$ -mediated inhibition in the inner medullary collecting duct (IMCD), and this occurs even in the presence of constant cAMP [30].

Binding of I receptor agonists, which also bind to  $\alpha_2$  receptors, increases salt and water excretion in the rat independent of AVP [16] and linked to multiple pathways. Two cAMP-mediated pathways have been indicated, one involving a PTX-sensitive G protein [28] and another that is PTX-insensitive [23]. Other effects of I receptor activation include PLC activation and generation of diacylglycerol and arachadonic acid [24] and stimulation of endogenous prostaglandin production [16]. Finally, Y receptor stimulation induces diuresis and natriuresis [14, 25, 26, 31, 32] and can cause inositol phosphate-dependent and independent calcium mobilization in some cell types that is attenuated by prostaglandin inhibitors [33-35].

## **1.2 Purpose of the Study**

The goal of this project is to identify the functional receptor-mediated mechanisms involved in the inhibition of AVP-stimulated salt and water permeability in the rat CCD. This will be accomplished using the isolated perfused tubule technique in which a single CCD segment is suspended between concentric pipettes in a bathing chamber on an

inverted microscope. Various receptor agonists and antagonists as well as specific signal pathway inhibitors will be added to the bathing solution. This technique allows for determination of the osmotic water permeability coefficient ( $P_f$ ) and characterization of salt transport using electrophysiological recordings of transepithelial voltage ( $V_t$ ), transepithelial resistance ( $R_t$ ), basolateral membrane voltage ( $V_{bl}$ ) and fractional resistance of the apical membrane ( $fR_{ap}$ ).

The specific aims of this project are:

- 1) Determine the involvement of calcium, prostaglandins, and protein kinase C in the signalling pathways used in the mechanism of alpha-2-mediated inhibition of AVP-stimulated transport in the CCD.
- 2) Determine the effect of the alpha-2 adrenergic agents oxymetazoline, ARC-239, and WB4101 on the alpha-2 mediated inhibition of AVP-stimulated transport in the CCD.
- 3) Determine the effect of agmatine on AVP-stimulated transport in the CCD.
- 4) Determine the effect of PYY on AVP-stimulated transport in the CCD.

## **Chapter II**

### **REVIEW OF LITERATURE**

The review of literature begins with a brief discussion on the mammalian nephron, with emphasis on the cortical collecting duct. The collecting duct is the final nephron segment where salt and water reabsorption can occur in the kidney. In addition, the collecting duct is under hormonal control, making it critical in the daily regulation of plasma osmolarity and blood pressure. The transporters and ion channels responsible for this regulation are discussed and include water channels, sodium channels, potassium channels, chloride channels, and sodium transporters. The specifics of hormonal control in the principal cell of the collecting duct is covered as well as some of the receptors known to reside there including vasopressin receptors, adrenergic receptors, imidazoline receptors, and Y receptors. Finally, some of the signalling pathways and second messengers involved in salt and water transport in the collecting duct are discussed, including G proteins, adenylyl cyclase and cAMP, protein kinase A, phosphatidylinositol, protein kinase C, and prostaglandins.

#### **2.1 Mammalian Nephron**

The kidney produces urine through the processes of filtration, reabsorption, and secretion. Plasma is filtered at the glomerulus, water and solutes are reabsorbed, and selected solutes are secreted into the tubular lumen. The functional unit of the kidney is

the nephron. The nephron consists of the glomerular capsule, proximal tubule, loop of Henle, distal tubule, and collecting duct (diagram 2). The collecting duct is subdivided into the cortical, outer medullary, and inner medullary collecting ducts, and each segment possesses distinct cell types and functions [36]. The ascending limb of the loop of Henle, distal convoluted tubule, and collecting duct are specialized with tightly regulated transport properties that allow the kidney to produce urine with a different composition from that of plasma [37].

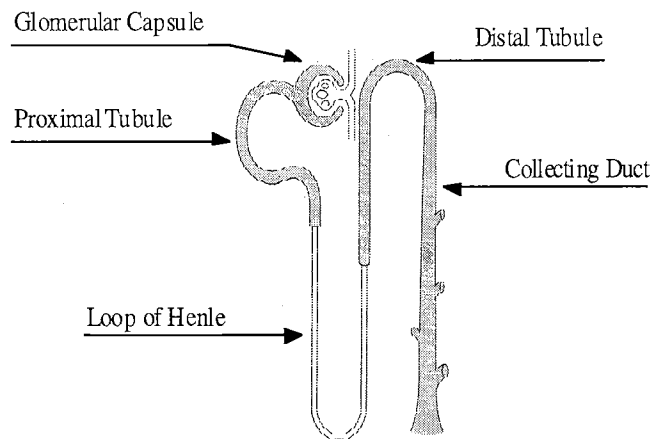


**Diagram 2.** The Mammalian Nephron.

The proximal tubule reabsorbs about 67% of the filtrate produced by the glomerulus, which includes water, sodium, chloride, potassium, and other solutes. In addition, the proximal tubule reabsorbs all of the filtered glucose and amino acids. The loop of Henle reabsorbs about 25% of the filtered sodium, chloride, and potassium from the thick ascending limb and about 15% of the filtered water from the thin descending limb. The distal tubule reabsorbs approximately 5% of the filtered load and the collecting duct

reabsorbs the remaining 2-3%, resulting in net sodium reabsorption of more than 99% of the filtered load. Quantitatively, the amount of filtrate reabsorbed in the collecting duct is small, but since it is the last segment of the nephron to influence sodium and water excretion it is critical in the determination of plasma osmolarity and volume.

## **2.2 Cortical Collecting Duct**

The cortical collecting duct (CCD) consists of two basic cell types. Intercalated cells are responsible for hydrogen and bicarbonate transport important in maintenance of acid-base balance [38]. Principal cells reabsorb sodium and water, and secrete potassium, giving them a major role in the regulation of blood pressure [37]. These responses are hormonally controlled by AVP and the mineralocorticoid aldosterone.

Both hormones stimulate sodium and potassium transport in the CCD and both have been shown to increase the amiloride-sensitive sodium conductance of the luminal membrane of the principal cell [39-42]. The increase in sodium permeability results from translocation of epithelial sodium channels from intracellular vesicles to the apical plasma membrane and/or the activation of cryptic channels already present in the membrane [5, 43-45].

AVP also increases water permeability in the principal cell. Water channels (aquaporins) are present in cytoplasmic vesicles within the cell and upon AVP stimulation these vesicles are translocated to the apical membrane thereby increasing

water permeability [3, 46]. AVP initiates this effect by binding to specific receptors that are located on the basolateral membrane of the principal cell [47] (diagram 3).

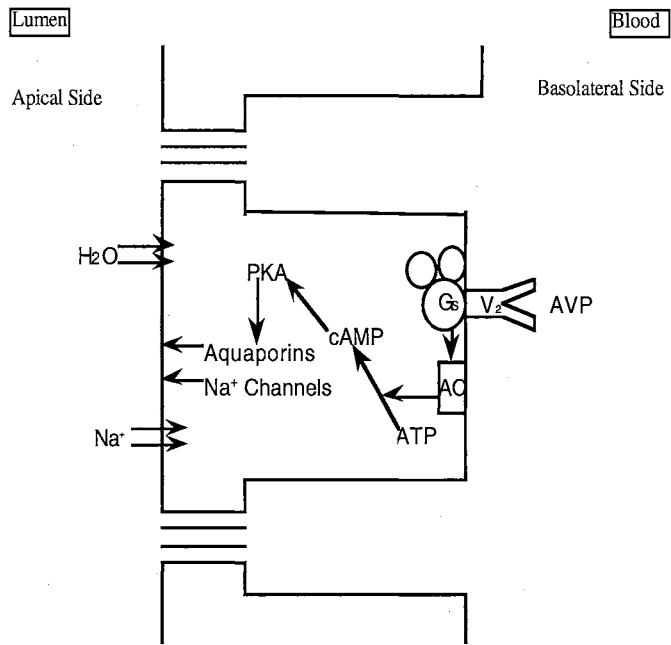


**Diagram 3.** In the principal cell of the cortical collecting duct, AVP binds to the  $V_2$  receptor located on the basolateral membrane. This binding activates a stimulatory G protein ( $G_s$ ) which then activates adenylyl cyclase (AC). AC catalyzes the formation of cAMP from ATP resulting in an increase in intracellular cAMP levels. The increase in cAMP leads to activation of other second messengers that ultimately induce the insertion of sodium and water channels, or aquaporins, into the apical membrane.

### 2.3 Transporters and Ion Channels in the CCD

Movement of solutes and water across epithelium occurs with the aid of epithelial transport proteins. These proteins are broadly catagorized as pumps, carriers, and channels. Pumps are active transporters, requiring energy from the hydrolysis of ATP to

move solute against a concentration gradient. Carriers are proteins that bind ions or specific substrates and move them across a membrane in a passive (no ATP required) or active (ATP required) manner. Carriers include cotransporters (symports) that carry two or more solutes in the same direction, or countertransporters (antiports) that move solutes in opposing directions. Channels are proteins that provide a pore allowing solute or water to passively diffuse across the membrane down a concentration gradient. The movement of solute involves active and passive processes while the movement of water is always passive.

In addition to water channels and epithelial sodium channels introduced in the previous section, the principal cell of the CCD contains potassium channels, chloride channels, and several ion transporters that allow stringent regulation of water and electrolyte movement. The most prominent ion transporter present is the sodium-potassium ATPase (Na/K-ATPase), which generates the electrochemical gradient that drives water and ion movement across cell membranes. Other sodium transporters that have been proposed in the principal cell include the sodium-chloride (NaCl) symport and sodium-hydrogen exchanger (NHE).

### ***2.3.1 Water Channels***

AVP stimulation results in the insertion of aquaporins (AQPs), intrinsic membrane proteins that function as water-selective channels, into the apical membrane of the principal cell. The AQP channels allow water to diffuse passively across the membrane. There are at least four mammalian AQPs characterized (AQP1 - AQP4) and each has

multiple names. The first to be identified was CHIP28 (channel-forming integral protein of 28 kDa) and was later called AQP-CHIP or AQP1 [48]. It is mercury-sensitive and found in two forms: a 28 kDa nonglycosylated form (CHIP28) and a 40-60 kDa glycosylated form (glyCHIP) [48]. AQP1 is the major water channel of the erythrocyte membrane [48], and is also found in the apical and basolateral membranes of the proximal tubule and thin descending limb of the loop of Henle [49-52].

AQP2, also called AQP-CD or WCH-CD (water channel-collecting duct), is found exclusively in the renal collecting duct and is responsible for AVP-regulated water transport across collecting duct cells [4, 46, 53]. AQP2 is mercury-sensitive and found only in the apical membrane and intracellular vesicles [46, 54]. Numerous studies have shown that AQP2 is transported to the apical membrane in the presence of AVP, and removed in the absence of AVP by a process termed the “shuttle hypothesis” [4, 46, 53, 55-59]. The mechanism of the shuttle hypothesis is still not fully understood, but evidence suggests that AQP2 housed in intracellular vesicles is targeted to the apical membrane with the aid of vesicle-associated membrane protein 1 (VAMP1) [60]. Vesicle-associated membrane protein 2 (VAMP2), also known as synaptobrevin, is implicated in the fusion of the vesicle to the plasma membrane [61]. Finally, the microtubule-associated protein dynein and the associated dynactin complex have been shown to play a role in vesicle trafficking to the membrane [62].

AQP3, also known as GLIP (glycerol-transporting integral protein) or BLIP (basolateral integral protein), is also found in renal collecting duct cells. Like AQP2, it is mercury-sensitive and permeable to water in the presence of AVP [63-65]. In contrast to

AQP2, AQP3 is confined to the basolateral membrane with no evidence of intracellular trafficking [66, 67] and is also permeable to urea and glycerol instead of being selective only for water [64, 68].

AQP4, also known as the mercury-insensitive water channel (MIWC), is the osmoreceptor found in the brain that senses the need for antidiuresis [69]. AQP4 is also found in the kidney inner medulla but not the cortical collecting duct [70]. Like AQP3, AQP4 is localized to the basolateral membrane but in contrast to AQP3, is not inhibited by mercury [71]. Also, unlike AQP2 and AQP3, water restriction does not increase AQP4 expression and it has been speculated that the AQP4 may provide a pathway for basolateral exit of water in the IMCD [70].

The general structure of the AQPs has been characterized by studies on the molecular structure of AQP1 (diagram 4). It is a homotetramer containing four independent aqueous units [48, 72, 73]. Each monomer has six membrane-spanning  $\alpha$ -helices which form a right-handed bundle around a central core [74, 75]. The six membrane-spanning regions are connected by five loops, three of which are extracellular (loops A, C, and E) and two that are cytosolic (loops B and D) [48, 76, 77]. The amino and carboxyl termini are both intracellular [46, 77].

The structure of AQP-2 is thus visualized to have an hourglass shape, and is referred to as the hourglass model [73]. Loops B and E are both hydrophobic, closely associated spatially, and share the same Asn-Pro-Ala motifs. This, along with the finding that mutations in either loop B or loop E greatly reduce permeability, indicate that this may

act as the central pore for the entry of water [73]. In addition, a cysteine residue at position 189 has been identified as the mercury-sensitive site [78].

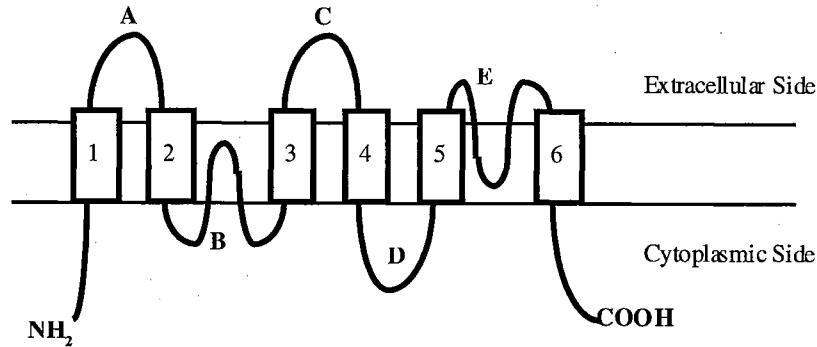


**Diagram 4.** Membrane topology of one aqueous unit of the AQP-2 water channel.

### 2.3.2 Sodium Channels

The sodium channels of the nephron fall into the class of epithelial sodium channels (ENaC) found in many tight, salt-reabsorbing epithelia. They are distinct from voltage-gated sodium channels, and are responsible for passive movement of sodium across apical or outward-facing membranes as the first step in the process of transepithelial sodium transport [45]. The ENaC channels allow sodium to diffuse down its electrochemical gradient into cells, where it is then extruded by the Na/K-ATPase located on the basolateral side (discussed in section 2.3.4). These channels are defined functionally as components of the membrane that move sodium into the cell by electrodiffusion without coupling to other solute flow and without direct use of metabolic energy. They are further defined pharmacologically by their sensitivity to the diuretic amiloride and its

analogs [79-82]. These amiloride-blockable channels have been classified into three groups: 1) channels with high selectivity to sodium over potassium ( $P_{Na}/P_K \geq 10$ ), low conductance ( $\sim 5$  pS), and long open and closed times (0.5-5.0 s); 2) channels with moderate selectivity ( $P_{Na}/P_K = 3-4$ ), high conductance (7-15 pS), and short open and closed times ( $\leq 50$  ms); 3) nonselective cation channels ( $P_{Na}/P_K \leq 50$ ), with high (23-28 pS) or low ( $\geq 3$  pS) conductances [83-85]. It is the highly selective, low conductance ENaC of the distal nephron that allows maintenance of total sodium balance [79, 86].

The ENaC from the distal nephron is composed of three homologous subunits: alpha ( $\alpha$ -ENaC), beta ( $\beta$ -ENaC), and gamma ( $\gamma$ -ENaC) which share 35% identity between them [87, 88] (diagram 5). All three subunits are glycosylated and each has two putative transmembrane domains (M1 and M2). Each subunit is a protein with a large hydrophilic loop ( $\sim 50$  kDa) between M1 and M2 in the extracellular space, and short hydrophilic  $NH_2$  and  $COOH$  terminals (9 and 10 kDa) in the cytoplasm. [87-90]. The transmembrane segments are predicted to have an  $\alpha$ -helical structure followed by a stretch of hydrophobic residues in a  $\beta$ -sheet structure [87, 89]. The extracellular loop contains about 500 residues and evidence suggests that the amiloride binding site resides in this domain on the  $\alpha$ -ENaC subunit [87, 89, 91, 92].

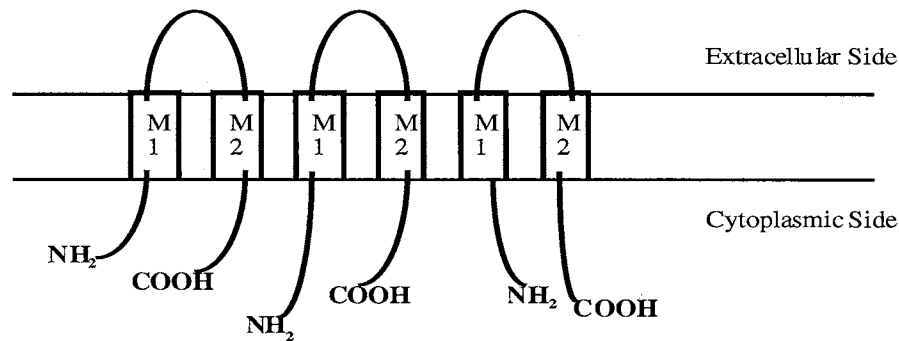


**Diagram 5.** Membrane topology of the epithelial sodium channel (ENaC) of the CCD.

The three ENaC subunits are well polarized and targeted only to the apical membrane and intracellular pools [93]. The subunits are coexpressed equally in the apical membrane and all three must be present for full activity of the channel. Studies have shown that  $\beta$ -ENaC and  $\gamma$ -ENaC subunits alone or together could not induce amiloride-sensitive currents. The  $\alpha$ -ENaC subunit alone or with either of the other two subunits induces only 2 to 10% of the maximal activity observed in the presence of all three subunits [93].

### 2.3.3 Potassium Channels

Potassium channels are classified into two broad groups based on their functional and biophysical properties. There are the delayed or outward rectifiers that are activated by depolarization, and the inward rectifiers that include the classical inward rectifying channel and the ATP-sensitive K channels [94]. The inward rectifiers are characterized by their ability to conduct K more readily into the cell than out of the cell and by a lack of

significant gating by voltage [95]. The classical inward rectifiers, also called the strong inward rectifiers, are found in excitable cells and function in the maintenance of the resting membrane potential and in regulating excitability. The ATP-sensitive K channels are weaker inward rectifiers than the classical and open and close in response to metabolic events [95, 96].

Potassium channels in the CCD serve three important functions. First, they maintain the lumen negative potential of the tubule cells, which is dependent on K conductances. The high intracellular concentration of K is generated by the basolateral Na/K-ATPase that extrudes Na from the cell in exchange for extracellular K and by the diffusion potential of K across the basolateral membrane [97]. Second, they recycle K across the basolateral membrane as a supply for the Na/K-ATPase. This recycling mechanism provides K to the extracellular fluid and safeguards continued turnover of the ATPase during extracellular K fluctuations. Third, they play a key role in K secretion. Electrophysiological studies have defined pathways for passive movement of K across basolateral and apical membranes [39, 96].

Patch-clamp analysis has led to the identification of at least four distinct K channels in principal cells [95, 98-101], and there is strong evidence that both apical and basolateral K channels contribute to K secretion. There are two classes of K channels in the apical membrane and two in the basolateral membrane. In the apical membrane, the maxi-K channel is activated by depolarization, has a large conductance of  $<100$  pS and a low open probability ( $P_o < 0.01$ ) [97]. The apical low-conductance K channel is activated by low pH or PKA, has a conductance of about 30 pS and a high open probability

( $P_o > 0.90$ ) [97, 99]. This channel is ATP-regulated and thus often referred to as the  $K_{ATP}$  channel [95] or the ROMK channel [95, 102]. The ROMK channel is a member of the family of inwardly rectifying potassium (IRK) channels and their expression is regulated by aldosterone and K [102]. Several variants of the ROMK channel have been identified, with ROMK1 and ROMK2 being found in the CCD, and consist of 2 membrane-spanning regions (M1 and M2) making it distinct from voltage-gated or ligand-gated ion channels [95]. The basolateral K channel is activated by hyperpolarization, has a conductance of 28 pS and a variable open probability [97]. In addition, an intermediate conductance channel located on the basolateral membrane has been described with a conductance of 85 pS [101]. This K channel is inhibited by high cytosolic calcium concentrations as opposed to the large conductance channel of the luminal membrane which is activated by high calcium levels [103].

#### ***2.3.4 Chloride Channels***

Chloride (Cl) is the predominant anion in the glomerular filtrate and over 99% of Cl and Na are reabsorbed along the nephron. The pathways of renal chloride transport may be transcellular or paracellular and are often coupled to Na transport. They are also involved in a variety of renal functions, including water and solute reabsorption, urinary acidification, cell volume regulation, and endosomal acidification. While the paracellular route is passive, the transcellular route involves membrane channels.

The CCD contains principal cells, primarily responsible for Na and K transport, and two types of intercalated cells. Type A ( $\alpha$ ) intercalated cells contain a bicarbonate ( $\text{HCO}_3$ )/Cl exchanger and a chloride channel on the basolateral membrane and are primarily responsible for hydrogen secretion. The type B ( $\beta$ ) intercalated cell contains a  $\text{HCO}_3$ /Cl exchanger and a chloride channel on the apical membrane, and a chloride channel on the basolateral membrane. Type B cells are primarily responsible for  $\text{HCO}_3$  secretion [104]. Intracellular microelectrode and patch-clamp studies indicate that principal cells have very little, if any, apical Cl conductance while the basolateral membrane is highly conductive to Cl [105, 106].

The two most prominent Cl channels in the CCD include the CLC (also known as the ClC, for chloride channel) and the CFTR (cystic fibrosis transmembrane conductance regulator). The CLC chloride channels are a family of channels with 9 members identified to date [107, 108]. These channels are the CLC-1, CLC-2, CLC-3, CLC-4, CLC-5, CLC-6, CLC-7, CLC-Ka/K1, and CLC-Kb/K2. Although they differ in their biophysical properties, distribution, and cellular compartmentalization, all share common structural features. The CLC channels consist of 10 to 12 transmembrane regions with cytoplasmic amino and carboxyl domains [109]. While 8 of these channels have been identified in the kidney, only the CLC-K2 has been identified in the rat CCD [110].

The CFTR channel is a chloride channel found in the apical membrane of many epithelial cells, and mRNA for the channel is expressed in all nephron segments [111]. It is a cAMP-regulated protein that is defective in cystic fibrosis, but evidence suggests that it is also a regulator for other membrane conductances. CFTR is expressed in all cell

types of the mouse and rabbit CCD [112] where it inhibits the ENaC channel [113, 114] and modulates the activity of renal ROMK2 channels [115, 116].

The CFTR has a voltage dependent low-conductance (9 pS) for chloride and is a member of a family of ATP binding cassettes (ABC). These membrane proteins are composed of two transmembrane domains, each with six membrane-spanning regions, and cytoplasmic amino and carboxyl terminals. The CFTR also contains two intracellular nucleotide binding domains and a large regulatory domain [111].

### ***2.3.5 Sodium-Potassium ATPase***

In renal tubular cells the Na/K ATPase is located exclusively on the basolateral membrane (see Diagram 11, page 55). The main function of this ATPase is to pump Na out of the cell and extracellular K into the cell using the energy from ATP hydrolysis. Although it may be considered an ion transporter (Na pump) or an enzyme (ATPase), both functions are achieved by this single protein complex. For each ATP molecule hydrolyzed, the Na/K-ATPase moves two K ions into the cell and three Na ions out of the cell. This unbalanced ion exchange causes the electrogenicity of the ATPase [117]. Molecular cloning has shown that the Na/K-ATPase is made up of two main subunits ( $\alpha$  and  $\beta$ ) [118]. The  $\alpha$  subunit consists of 10 transmembrane domains with cytoplasmic amino and carboxyl termini, and a long intracytoplasmic loop. The cytoplasmic domain contains binding sites for sodium and ATP and a phosphorylation site, and the extracellular domain contains binding sites for potassium and ouabain, and is therefore

considered to be the catalytic subunit [117]. The  $\beta$  subunit is smaller than the  $\alpha$ , and contains a single transmembrane domain with several glycosylation sites. The  $\beta$  subunit assists in the folding of newly synthesized  $\alpha$  subunits and stabilizes the  $\alpha$  subunits within the plasma membrane [119]. Although the  $\beta$  subunit has no enzymatic or transport activity, its association with the  $\alpha$  subunit is necessary for ATPase and pump activity [120].

### ***2.3.6 Sodium Transporters: Na/Cl Symport and Na/H Exchanger***

The principal cell of the rat CCD contains sodium transporters in addition to the Na/K-ATPase discussed in the previous section. Experimental studies show the existence of sodium-chloride (Na/Cl) and sodium-hydrogen (Na/H) cotransport and exchange mechanisms, respectively. Evidence of a neutral Na/Cl cotransporter (symport) within the apical membrane comes from experiments using isolated rat CCDs in which certain hormones inhibit sodium transport without changing transepithelial voltage [9, 121]. In CCDs from deoxycorticosteroid (DOC)-treated rats, hydrochlorothiazide reduces sodium and chloride reabsorption without effecting transepithelial voltage, and amiloride decreases sodium reabsorption by only 50% [122]. DOC is converted to corticosterone and then to aldosterone by hydroxylase enzymes in the adrenal cortex, thereby increasing Na channel activity and Na absorption. Hydrochlorothiazide is an inhibitor of NaCl transport and amiloride is a Na channel inhibitor. The finding that half of the net sodium absorption can be inhibited by thiazides and half can be inhibited by amiloride indicates

the rat CCD contains more than one mechanism of sodium entry. There is conflicting data on this point, as studies on principal cells of amiloride-treated rats produces no intracellular depolarization with the addition of ouabain [39]. Depolarization would have occurred if sodium were allowed across the apical membrane *via* another transporter. The actual location of this proposed CCD Na/Cl symport is unknown, and it is possible that it resides in cells that do not contain epithelial sodium channels.

The principal cell of the rat CCD may also contain a neutral Na/H exchanger (antiport)[123]. There are four types of Na/H exchangers known to exist, designated NHE-1, NHE-2, NHE-3, and NHE-4 [124]. NHE-2 is found mostly in the proximal tubule and inner medullary collecting duct and NHE-3 is found in the proximal tubule and thick ascending limb of the rat kidney [125]. NHE-4 is found in the rat inner medullary collecting duct [126]. The NHE-1 is expressed ubiquitously and is located on the basolateral membrane [127, 128].

The NHE-1 isoform, designated as the 'housekeeping' isoform, is inhibited by amiloride and the imidazoline agonist moxonidine [128]. It is important in intracellular pH and cell volume regulation and may play a role in essential hypertension [124, 129]. The NHE-1 exchanger is a membrane protein of 815 amino acids with 12 transmembrane domains and an amiloride binding site on the 4th membrane-spanning region [130]. There is a hydrophobic domain within NHE-1 thought to be responsible for the transport of sodium and hydrogen, and a hydrophilic domain within the cytoplasmic carboxyl terminus that is affected by protein kinases [130, 131]. There are several potential phosphorylation sites for PKC and PKA in the NHE-1 isoform and activation of PKC by

phorbol 12-myristate 13-acetate (PMA) augments the activity of NHE-1 [131, 132]. In the rat CCD, NHE-1 is responsible for regulation of cellular pH in the principal cell and is activated by PKC and inhibited by PKA [123].

## **2.4 Hormonal Control of Salt and Water Transport in the CCD**

Although salt and water transport occur in several places along the nephron, final regulation occurs in the collecting duct to insure that daily excretion or output is equal to dietary intake or input. This regulation is controlled by hormones in the CCD. The most prominent influences are made by AVP, mineralocorticoids, catecholamines, natriuretic peptides, and endothelin. The following review summarizes these hormones and their effects in the collecting duct with particular emphasis on effects within the rat CCD.

### ***2.4.1 Aldosterone***

Aldosterone increases the amiloride-sensitive sodium conductance of the apical membrane thereby increasing sodium reabsorption in the rat CCD [2, 39, 133]. Aldosterone increases sodium reabsorption in the principal cell of the CCD in two ways: first by activation of sodium channels located on the apical membrane and second by increasing the activity of the Na/K-ATPase on the basolateral membrane. These events also increase potassium secretion [134, 135]. Thus, sodium absorption is a two-step process involving the passive entry of sodium from the tubular lumen into the cell through apical sodium channels followed by active extrusion through the basolateral

Na/K-ATPase pump into the serosal compartment. While some control of sodium transport occurs at the basolateral step, most of the ion movement is controlled by the apical ENaC sodium channel [5].

The increase in sodium transport by aldosterone occurs slowly and requires gene expression and protein synthesis [2, 136, 137]. Aldosterone, a steroid hormone, enters the cell by diffusion and binds to cytoplasmic receptors which then migrate as a complex to the nucleus. There it binds to DNA and promotes the synthesis of mRNA and specific proteins [138]. The resulting transport response has been shown to be dependent on this synthesis since it can be prevented by inhibitors of protein synthesis and mRNA [138, 139]. The end result is an increase in the amiloride-sensitive sodium conductance of the apical membrane which allows sodium to enter the cell *via* its electrochemical potential gradient.

The mechanism for the increased sodium permeability has been a topic of much debate. The current and most accepted theory is that ENaC channels (discussed in section 2.3.2) exist in the apical membrane in both active and inactive states, and that aldosterone increases sodium transport by activating inactive or “cryptic” channels [42, 43]. This activation may be associated with methylation of inactive channels [140].

#### ***2.4.2 Vasopressin***

Vasopressin (AVP) increases sodium reabsorption and water permeability in the principal cell of the CCD [141-143]. Using the isolated perfused tubule technique,

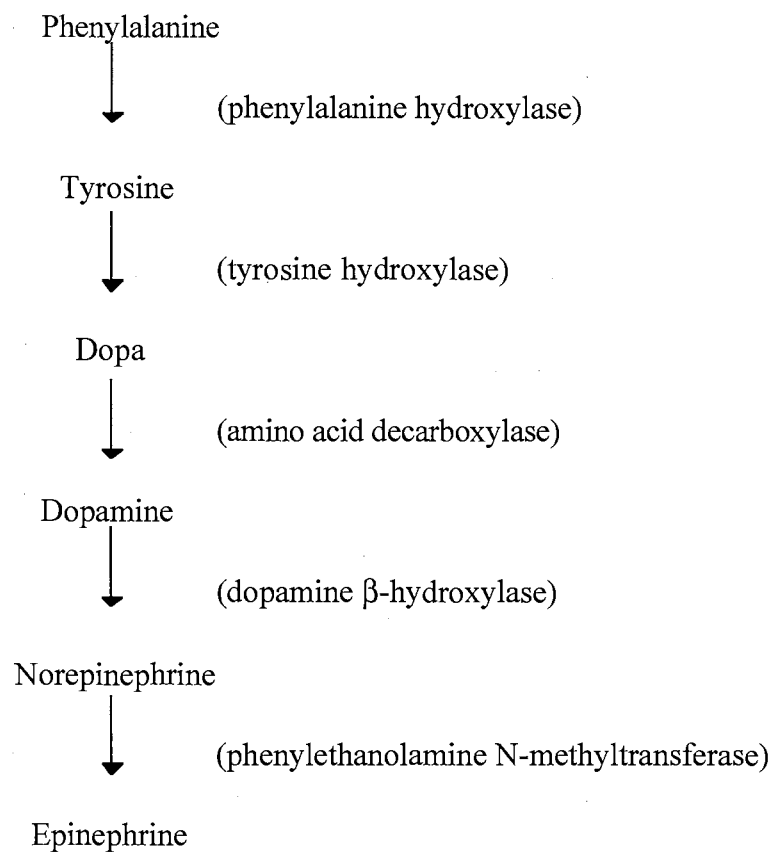
investigators have shown that AVP increases lumen-to-bath sodium transport and keeps it elevated for up to 5 hours [142]. In addition, AVP increases osmotic water permeability ( $P_f$ ) in the rat CCD from zero to as high as 1000  $\mu\text{m}/\text{sec}$  [144]. Using electrophysiological methods, AVP and non-hydrolyzable cAMP analogs have been shown to increase apical membrane sodium conductance [39, 40].

As with aldosterone, the increase in AVP-stimulated sodium transport is due to an increased activity of amiloride-sensitive ENaC channels (discussed in section 2.3.2) in the apical membrane [2, 11, 142, 145]. In contrast to aldosterone, these effects appear to be due to an increase in the number of ENaC channels in the apical membrane rather than activation of channels that are already present [3, 43, 146]. The additional ENaC channels are contained in vesicles located in the cytoplasm and are transported to the apical membrane in the presence of AVP [147-149].

AVP induces formation of coated pits and insertion of intramembrane particles (IMP) into plasma membranes [143, 150-153] indicating that the ENaC channels enter the lipid bilayer *via* clathrin-mediated endocytosis [153]. While some of the IMPs are associated with insertion of sodium channels as previously mentioned, others are involved in water channel trafficking. AVP has been shown to induce water permeability in the CD *via* the relocation of AQPs (discussed section 2.3.1) from intracellular vesicles to the apical membrane [3, 150, 154, 155]. In addition, the removal of AVP results in the removal of these channel proteins from the membrane [152, 156]. Recent studies have suggested that the vesicle-targeting proteins synaptobrevin-2 and syntaxin-4 may play a role in this process [155].

### 2.4.3 Epinephrine and Norepinephrine

Epinephrine and norepinephrine are catecholamines that are released from the adrenal medulla and bind to adrenergic receptors (discussed in section 2.5.2). Biosynthesis of catecholamines occurs in the adrenal chromaffin cell by the following pathway, with responsible enzymes in parentheses:



Epinephrine and norepinephrine are also neurotransmitters synthesized within and released from nerve cells. The adrenal medulla secretes more epinephrine than norepinephrine, while nervous tissue releases predominantly norepinephrine. Thus when

considering the effects of catecholamines on renal function it should be noted that epinephrine is the principal circulating adrenergic hormone.

In the isolated perfused rat kidney, norepinephrine or epinephrine perfused at constant pressure increases sodium reabsorption and increases free water clearance [157]. Epinephrine and norepinephrine bind differentially to all classes of adrenergic receptors (alpha-1, alpha-2, beta-1, beta-2). Specifically, beta-2 receptors are more sensitive to epinephrine than norepinephrine, and are more sensitive to epinephrine than are the alpha-1 receptors. Thus the net effect of infusion of epinephrine may involve summation of effects at various sites in the nephron [158]. In the isolated perfused rat CCD, alpha-1 and alpha-2 receptors are present, with a predominance of the alpha-2 subtype [159]. Epinephrine and norepinephrine binding to the alpha-2 adrenergic receptor suppresses intracellular cAMP stimulation by AVP [29, 160, 161].

#### ***2.4.4 Dopamine***

Dopamine is another catecholamine synthesized in neurons as a precursor to norepinephrine and epinephrine, however renal dopamine is also produced independently of nerve activity. Renal dopamine is synthesized in proximal tubule cells by the action of amino acid decarboxylase (AADC) on L-3,4-dihydroxyphenylalanine (L-DOPA) [162, 163]. L-DOPA enters the cell *via* a sodium transporter in the apical membrane [164] and is decarboxylated to dopamine, which exits the cell apically or basolaterally [163]. The basolateral dopamine transporter is dependent on sodium and pH, and little is known about the apical transporter [165]. Dopamine regulates the activities of various renal

sodium transporters, including the Na/K-ATPase and Na/H exchanger, and promotes sodium excretion [166-169]. In contrast to epinephrine and norepinephrine, which cause natriuresis by activation of adrenergic receptors, dopamine binds to specific dopamine receptors [170]. There are at least five dopamine receptor subtypes which are divided into two main classes, the D<sub>1</sub>-like and the D<sub>2</sub>-like. The D<sub>1</sub>-like division includes the D<sub>1</sub> and D<sub>5</sub> receptors and the D<sub>2</sub>-like division includes the D<sub>2</sub>, D<sub>3</sub>, and D<sub>4</sub> receptors [170].

In the rat CCD, the D<sub>1</sub> and D<sub>4</sub> receptors are expressed [171] and dopamine administration results in inhibition of AVP-stimulated sodium reabsorption and osmotic water permeability [168]. The natriuretic and diuretic effects in the CCD appear to be mediated by the D<sub>4</sub> subtype [168, 171] and occur *via* the inhibition of cAMP accumulation [12, 172].

#### **2.4.5 Serotonin**

In the proximal tubule, AADC converts L-5-hydroxytryptophan (L-5-HT) to serotonin (5-HT) [173-175]. In contrast to dopamine, which causes natriuresis and diuresis, renal serotonin promotes sodium and water reabsorption [163, 176]. There are at least 10 types of 5-HT receptors (5-HT<sub>1A</sub>, 5-HT<sub>1B</sub>, 5-HT<sub>1C</sub>, 5-HT<sub>1D</sub>, 5-HT<sub>1E</sub>, 5-HT<sub>2A</sub>, 5-HT<sub>2B</sub>, 5-HT<sub>3</sub>, 5-HT<sub>1P</sub>, 5-HT<sub>4</sub>) which are divided into three major families (5-HT<sub>1</sub>, 5-HT<sub>2</sub>, and 5-HT<sub>3</sub> receptor families) [177]. The 5-HT<sub>1</sub> family has the highest affinity for 5-HT and is coupled to an inhibitory G protein that inhibits adenylyl cyclase. The 5-HT<sub>2</sub> family displays a relatively low affinity for 5-HT and high affinity for 5-HT

antagonists, and is linked to phosphatidylinositol turnover. The 5-HT<sub>3</sub> receptor family mediates the excitatory effects of 5-HT [177].

In the kidney, the 5-HT<sub>1A</sub> and 5-HT<sub>1B</sub> receptors have been located [163, 178], but the antinatriuretic effect of 5-HT is attributed to the 5-HT<sub>1A</sub> receptor in the rat [163]. Histochemical mapping of 5-HT<sub>1A</sub> receptors is identical in human and rat kidneys, and the receptor is found in the thick ascending limb, distal convoluted tubule, connecting tubule, and principal cells of the cortical collecting duct [179].

#### ***2.4.6 Atrial Natriuretic Peptide***

Atrial natriuretic peptide (ANP) is a peptide hormone secreted by the atria of the heart in response to increased vascular volume [180, 181]. In the vasculature, ANP reduces blood pressure by inhibiting sympathetic output and by ANP-receptor mediated relaxation of vascular smooth muscle cells [181]. ANP also inhibits renin and aldosterone secretion, and in the kidney ANP stimulates natriuresis and diuresis [182-184].

ANP binds to cell surface natriuretic peptide receptors (NPRs). There are three NPRs (NPR1, NPR2, and NPR3), each with a single transmembrane region and an extracellular binding domain [185]. NPR1 is expressed in the kidney, vasculature, and adrenal glands. NPR2 is found in the brain and pituitary gland and may have a role in neuroendocrine regulation. NPR3 is the most widely expressed, being found in most of the major endocrine glands, kidney, vasculature, and lungs [185].

In the rat and rabbit IMCD, ANP inhibits sodium reabsorption [186-190] and AVP-stimulated osmotic water permeability [186, 189]. ANP exerts this action through the second messenger cGMP, which inhibits sodium reabsorption by reducing the open probability of the ENaC channel [191]. The mechanism by which ANP inhibits water permeability has not been determined, but does not appear to involve inhibition of cAMP accumulation within the cell [192, 193]. In the CCD, reports of the effects of ANP are contradictory. ANP has been reported to inhibit chloride transport in the presence and absence of AVP, and to inhibit water absorption by 50% in isolated rabbit tubules [9, 194]. In contrast, more recent reports in the rat CCD could find no effect of ANP on sodium or water permeability [195-197].

#### ***2.4.7 Urodilatin***

Urodilatin is a member of the family of natriuretic peptides, and is processed to a 23-amino acid peptide hormone from the same precursor as ANP [198]. It is synthesized in renal distal tubule and connecting tubule epithelial cells and interacts with luminal receptors to regulate sodium and water reabsorption. Urodilatin binds to the NPR1 receptor (also called NPR-A receptor) in the same way as ANP, and stimulates formation of cGMP [199]. cGMP-dependent protein kinase is then activated which in turn inhibits sodium reabsorption *via* the amiloride-sensitive ENaC channel (discussed in section 2.3.1) [200]. Further sodium regulation occurs by inhibition of renin secretion and inhibition of the stimulatory effect of angiotensin II on aldosterone release [198]. In addition,

relaxation occurs in kidney arterial smooth muscle *via* a reduction of intracellular calcium levels [201].

The primary role of urodilatin is natriuretic and diuretic [202, 203]. In humans, urodilatin induces strong diuresis and natriuresis under different sodium diets [203]. In rats, urodilatin increases urine flow and sodium excretion, and reduces blood pressure [183]. Microperfusion studies demonstrate that urodilatin induces sodium and water reabsorption in the rat IMCD [190, 204]. To date, there is no evidence that urodilatin has any effect in the CCD [190, 197].

#### **2.4.8 Endothelin**

Endothelins (ETs) are a family of endothelial cell-derived vasoactive substances [205] of which here are three members (ET-1, ET-2, and ET-3) [206]. ET-1 is made by endothelial cells, airway epithelial cells, macrophages, fibroblasts, cardiomyocytes, and some neurons [205]. More recently, IMCD cells have been shown to produce ET-1 [207]. ET-2 is expressed in intestinal epithelial cells and ET-3 is expressed in intestinal and renal tubular epithelial cells and neurons [205, 208].

Two ET receptors (ET<sub>A</sub> and ET<sub>B</sub>) have been identified in mammals and both contain 7 transmembrane regions [209]. Each receptor activates an overlapping set of G proteins, leading to diverse responses such as activation of phospholipase C and increases in intracellular calcium [210]. ET<sub>A</sub> has higher affinity for ET-1 and ET-2 over ET-3, and ET<sub>B</sub> has equal affinities for all three endothelin peptides [209]. ET<sub>A</sub> and ET<sub>B</sub> receptors

have been identified in vessel and airway smooth muscle cells, heart, liver, brain, bone, kidney, and within the reproductive tract [209]. In the rat kidney, ET<sub>A</sub> receptor mRNA is found only in the glomerulus, arcuate artery, and vasa recta whereas ET<sub>B</sub> receptor mRNA is found in those locations as well as the medullary and cortical collecting duct [211, 212].

Endothelin, specifically ET-1, has direct tubular actions that appear to be localized mainly to the IMCD where it inhibits AVP-stimulated cAMP accumulation and osmotic water permeability [213-215]. The effects of ET-1 on sodium transport has been further explored in rats lacking the ET<sub>B</sub> receptor gene which results in a salt-sensitive hypertension [216]. In another study, rats treated with deoxycorticosterone acetate (DOCA) exhibited significant hypertention when an ET<sub>B</sub> receptor-specific antagonist was administered [217]. These findings indicate that the effects of ET-1 on sodium transport are mediated by the ET<sub>B</sub> receptor in the rat IMCD, which acts by tonically inhibiting ENaC activity [215-217].

## **2.5 Membrane Receptors in the CCD**

The CCD is a major site of hormonally regulated sodium and water transport and each hormone binds with varied affinity to specific receptors. Section 2.4 reviewed some of the major hormones influencing sodium and water permeability in the kidney. The present section details vasopressin and adrenergic receptor structure and function,

and introduces imidazoline and Y receptors as modulators of AVP-stimulated sodium and water permeability.

### ***2.5.1 Vasopressin Receptors***

AVP acts on at least two types of receptors,  $V_1$  and  $V_2$ , classified by their second messengers. Both contain seven hydrophobic transmembrane domains characteristic of G protein-coupled receptors [218-220]. In addition both are found in the kidney, but with distinct mechanisms of action [221-223]. The  $V_1$  receptor is coupled to phospholipase C and therefore produces 1,2,4-inositol triphosphate and diacylglycerol. This leads to mobilization of intracellular calcium and inhibition of cAMP formation *via* calcium-dependent prostaglandin synthesis [223], and influences blood pressure, glycogenolysis, and liver regeneration [224, 225]. This  $V_1$  receptor has been further subdivided into  $V_{1a}$  and  $V_{1b}$  subtypes. The  $V_{1a}$  is found in many tissues, including the kidney [222, 226, 227] where it appears to be associated with interstitial cells and in vascular elements adjacent to collecting ducts [222, 226]. The  $V_{1b}$  receptor has been localized to the anterior pituitary [228].

The  $V_2$  receptor is coupled to adenylyl cyclase and has been shown to mediate the antidiuretic effects of AVP in the collecting duct [3, 47, 221] (diagram 3, page 9). AVP stimulates sodium and water transport from the basolateral, but not the apical, side of collecting duct cells indicating that the  $V_2$  receptor is localized to the basolateral

membrane [141, 143, 229]. The specific site of hormone binding is found on the second extracellular domain of the receptor [230].

### ***2.5.2 Adrenergic Receptors***

Adrenergic receptors, or adrenoceptors, are divided into two families ( $\alpha$  and  $\beta$ ) and can be distinguished pharmacologically based on their responses to epinephrine, norepinephrine and isoproterenol [231, 232]. The  $\alpha$  adrenoceptors are responsive to the naturally occurring catecholamines epinephrine and norepinephrine but show only a weak response to the synthetic agonist isoproterenol [232]. The  $\beta$  receptors are characterized by a strong response to isoproterenol and lower response to the natural catecholamines [231].

The  $\alpha$  receptors are divided into subtypes,  $\alpha_1$  and  $\alpha_2$ , based on their affinity for agonists and antagonists. The  $\alpha_1$  receptor has a higher affinity for phenylephrine than do the  $\alpha_2$  receptors, whereas clonidine and yohimbine selectively bind to the  $\alpha_2$  receptors with less effect on the  $\alpha_1$  receptors [233, 234]. Binding to  $\alpha_1$  receptors initiates a G protein mediated activation of phospholipase C and leads to the release of calcium from the endoplasmic reticulum in smooth muscle cells [235]. In contrast, the effect of  $\alpha_2$  receptor binding is an inhibition of adenylyl cyclase and a decrease in intracellular cAMP and is mediated by a pertussis-toxin sensitive inhibitory G protein [232].

Binding studies have identified at least three subtypes of the  $\alpha_2$  adrenoceptor ( $\alpha_{2A}$ ,  $\alpha_{2B}$ , and  $\alpha_{2C}$ ), all of which are activated nonselectively by epinephrine and

norepinephrine [233, 236-240]. All of the  $\alpha_2$  subtypes can be blocked by yohimbine and rauwolscine, although the affinity varies [241]. The  $\alpha_{2A}$  subtype is widely distributed in tissues and has a higher affinity for oxymetazoline over prazosin. The  $\alpha_{2B}$  subtype is also widely distributed but has a higher affinity for prazosin than for oxymetazoline [237]. The  $\alpha_{2C}$  receptor is expressed in the opossum kidney (OK) cell line [242]. An additional subtype,  $\alpha_{2D}$ , has been found in bovine pineal gland and may represent a species homologue of the  $\alpha_{2A}$  subtype [243].

Clonidine has been characterized as the prototypical  $\alpha_2$  agonist which inhibits AVP-stimulated water and sodium permeability [244]. Yohimbine is the prototypical  $\alpha_2$  antagonist and reverses the effects of clonidine [234]. The non-selective endogenous adrenergic agonist epinephrine and the  $\alpha_2$ -selective agonist dexmedetomidine have also been shown to completely inhibit AVP-stimulated transport in the collecting duct [7, 8, 29], and other agonists and antagonists have been tested with varied degrees of inhibition at given concentrations.

### ***2.5.3 Imidazoline Receptors***

Recently, a new class of receptors called imidazoline (I) receptors have been implicated in this AVP-mediated event. Imidazolines are compounds that contain an imidazole ring structure (diagram 6) and include some adrenergic agents [21, 245, 246] (see appendices A and B). Clonidine, for example, is an  $\alpha_2$  agonist that is also an imidazoline.

The antihypertensive action of clonidine was originally thought to be *via*  $\alpha_2$  adrenoceptor activation in the central nervous system [244]. It has since been shown that the effect of clonidine is mediated, at least in part, by activation of specific imidazoline receptors [21, 247, 248]. Studies in the rat kidney have shown that activation of I receptors increases sodium and water excretion [15, 16, 249].

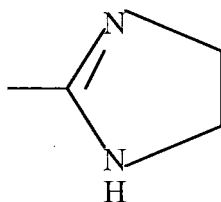


**Diagram 6.** Imidazole Ring Structure. The imidazole ring may be attached to NH or to C of the side group.

Like the adrenergic receptors, I receptors are subdivided into  $I_1$  and  $I_2$  subtypes that bind with varied affinity to different agonists and antagonists [250, 251]. The  $I_1$  receptor displays a high affinity for clonidine by preferentially binding [ $^3$ H]-pNH<sub>2</sub>-clonidine and [ $^3$ H]-clonidine, and is thought to mediate the fall in arterial pressure attributed to imidazolines [24, 247, 248, 252, 253]. The pharmacologic profile shows the highest affinity for imidazolidines (imidazoline ring attached to NH) such as clonidine and moxonidine, medium affinity for imidazolines (imidazoline ring attached to C) such as idazoxan and phentolamine, and low affinity for guanidines and guanidides (guanabenz, amiloride) [254].

The I<sub>1</sub> receptor site is selectively localized to plasma membranes [254] and has been shown to act *via* a pertussis toxin-sensitive G protein [28]. Activation of the receptor leads to production of the second messenger diacylglyceride through direct activation of phosphatidylcholine-selective phospholipase C. I<sub>1</sub> receptor stimulation in PC12 cells (pheochromocytoma cells which lack  $\alpha_2$  receptors) also elicits release of arachidonic acid and prostaglandins, resulting from the action of diacylglyceride lipase on accumulated diacylglyceride [24]. The I<sub>1</sub> receptor may be further divided, based on the affinity for cimetidine, into subtypes I<sub>1A</sub> (cimetidine-sensitive) and I<sub>2B</sub> (cimetidine-insensitive) [255].

The I<sub>2</sub> receptor preferentially binds [<sup>3</sup>H]-idazoxan and [<sup>3</sup>H]-cirazoline and its pharmacologic profile shows the highest affinity for imidazolines (idazoxan, cirazoline) with a low affinity for clonidine [250, 256]. These receptors are found associated with mitochondrial membranes, with the receptor site located mainly on the external membrane of the mitochondria. The I<sub>2</sub> receptor is associated with the monoamine oxidase (MAO) system, with no involvement of G proteins [257, 258]. This mitochondrial specific binding site may be associated with the catalytic site of the MAO enzyme, and therefore may be a regulatory site [259]. In addition, I<sub>2</sub> receptors in different tissues have been shown to display high and low affinities for amiloride supporting the existence of I<sub>2</sub> receptor subtypes, I<sub>2A</sub> (amiloride-sensitive) and I<sub>2B</sub> (amiloride-insensitive) [250, 258].

The discovery of the first candidate for an endogenous imidazoline receptor ligand actually occurred before the characterization of imidazoline receptors as separate from  $\alpha_2$  receptors. In 1984, clonidine-displacing substance (CDS) was purified from human brain and shown to displace [<sup>3</sup>H]-clonidine with high affinity, although it was thought at the

time to be due to its  $\alpha_2$  selectivity [260]. Later, CDS was found to competitively bind with high affinity to I receptors [22] but its structure remained unknown.

In 1994, a CDS called agmatine was isolated from bovine brain. Agmatine, an arginine metabolite, binds with high affinity to  $\alpha_2$ , I<sub>1</sub> and I<sub>2</sub> receptors making it the first endogenous imidazoline receptor ligand of known structure [261, 262]. Further studies have found that agmatine displays preferential affinity for the I<sub>1</sub> binding site [263-265]. In human platelets the affinity of agmatine for the I<sub>1</sub> receptor subtype was 2200-fold greater than that of the I<sub>2</sub> subtype, 1400-fold greater than that of the  $\alpha_{2A}$  adrenoceptors, 5000-fold greater than the  $\alpha_{2B}$  adrenoceptors, and 800-fold over the  $\alpha_{2C}$  adrenoceptors [264].

Agmatine may be an important neurotransmitter in mammals. It is synthesized in the brain and stored in synaptic vesicles in axon terminals [266]. Agmatine is released by depolarization in a calcium-dependent manner and is inactivated by reuptake or enzymatic degradation [267]. Reuptake into synaptosomes is calcium-dependent and inhibited by calcium channel blockers [268]. Enzymatic degradation occurs through the action of agmatinase, which hydrolyses agmatine to putrescine and urea [269].

The substrate for the production of agmatine is arginine, which enters the cell by facilitated transport and is converted *via* the enzyme arginine decarboxylase (ADC) on the mitochondrial membrane [269]. Once synthesized, agmatine can bind to I<sub>2</sub> receptors on the mitochondrion or to  $\alpha_2$  adrenergic, and possibly I<sub>1</sub> receptors on the plasma membrane. It may also be released extracellularly since agmatine has been found in

plasma. The synthesis of agmatine is thought to be regulated by feedback inhibition of ADC within the cell [270](diagram 7).

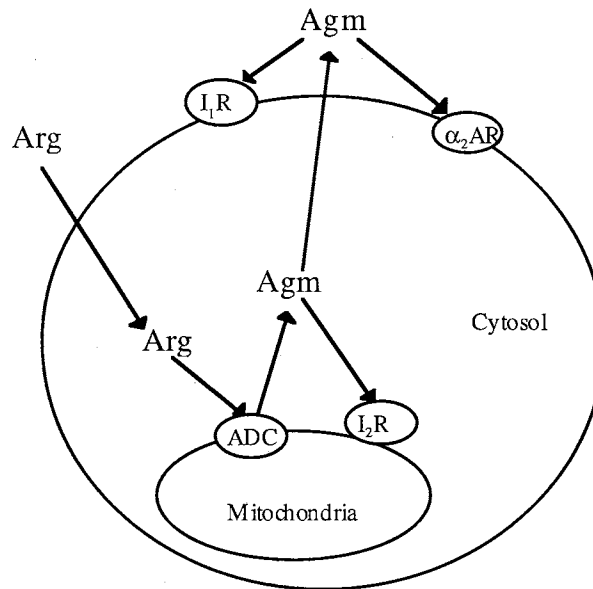


**Diagram 7.** Biosynthesis of Agmatine. Arginine is converted to agmatine by arginine decarboxylase located in the mitochondrial membrane. Agmatine may bind to imidazoline receptors on the mitochondrial membrane, or leave the cell and bind to imidazoline or alpha 2-adrenergic receptors on the plasma membrane. Arg, arginine; Agm, agmatine; ADC, arginine decarboxylase; I<sub>1</sub>R and I<sub>2</sub>R, imidazoline receptors; α<sub>2</sub>AR, alpha 2-adrenergic receptor.

Although it was previously known to occur in plants, bacteria, and lower life forms, the discovery of ADC in rat brain indicates that the source of agmatine is endogenous since ADC is the enzyme involved in the rate-limiting step in agmatine biosynthesis. Of additional interest is the localization of ADC to mitochondrial membranes since that is also the location of I<sub>2</sub> receptors [261]. Agmatine has been shown to be widely distributed in the body with its rank order of concentration being stomach > small intestine >> adrenal > heart > brain > plasma [262]. ADC activity has been identified in the kidney

cortex and medulla and diamine oxidase, an enzyme shown to metabolize agmatine, has been localized to the kidney glomeruli [269].

Relatively little is known about the biological actions of agmatine. It is a cation and has been shown to open up some ion channels by activation of nicotinic acetylcholine receptors [271]. Agmatine may also have a role in insulin-glucose metabolism since it was shown to facilitate the release of insulin from pancreatic cells exposed to glucose [272]. What is known is that agmatine does not mimic the actions of clonidine completely. Agmatine does not contract vascular smooth muscle and is thought to decrease sympathetic nerve activity and arterial pressure when injected i.v. by blocking sympathetic ganglionic transmission [270].

In rats, microperfusion of agmatine into renal interstitium and the urinary space of the surface glomeruli produces reversible increases in the single nephron filtration rate (SNFR) and absolute proximal reabsorption (APR). Yohimbine (an  $\alpha_2$  antagonist) produced the opposite effects and BU-224 (an  $I_2$  agonist) duplicated agmatine's effects on SNFR but did not effect APR [269]. Thus the effects of agmatine on SNFR and APR appear to be dissociable and mediated by different mechanisms and may constitute a novel endogenous regulatory mechanism in the kidney.

#### ***2.5.4 Y Receptors (Neuropeptide Y and Peptide YY)***

NPY and PYY bind with high affinity to Y receptors, so named because they have many tyrosine residues, and have been shown to affect salt and water transport in the

kidney. NPY and PYY are both members of the pancreatic polypeptide family that also contains pancreatic polypeptide (PP) [273].

NPY is a neurotransmitter that is widely distributed in central and peripheral neurons and is co-stored and released with norepinephrine (NE) from perivascular nerve fibers upon sympathetic stimulation [274]. Coexisting NPY and NE act synergistically to regulate renal tubular Na/K-ATPase activity [275-278] and NPY has been shown to potentiate the effects of NE by sensitization of arteries. This effect occurs postjunctionally [274, 279] and depends on the presence of sodium [275]. In the CCD, NPY decreases AVP-stimulated hydraulic conductivity and cAMP was found to play a role in this response [26].

While NPY is considered a neurotransmitter, the structurally related PYY is a gut hormone found in the small intestine and colon. PYY is released from the endocrine cells of the lower intestine in response to food and acts on the gastrointestinal system to slow intestinal motility and increase intestinal transport of salt and water [280, 281]. In the CCD, preliminary studies have indicated that PYY decreases sodium transport [32].

NPY and PYY both act on Y receptors which are found in many tissues, including the kidney where they have segment-dependent effects in the nephron [13, 32, 282, 283]. Binding studies have identified up to five Y receptor subtypes ( $Y_1$ - $Y_5$ ) [284]. NPY and PYY bind equally well to the  $Y_1$  and  $Y_2$  receptors, both of which have been found in the kidney [285]. The  $Y_3$  receptor has a higher affinity for NPY over PYY [286] while the  $Y_4$  receptor binds only PP with high affinity [287] and neither has been localized to the kidney. The  $Y_5$  receptor is localized to the brain [287, 288] and binds NPY, PYY and PP

where it is involved in the regulation of feeding behavior [289]. The  $Y_5$  receptor has also been indicated in some of the renal effects of NPY [32].

All of the known Y receptors are coupled to pertussis toxin-sensitive G-proteins [34]. The signalling mechanisms for the different receptor subtypes appear to be similar, although no distinct signal transduction pathways have been identified. Inhibition of adenylyl cyclase is the typical response as with other  $G_i/G_o$ -coupled receptors [290], but other responses have been reported. These include inhibition of calcium channels [34, 278] and stimulation of Na/K-ATPase activity [277, 278].

## **2.6 Signalling Pathways and Second Messengers in the CCD**

AVP action represents the prototypical example of a hormonal effector acting through a stimulatory G protein and adenylyl cyclase activation of cAMP-dependent signalling in the CCD (see section 2.5.1). Protein kinase A (PKA) is a known second messenger in this system, but much of the signal transduction pathway remains unknown. This section reviews G proteins and some of the second messengers and pathways that are involved in regulation of AVP-stimulated sodium and water transport in the CCD. These second messengers and pathways include adenylyl cyclase, PKA, phosphatidylinositol hydrolysis, protein kinase C (PKC), prostaglandins, and calcium.

### 2.6.1 G Proteins

G proteins are a family of proteins involved in a variety of signal transduction pathways, including phospholipid metabolism, intracellular vesicle trafficking, and ion channel regulation [27, 291]. These proteins are divided into two major classes, heterotrimeric G proteins and monomeric G proteins.

The heterotrimeric G proteins have a high molecular weight and consist of three subunits:  $\alpha$  ( $M_r$  39,000-52,000),  $\beta$  ( $M_r$  35,000-36,000), and  $\gamma$  ( $M_r$  8,000-10,000). There are various heterotrimeric G proteins, characterized by their  $\alpha$  subunits because they are the most diverse and are thought to be responsible for the specificity of receptor and effector interactions [292-294]. The most important ones that act in the kidney are  $G_s$ , a stimulatory G protein that activates hormone-sensitive adenylyl cyclase [295] and  $G_i$ , an inhibitory G protein that inhibits adenylyl cyclase.

The monomeric G proteins have a low molecular weight and consist of a single  $\alpha$  subunit ( $M_r$  19,000-29,000). These proteins have been shown to be important in target protein regulation and oncogenesis, and include the Ras and Rab family of proteins [291]. Both classes are defined by the ability of the  $\alpha$  subunit to bind and hydrolyze guanine nucleotides [27].

G protein-mediated signals are initiated *via* binding by G protein-coupled receptors (GPCR). The GPCRs all have seven membrane-spanning domains of 20-25 hydrophobic residues in the form of  $\alpha$ -helices. There is an extracellular amino terminus, three extracellular loops, three intracellular loops, and an intracellular carboxyl terminus.

Agonists interact with the extracellular and transmembrane domains. The intracellular domains interact with G proteins which contain phosphorylation sites and transduce the signal to the interior of the cell [296](diagram 8).

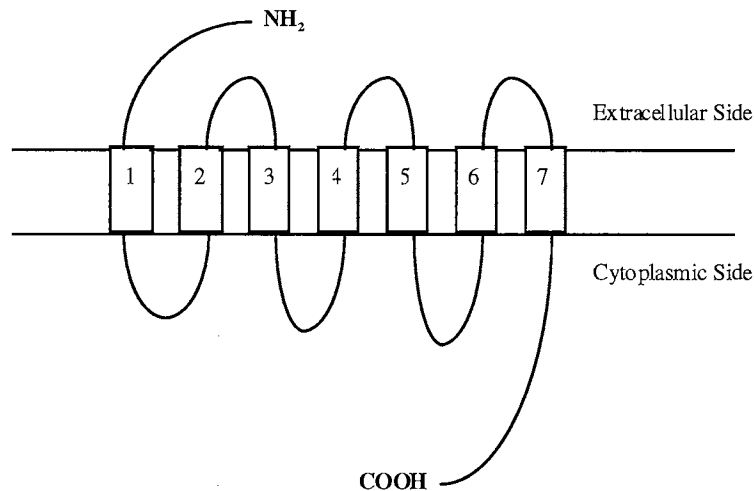


**Diagram 8.** Topology of the G Protein-Coupled Receptor. The family of G protein-coupled receptors all contain 7 transmembrane regions, an amino extracellular terminus, a carboxyl intracellular terminus, and 3 intracellular loops involved in G protein binding.

In renal epithelia, G proteins mediate AVP-stimulated sodium and water permeability through a basolateral G<sub>s</sub> mechanism, and this action can be modulated by different receptors through a G<sub>i</sub> mechanism [218, 294, 297]. The G<sub>s</sub> protein stimulates adenylyl cyclase which in turn causes an accumulation of cAMP within the cell. The increase in cAMP activates PKA [298, 299] and leads to the insertion of water channels and sodium channels into the apical membrane. Activation of a basolateral G<sub>i</sub> protein by  $\alpha$ -adrenergic agents inhibits sodium and water permeability [7, 29, 300] by mechanisms not yet fully understood (diagram 9).

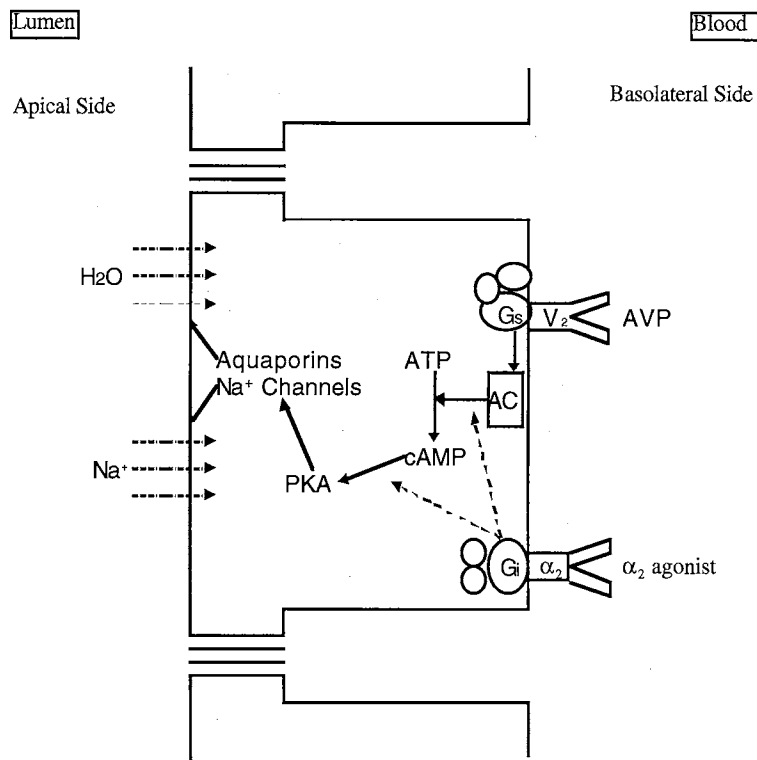


**Diagram 9.** Alpha-2 Receptor in the Principal Cell. Alpha-2 ( $\alpha_2$ ) agonists bind to the  $\alpha_2$ -adrenergic receptor and inhibit AVP-stimulated water and sodium permeability.

The signalling pathways for AVP-stimulated sodium and water transport in the CCD and inhibition of this transport are not completely known, but it has been shown that second messengers in addition to cAMP are involved [29, 30, 301]. These second messengers may include calcium [302], PKC [44, 298, 303, 304], and prostaglandin E<sub>2</sub> [305-308].

### ***2.6.2 Adenylyl Cyclase and cAMP***

Adenylyl cyclase (AC) integrates the positive and negative signals that act through G protein-coupled receptors to regulate intracellular levels of cAMP [27]. The structure of AC consists of two subunits (M1 and M2) with six transmembrane domains each [309]. There is a large cytoplasmic loop between the two subunits (C1) and a large extracellular loop between transmembrane regions 9 and 10 that is the site for glycosylation [310]. There are at least 9 isoforms of mammalian AC identified so far [311-315]. All of the isoforms have been found in the brain and all are stimulated by the G<sub>s</sub>  $\alpha$  subunit of the G protein, and this requires both the C1 domain as well as the carboxyl terminus [316]. The inhibitory G<sub>i</sub>  $\alpha$  subunit inhibits only AC types 1, 5, and 6, and occurs in the C1 regions of AC types 1 and 5 [317]. In the principal cell of the rat collecting duct, the type 6 AC isoform has been localized where it elicits a calcium-dependent inhibition of cAMP [318]. The  $\beta\gamma$  subunit of the G protein inhibits type 1 and stimulates types 2 and 4 [310, 319] and occurs in the C1 region of the AC type 1 isoform [317].

### ***2.6.3 Protein Kinase A***

Binding of the  $\alpha$  subunit of the G protein to adenylyl cyclase activates the enzyme which in turn catalyzes the conversion of ATP to cAMP [319]. cAMP is bound to PKA enzymes, which are composed of two regulatory and two catalytic subunits [320]. The PKA catalytic subunits, which are the main effectors of cAMP, dissociate from cAMP-saturated regulatory subunits and phosphorylate numerous downstream targets.

Diversification of the pathway occurs at the PKA level because various PKA anchoring proteins (AKAPs) can sequester PKA molecules until the arrival of cAMP [321, 322]. The AKAPs represent a family of functionally related molecules characterized by their interaction with the type I or type II regulatory subunits of PKA. In addition, AKAPs contain unique targeting sequences that direct the PKA-AKAP complex to specific intracellular locations [321]. One of these targets is the aquaporin 2 water channel (AQP-2), which is translocated to the apical membrane upon phosphorylation [323].

#### ***2.6.4 Phosphatidylinositol Breakdown***

One of the ways that vasopressin increases levels of calcium within the cell is by initiating calcium release from intracellular stores, which is dependent on inositol-1,4,5-trisphosphate (IP<sub>3</sub>) generation [302]. Phospholipase C (PLC) hydrolyzes phosphatidylinositol bisphosphate (PIP<sub>2</sub>) into two breakdown products, diacylglycerol (DAG) and IP<sub>3</sub>. IP<sub>3</sub> initiates the mobilization of calcium [324, 325] and DAG in the presence of calcium directly binds to and activates PKC. The increase in calcium may also lead to activation of other calcium-dependent kinases [302].

#### ***2.6.5 Protein Kinase C***

The ultimate consequence of DAG formation is the activation of PKC. PKC represents a family of enzymes that phosphorylate serine or threonine residues on various intracellular proteins and are responsible for a wide range of cellular functions. There are

12 isozymes identified so far and they are classified into three subfamilies [326]. The classical PKC (cPKC) includes the  $\alpha$ ,  $\beta$ I,  $\beta$ II, and  $\gamma$  isozymes and is dependent on activation through cofactors like DAG and calcium. The second group includes the novel PKC (nPKC) including  $\delta$ ,  $\epsilon$ ,  $\theta$ ,  $\eta$ , and  $\mu$ , and are also activated by DAG but are calcium independent. The third group, or atypical PKC (aPKC), includes  $\zeta$ ,  $\iota$ , and  $\lambda$ , and require only phosphatidylserine for activation [324, 326]. Of all the PKC isoforms, only PKC $\alpha$  has been localized to the CCD [326]. As with PKA, anchoring proteins play an integral part of PKC activity. These anchoring proteins for PKC are called RACKs (receptors for activated C-kinase) [327, 328] and have been proposed to impart isozyme selectivity within the cell [328].

### ***2.6.6 Prostaglandins***

Prostaglandins (PGs) are a family of diverse autocooids derived from the cyclooxygenase-mediated metabolism of arachadonic acid. Five primary prostanoids are produced and each one interacts with a different G protein-coupled receptor [329]. PGE<sub>2</sub> is produced in the kidney and the highest rate of synthesis occurs in the collecting duct where it plays a role in salt and water transport [329]. Studies investigating the effects of exogenous PGE<sub>2</sub> administration demonstrate varied results depending on the PG receptor involved as well as major species differences [6, 10, 330]. In the rat CCD, exogenous PG has little effect on AVP-stimulated salt or water transport [6, 330, 331]. Endogenous PG production however, has been shown have an antinatriuretic and

antidiuretic effect by reversing alpha-2 adrenoceptor effects [332]. This occurs by a direct stimulation of PG synthesis by vasopressin [329, 333]. The mechanism of action of PGE<sub>2</sub> may involve release of calcium from intracellular stores and subsequent activation of PKC [10, 306].

### **2.6.7 Calcium**

In the mammalian collecting duct, AVP increases intracellular free calcium concentrations [334-336]. AVP binds to two receptors: V<sub>1</sub> receptors which activate phospholipase C and release intracellular calcium through phosphatidylinositol hydrolysis [302]; and V<sub>2</sub> receptors which are coupled to adenylyl cyclase and cAMP generation (discussed in section 2.1.5). Radioligand binding studies have shown that the V<sub>2</sub> receptor is more abundant in the collecting duct, and that the V<sub>1</sub> receptor is localized in vascular and interstitial cells rather than in tubules themselves [221]. In addition, AVP was shown to increase intracellular calcium levels in mouse collecting duct cells and isolated rat IMCDs independent of adenylyl cyclase activation [336-338].

Two phases of cellular free calcium mobilization are evident after the addition of AVP. There is an early phase derived from the intracellular calcium pool and a sustained phase that depends on extracellular calcium [325, 335]. In rabbit CCDs, reduced extracellular calcium causes a reduction in the hydrosmotic effect of AVP [339-341]. Evidence suggests that calcium inhibits AVP action by stimulation of PLC and the subsequent activation of PKC inhibits cAMP formation [341].

In summary, the mammalian nephron regulates blood pressure and plasma osmolarity, and reabsorption of sodium and water in the collecting duct is the final step of this regulation. The cortical segment of the renal tubule contains principal cells that possess water channels, ion channels and ion transporters. The tubular reabsorption of sodium and water is under hormonal stimulation and the influence of some of the major players is shown in table I. In addition, multiple second messengers and signalling pathways are implicated in these responses, including G proteins, adenylyl cyclase, PKA, PKC, prostaglandins, and calcium.

<u>Hormone</u>	<u>Sodium reabsorption</u>	<u>Water reabsorption</u>
Aldosterone	stimulates	stimulates
Vasopressin	stimulates	stimulates
Epinephrine	inhibits	inhibits
Dopamine	inhibits	inhibits
Serotonin	stimulates	stimulates
Atrial Natriuretic Peptide	inhibits	inhibits
Urodilatin	inhibits	inhibits
Endothelin	inhibits	inhibits

**Table I.** Hormonal Effects on Sodium and Water Reabsorption in the CCD.

## **Chapter III**

### **RESEARCH DESIGN AND METHODS**

#### **3.1 Animals**

Young, pathogen-free Sprague-Dawley rats (50-100 g body weight) were obtained from the Oklahoma State University College of Osteopathic Medicine animal facility or purchased from Harlan Sprague-Dawley Inc. (Indianapolis, IN). Animals were housed in a separate room in the animal facility in plastic bins with adequate bedding, and maintained on standard rat chow and tap water ad libitum. Rats were kept on a 12 hour light and 12 hour dark cycle. Some of the rats were given a low sodium diet to allow for more pronounced electrophysiological responses due to increased levels of endogenous mineralocorticoids which increase sodium transport. Animal facilities were under the direction of full-time animal caretakers, and this project was approved by the Oklahoma State University College of Osteopathic Medicine Animal Use Committee. The College of Osteopathic Medicine complies with the NIH policy of animal welfare of the Animal Welfare Act and all other applicable laws.

All animals were killed by decapitation. Although the Panel on Euthanasia of the American Veterinary Medical Association recommends anesthesia before decapitation, it has been found that decapitation can be accomplished rapidly in these small rats with a minimum of excitement in comparison to the restraint and injection of anesthetics. In addition, many circulating hormones affect the transport characteristics of the collecting

duct, so excessive handling of the animals may alter plasma levels of adrenal corticoids, catecholamines, and vasopressin.

### 3.2 Isolation and Perfusion of Renal Tubules

After decapitation, both kidneys were removed and placed in cold dissecting solution containing 6% bovine albumin. The kidney capsules were removed and 4 or 5 cross-sectional slices were cut from each kidney and placed in a chilled ( $\sim 17^{\circ}\text{C}$ ) dissection solution in order to slow metabolic processes temporarily. A section of the cortical collecting duct (CCD) was then dissected from the renal slices and was identified by the presence of specific morphological and structural features [36, 342].

The isolated CCD was transferred to room-temperature bathing solution in a Lucite perfusion chamber on the stage of an inverted microscope. The tubule was mounted between concentric pipettes and suspended in the bathing solution (diagram 10).

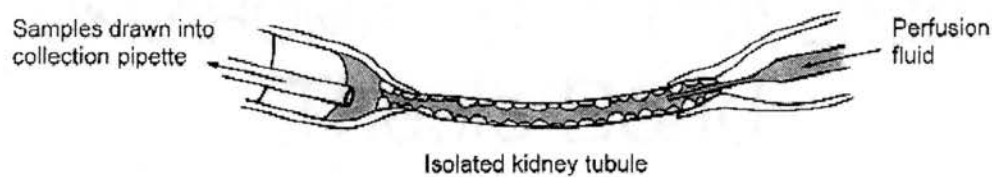


**Diagram 10.** Isolated Perfused Tubule Technique. A single cortical collecting duct is suspended from concentric pipettes in a bathing solution on an inverted microscope. A perfusion solution is moved through the tubule using air pressure. All solutions were maintained at  $37^{\circ}\text{C}$ .

On the perfusion side of the suspended tubule, an inner pipette was inserted into the tubular lumen and perfusion was initiated using air pressure. The other end of the tubule

was held in place by the tip of the collection pipette, which had been dipped in Sylgard (Dow-Corning, Midland, MI) to provide a seal so that the luminal perfusate was completely isolated from the bathing solution. The bathing solution flowed constantly from a temperature regulated reservoir so changes in the bathing solution could occur without a change in temperature.

### 3.3 Solutions

The compositions of the bath, perfusion, and dissecting solutions are shown in table II. Perfusion and bath solutions were bubbled with a 95% O<sub>2</sub>/5% CO<sub>2</sub> gas mixture for 30 minutes prior to use. All concentrations are in mM and the dissecting solution contained 6% bovine albumin to keep the tubule from sticking to the glass dissecting chamber and transfer pipette.

	<u>BATH</u>	<u>PERFUSION</u>	<u>DISSECTING</u>
NaCl	130	88	106
NaHCO <sub>3</sub>	25	-	25
KCl	5	5	5
Glucose	5	0.5	8.3
MgCl <sub>2</sub>	1	0.5	0.5
CaCl <sub>2</sub>	1.5	1.5	1.5
Phosphate Buffer	2	2.5	2
Na Acetate	5	5	5
Urea	-	-	1
pH	7.4	6.6	7.4
Osmolality (mOsm)	295	184	296

**Table II.** Composition of Solutions.

### 3.4 Osmotic Water Permeability (Flux) Experiments

#### 3.4.1 Determination of $P_f$

As noted above, the perfusate was made hypotonic to the bathing solution (184 vs 310 mOsm/Kg H<sub>2</sub>O) in the flux experiments in order to create an osmotic gradient across the epithelium. Dialized <sup>3</sup>H-methoxy inulin or <sup>14</sup>C-carboxyl inulin was added to the perfusate as a volume marker. Samples of perfusate were collected in a calibrated volumetric pipette and counted in a scintillation counter.

Perfusion rate ( $V_i$ ) was determined as

$$V_i = (V_o)^3 H_o / ^3 H_i$$

where <sup>3</sup>H<sub>o</sub> is the inulin concentration in the collection pipette and <sup>3</sup>H<sub>i</sub> is the inulin concentration in the perfusate.  $V_o$  is the rate of collection and was measured directly as the time to fill a calibrated constant volume pipette.

Hydraulic conductivity ( $L_p$ ) was determined as

$$L_p = V_i C_i / RTA [(C_i - C_o) / (C_i C_o C_b) + (1/C_b) 2 \ln ((C_o - C_b) C_i) / ((C_i - C_b) C_o)]$$

where  $C_i$ ,  $C_o$ , and  $C_b$  is the osmolality in mOsm/kg H<sub>2</sub>O for perfusate, collected fluid, and bath, respectively.  $R$  is the gas constant,  $T$  is the temperature in °K, and  $A$  is the tubular area in cm<sup>2</sup> calculated from the measured tubule length and internal diameter [343].

Osmotic water permeability ( $P_f$ ) was determined as

$$P_f = (L_p) RT / V_w \text{ where } V_w \text{ is the molar volume of water.}$$

In the CCD, the  $P_f$  in the absence of AVP is near zero as apical water channels are confined to intracellular vesicles [4, 8, 154]. Reif *et al* [142] report basal  $P_f$  values in the rat CCD in the absence of AVP to range from 20-30  $\mu\text{m}/\text{sec}$  and to increase to over 400  $\mu\text{m}/\text{sec}$  with AVP stimulation. Chen *et al* [144] report that 220 pM AVP increases  $P_f$  from 0 to  $981 \pm 120$   $\mu\text{m}/\text{sec}$  in isolated rat CCDs. Studies by Hawk *et al* [344] and Rouch *et al* [7, 8] found basal  $P_f$  to range from 0 to 35  $\mu\text{m}/\text{sec}$ , and to be increased with 220 pM AVP to a range of 602-835  $\mu\text{m}/\text{sec}$ .

### **3.4.2 Study Design for Flux Experiments**

Once a collecting duct was mounted and perfusion was initiated, the bathing solution was slowly warmed to 37°C and equilibrated for 20 minutes. The experiments consisted of this initial control period and two to four experimental periods. In each period, three individual samples were taken from the collection pipette after a 15-20 minute equilibration time and averaged for a single  $P_f$  value. Subsequent periods began with the addition or removal of an experimental agent to the bathing solution. Dexmedetomidine, an  $\alpha_2$  agonist that has been shown to inhibit AVP-stimulated permeability by more than 95%, and atipamezole, an  $\alpha_2$  antagonist that has been shown to reverse this inhibition were both used at 1  $\mu\text{M}$  [8]. The cAMP non-hydrolyzable analog 8-CPT-cAMP was used at 100  $\mu\text{M}$ . Oxymetazoline, WB4101, ARC239, agmatine, idazoxan, and rilmenidine were used in 1  $\mu\text{M}$  concentrations. Staurosporine, a PKC inhibitor, was used at 10 nM

and 100 nM and indomethacin, a prostaglandin synthesis inhibitor, was used at 5  $\mu\text{M}$  [8].

AVP was used at 220 pM [8] and PYY at 10 nM and 100 nM concentrations [345].

### 3.5 Electrophysiology Experiments

#### 3.5.1 Determination of $V_p$ , $R_p$ , $V_{bl}$ , and $fR_{ap}$

The isolated perfused tubule technique can also be used to measure the electrophysiological parameters across an epithelial layer as depicted in diagram 11.

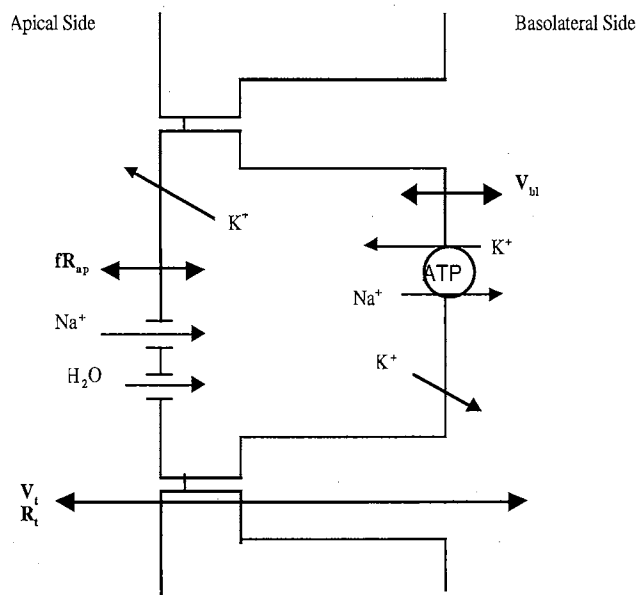


**Diagram 11.** Electrophysiological Measurements in the Principal Cell.  $V_t$  is the transepithelial voltage and is lumen negative,  $R_t$  is the transepithelial resistance,  $V_{bl}$  is the voltage across the basolateral membrane, and  $fR_{ap}$  is the fractional resistance of the apical membrane.

A Luigs-Neuman (Rattingen, FRG) in vitro perfusion system was used to provide electrical sealing on both sides of the suspended tubule (diagram 12). The perfusion

pipette was made from double-barrelled theta glass. Electric current from a stimulator (Grass S88) was sent through a silver wire inserted into one side of the pipette while the other side was used to measure transepithelial voltage ( $V_t$ ). The double barrel pipette also allowed for rapid changes in the luminal perfusate by changing pressure from one side to the other *via* a valve system.

### Electrophysiology in Kidney Tubule

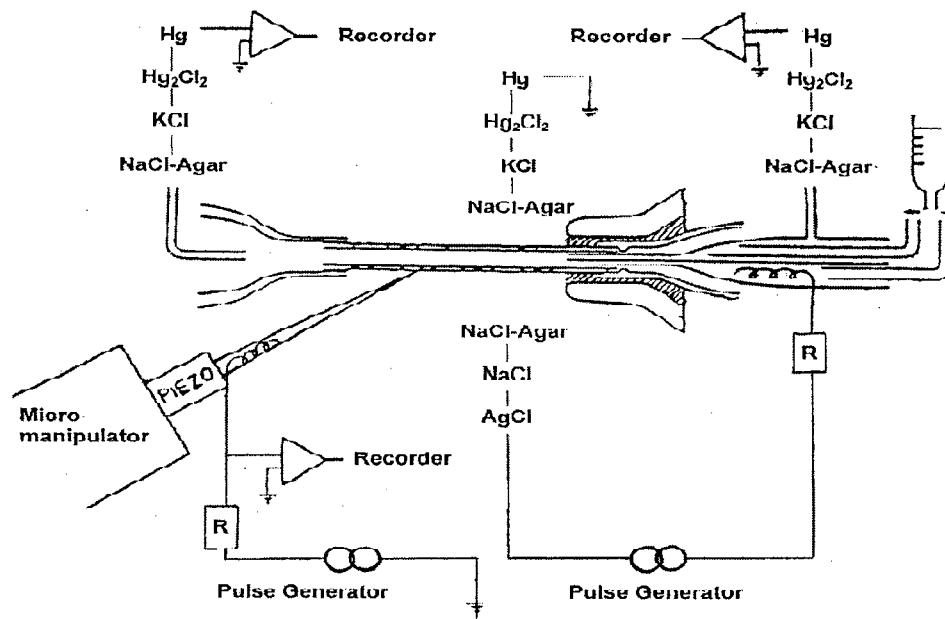


**Diagram 12.** Electrophysiology Experimental Setup. See text for explanation.

$V_t$  (mV) was continuously measured through the perfusion pipette which was connected to a high impedance electrometer (Keithley 614) by an agar bridge. Another agar bridge was inserted into the collection pipette to measure voltage at the other end of the tubule. Current pulses of 40-80 nA at 80 msec duration and a rate of 8 pulses/minute were injected, and voltage deflections at both ends of the tubule are measured.  $R_t$  was

calculated according to cable analysis for a terminated cable of length L [346]. The transepithelial length constant of the tubule,  $\lambda_t$ , is determined from the voltage deflections at the perfusion end ( $\Delta V_o$ ) and collection end ( $\Delta V_L$ ) of the tubule and is given by the following equation

$$L/\lambda = \cosh^{-1}(\Delta V_o/\Delta V_L)$$

Transepithelial resistance (in  $\Omega\cdot\text{cm}^2$ ) was determined by the equation

$$R_t = 2\sqrt{\pi\lambda_t^3 R_{in} R_i} \sqrt{\tanh(L/\lambda_t)}$$

where  $R_{in}$  is the input resistance measured in ohms ( $\Omega$ ) and  $R_i$  is the resistance of the perfusion solution (in  $\Omega\cdot\text{cm}$ ) measured using conductance meter (YSI).

Basolateral membrane voltage ( $V_{bl}$ ) (in mV) was measured by cell impalement. Single barrel microelectrodes made with a vertical pipette puller (Sutter P-30) were filled with 1M KCl, yielding resistances of 80-200 M $\Omega$ . The microelectrode was mounted on a motorized micromanipulator (Adams and List) and the basolateral membrane impaled using a piezoelectric driver (Fine Science Tools PM-10). The microelectrode was connected to one channel of the electrometer for intracellular voltage measurements.

The fractional resistance of the apical membrane ( $fR_{ap}$ ) was determined from the ratio of the voltage deflections across the apical membrane to that of the epithelia at the point of impalement and was calculated by the equation

$$fR_{ap} = R_a / (R_a + R_b) = \Delta V_a / \Delta V_b$$

where  $R_a$  and  $R_b$  are the apical and basolateral cell membrane resistances, respectively, of the impaled cell.

Basal sodium transport in the rat CCD in the absence of AVP is very low [2, 8, 11, 39, 347]. Schafer *et al* [172] found the basal value of  $V_t$  was  $-2.5 \pm 0.03$  mV and AVP hyperpolarized  $V_t$  to  $-19.3 \pm 3.2$  mV in isolated rat CCDs. Schlatter and Schafer [39] report the basal  $V_t$  to be  $-5.1 \pm 0.7$  mV and  $R_t$  to be  $51 \pm 4$   $\Omega \cdot \text{cm}^2$  in the rat CCD. In that study, 220 pM AVP hyperpolarized  $V_t$  to  $-16.1 \pm 1.4$  mV and decreased  $R_t$  to  $39 \pm 2$   $\Omega \cdot \text{cm}^2$ . In addition, data obtained from impaled principal cells show that AVP depolarizes the apical membrane from  $79 \pm 1$  to  $66 \pm 2$  mV and decreases  $fR_{ap}$  from  $0.76 \pm 0.04$  to  $0.70 \pm 0.04$ . Rouch *et al* [8] report control  $V_t$  to be  $0 \pm 0.03$  mV with AVP hyperpolarization bringing it down to  $-2.6 \pm 0.2$  mV, and control  $R_t$  values to be  $30 \pm 4$   $\Omega \cdot \text{cm}^2$  with AVP decreasing it to  $24 \pm 5$   $\Omega \cdot \text{cm}^2$ .

### ***3.5.2 Study Design for Electrophysiology Experiments***

Once a tubule was mounted on the concentric pipettes, the bathing solution was warmed to 37°C and equilibrated for 5 -10 minutes. After the control period, AVP was added to the bath to stimulate sodium transport. This hyperpolarized  $V_t$  and reduced  $R_t$ . Experimental periods began with the addition or removal of an agent to the bathing solution and a minimum of 5 minutes was allowed before proceeding to the next period.

A cellular impalement may have been obtained once  $V_t$  stabilized. A perfusion solution containing 10  $\mu\text{M}$  amiloride, a sodium channel blocker, was used to determine if the impaled cell was a principal cell. Amiloride completely hyperpolarizes the apical and basolateral membranes even in the presence of AVP, indicating that the only route of

sodium entry into the principal cells occurs *via* amiloride sensitive sodium conductance [39], and amiloride alters  $V_{bl}$  in principal cells. Intercalated cells do not contain sodium channels and therefore do not show this response. Impalements were considered successful if the following criteria were met: 1) voltage was reached rapidly upon impalement; 2) voltage remained stable for at least 5 minutes; 3) voltage returned to baseline when the electrode was removed from cell; 4) pipette tip resistance did not change over the course of the experiment.

### 3.6 Statistical Analysis

The experimental design of these studies allow for each renal tubule to serve as its own control with three or four subsequent treatment groups. These types of experiments are called repeated-measures designs. The total variability of this design can be broken down into three components: variability between subjects, variability between subject's responses, and variability due to the treatments. Repeated-measure designs are more powerful than ordinary designs because the variability between subjects can be isolated so the analysis can focus more precisely on the treatment effects. The recommended approach for analyzing this type of data is called the analysis of variance (ANOVA) [348-350].

The ANOVA is the multigroup generalization of the  $t$  test. Like the  $t$  test, ANOVA complies with the assumptions that the samples are randomly distributed with the same standard deviations. Unlike the  $t$  test, the ANOVA compares more than two groups and

answers the question of whether or not differences are due to random sampling variation. It also protects the researcher by first asking if there are any differences at all among the groups. If the ANOVA test is significant then the answer is yes, and the investigator can then make comparisons between groups or combinations of groups [349].

The F statistic is used to conduct an ANOVA, and is the ratio of population variance of means from different treatment groups to an estimate of population variance computed from the variance within each treatment group. Therefore, when F is a large number the conclusion is that at least one of the treatments had an effect. To answer further questions about which treatments had effects, multiple contrasts and comparisons can be made. In testing a contrast, the differences of interest are concentrated into a single degree of freedom producing a more powerful test. This allows a very specific hypothesis to be tested, such as “AVP will increase water reabsorption”, after the ANOVA has determined that a difference exists [348, 349].

Because the design of these experiments allow each individual collecting duct to act as its own control and also allows for influences of one experimental period upon another, the one-way ANOVA statistical test is appropriate [348] (Payton, M.E., personal communication). A minimum of four and a maximum of eight experiments were conducted in each protocol. Results obtained from the experimental periods were examined using ANOVA with repeated measures and significance was determined using contrasts between selected periods with the SuperANOVA™ (Abacus Concepts, Berkeley, CA) computer program with a level of significance set at  $P < 0.05$ . The type III sums of squares is designed to remove all the other effects in the model before testing

the effect in question. This is appropriate when the investigator wants to assess the effect of terms in the model when it is felt that each level of the factors in the experiment should have equal weight.

Results from all experiments are shown in graph form and reported as mean  $\pm$  SE (standard error of the mean). This technique of reporting SE is informative but misleading. When treatment effects are small and group variability is high, SE bars may overlap, leading to the impression that no significant difference exists. This is not necessarily true, however, and subsequent conclusions will often be faulty. This method does well in representing the relative variability of the data, but researchers should not try to draw inference to the equality of the means based on the SE bars, [351]. Raw data and statistical values are found in appendix D.

## Chapter IV

# SECOND MESSENGERS IN THE ALPHA 2-MEDIATED INHIBITION OF AVP- STIMULATED TRANSPORT IN THE CCD

### 4.1 Introduction

One of the major stimulators of sodium and water reabsorption in the CCD is arginine vasopressin (AVP), and this response is inhibited by alpha-2 ( $\alpha_2$ ) agonists. The mechanism of  $\alpha_2$ -mediated inhibition occurs through an inhibitory G protein ( $G_i$ ) coupled to adenylyl cyclase that blocks the formation of intracellular cAMP from ATP. Recent evidence has shown that  $\alpha_2$  agonists are capable of inhibiting AVP-stimulated sodium and water transport in the CCD in the presence of non-hydrolyzable cAMP analogs, suggesting an alternate signalling pathway [29]. Some of the main intracellular second messengers that have been indicated in the mechanism of  $\alpha_2$ -mediated inhibition of AVP-stimulated sodium and water transport include prostaglandins, PKC, and calcium. In the rabbit CCD, staurosporine inhibits the prostaglandin  $E_2$  ( $PGE_2$ )-induced reduction in  $P_f$  [306] and inhibits sodium transport *via* an increase in intracellular calcium concentrations [352]. In mouse distal tubule cells,  $\alpha_2$  receptors activate phospholipase C and increase PKC activity [353]. In the rat inner medullary collecting duct (IMCD),  $PGE_2$  inhibits  $P_f$  at a post-cAMP site linked to PKC activation [307]. Also in the rat IMCD, indomethacin, a known prostaglandin inhibitor, and staurosporine both reverse  $\alpha_2$ -mediated inhibition of AVP- and cAMP-stimulated  $P_f$  [30], but such studies have not yet been done in the rat

CCD. The purpose of the present study is to determine the effects of decreased extracellular calcium levels, decreased intracellular PKC levels, and decreased endogenous prostaglandin synthesis on the  $\alpha_2$ -mediated inhibition of AVP-stimulated  $P_f$ ,  $V_t$ , and  $R_t$  in the rat CCD. The hypothesis is that all three second messengers play a role in the  $\alpha_2$ -mediated mechanism.

## 4.2 Methods

After dissection, CCDs were mounted on concentric pipettes and a control period was initiated as described in section 3.2. Nine flux protocols were used, all having an initial control period and a second period where 220 pM AVP was added to the bath. Protocols are listed in table III.

Protocol	Period				
	1	2	3	4	5
1	Control	AVP	AVP	AVP	
2	Control	AVP	LC AVP	AVP	Control
3	Control	AVP	AVP+D	AVP+D+A	
4	Control	AVP	LC AVP+D	AVP	
5	Control	AVP	LC AVP+D+Q	AVP	
6	Control	AVP	AVP+D	AVP+D+I+S	AVP+D
7	Control	AVP	AVP+D	AVP+D+I	AVP+D
8	Control	AVP	AVP+D	AVP+D+S (10nM)	
9	Control	AVP	AVP+D	AVP+D+S (100nM)	

**Table III.** Protocols to Investigate Second Messengers.

AVP, arginine vasopressin; LC, 0.1  $\mu$ M calcium bath; D, dexmedetomidine; A, atipamezole; Q, quin-2AM; I, indomethacin; S, staurosporine.

Protocol 1 served as an AVP control experiment to determine the stability of the AVP response over three experimental periods. Protocol 2 was to determine if extracellular calcium is required for the AVP response, so a low calcium bath (0.1 mM  $\text{Ca}^{2+}$ ) was substituted for normal bath (1.5 mM  $\text{Ca}^{2+}$ ) in one period. This also allowed for comparisons between the control experiment and low calcium experiment. Protocol 3 was done to determine the effect of the  $\alpha_2$  agonist dexmedetomidine (1  $\mu\text{M}$ ) and  $\alpha_2$  antagonist atipamezole (1  $\mu\text{M}$ ) on AVP-stimulated water transport and served as an  $\alpha_2$  control experiment. Protocol 4 was to determine if extracellular calcium is necessary for the  $\alpha_2$  effect by investigating the effect of dexmedetomidine in a low calcium bath. This allowed for the comparison of protocols 3 and 4. Protocol 5 was done to determine if intracellular calcium is required for the  $\alpha_2$  effect by investigating the effect of dexmedetomidine in a low calcium bath in the presence of an intracellular calcium chelator (60  $\mu\text{M}$  Quin-2 AM).

Protocol 6 was undertaken to determine the combined effect of prostaglandin and PKC inhibition on the  $\alpha_2$  effect using the prostaglandin synthesis inhibitor indomethacin and the PKC inhibitor staurosporine. Indomethacin was used at 5  $\mu\text{M}$  because previous studies have shown this concentration to be effective in inhibiting prostaglandin effects in the rat IMCD [307, 354]. Staurosporine was used initially at 10 nM based on results from previous studies in the rat IMCD [307] and rat CCD [8]. Protocol 7 was done to determine if indomethacin has an effect by itself. Protocol 8 was undertaken to determine if staurosporine has an effect by itself and protocol 9 was done to determine if increasing

staurosporine concentration from 10 nM to 100 nM would cause an effect when low dose PKC inhibition did not.

Two additional sets of experiments were conducted using electrophysiology techniques described in section 3.5 as an indicator of epithelial sodium channel activity. These studies mimicked protocol 2 using a low calcium bath, and protocol 6 using the PKC and prostaglandin inhibitors as shown in Table III.

### 4.3 Source of Biochemicals

AVP, quin-2AM, 8CPTcAMP, indomethacin and staurosporine were purchased from Sigma Chemical Co. (St. Louis, MO). Dexmedetomidine and atipamezole were obtained from Orion Pharma (Turku, Finland) and <sup>3</sup>H-inulin was purchased from New England Nuclear (Boston, MA).

### 4.4 Results

In protocol 1, AVP significantly increased  $P_f$  and maintained it for three consecutive periods (figure 1A). In protocol 2, this AVP effect was not diminished by substituting the normal bath calcium concentration of 1.5  $\mu$ M with a bath containing only 0.1  $\mu$ M calcium (figure 1B). Figure 1C shows there is no difference in AVP response between groups in the normal bath and low calcium bath conditions. In protocol 3, dexmedetomidine inhibited AVP-stimulated  $P_f$  ( $p < .01$ ) and atipamezole reversed the inhibition ( $p < .05$ ) (figure 2A). In protocol 4, the low calcium bath (LC) did not impair

the ability of dexmedetomidine to inhibit AVP-stimulated  $P_f$  ( $p < .05$ ) (figure 2B). Figure 2C shows there is no significant difference in the effects of dexmedetomidine between normal and LC conditions. Of additional interest is the observation that there was no significant difference between the final periods which contained AVP, dexmedetomidine, and atipamezole in protocol 3 whereas protocol 4 contained only AVP (figure 2C). In the fifth protocol, the intracellular calcium chelator quin-2AM was used in conjunction with a LC bath, AVP, and dexmedetomidine. In this study, the CCD was in the presence of the chelator for 30 minutes. Results indicate that tubule damage occurred allowing water to leak into the tubule resulting in a negative  $P_f$  in the last two experimental periods (figure 2D).

In protocol 6, indomethacin and staurosporine were both present in the bathing solution. Dexmedetomidine inhibited AVP-stimulated  $P_f$  ( $p < .001$ ) and the addition of 5  $\mu\text{M}$  indomethacin and 1  $\mu\text{M}$  staurosporine resulted in a 53% reversal ( $p < .05$ ) (figure 3A). All experimental periods are different from the control period ( $p < .05$ ). The first and second AVP+Dex periods were not different from each other and the AVP period is not different from the fourth period in which both agents were in the bath. In protocol 7, the indomethacin alone study, dexmedetomidine inhibited AVP-stimulated  $P_f$  ( $p < .001$ ) with no reversal upon addition of indomethacin to the bath. There was a difference between the control period and the first AVP+Dex period ( $p < .05$ ), but no difference in the fourth period in which indomethacin was present or the final AVP+Dex period versus control (figure 3B). In protocol 8, with staurosporine at 10 nM, dexmedetomidine inhibited AVP-stimulated  $P_f$  ( $p < .001$ ) with no reversal upon addition of 10 nM staurosporine to

the bath (figure 3C). Finally, in protocol 9, staurosporine was used at 100 nM and reversed dexmedetomidine-induced inhibition ( $p < .05$ ) (figure 3D).

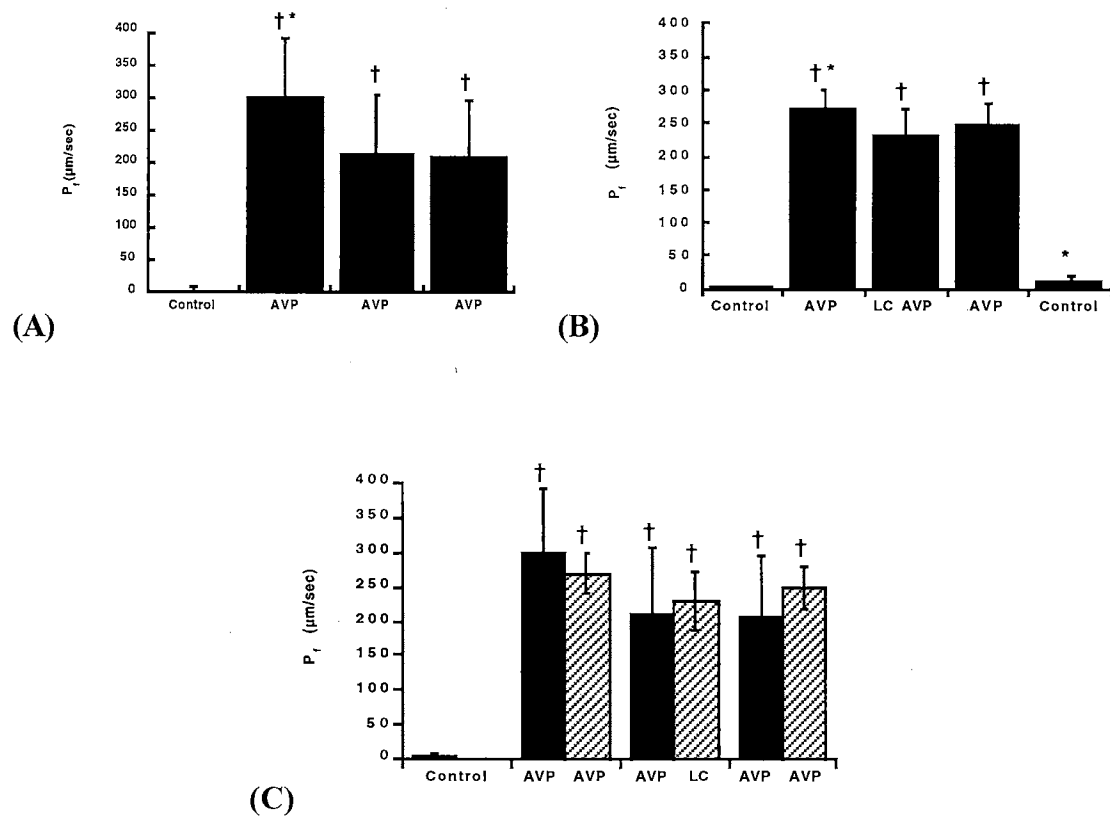


**Figure 1.** AVP-stimulated  $P_f$  under standard and low calcium conditions. **(A)** AVP time-control study. The sequence of experimental periods is shown on the horizontal axis. After the control period, 220 pM AVP was added to the bath and  $P_f$  increased significantly ( $p < .001$ ). There was an insignificant decrease in  $P_f$  in the second and third AVP periods.  $n=4$ . **(B)** Low calcium bath does not affect AVP-stimulated  $P_f$ . Switching from 1.5 mM concentration of calcium to 0.1 mM calcium had no effect on  $P_f$ .  $n=4$ . **(C)** Standard bath vs low calcium bath. Comparison between normal calcium (1.5 mM) and low calcium bath experiments shows no difference between groups in any period. Solid bars represent protocol 1 and hatched bars represent protocol 2.

AVP, arginine vasopressin; LC, 0.1 µM calcium bath.

† = different from control period. \* = different from previous period.

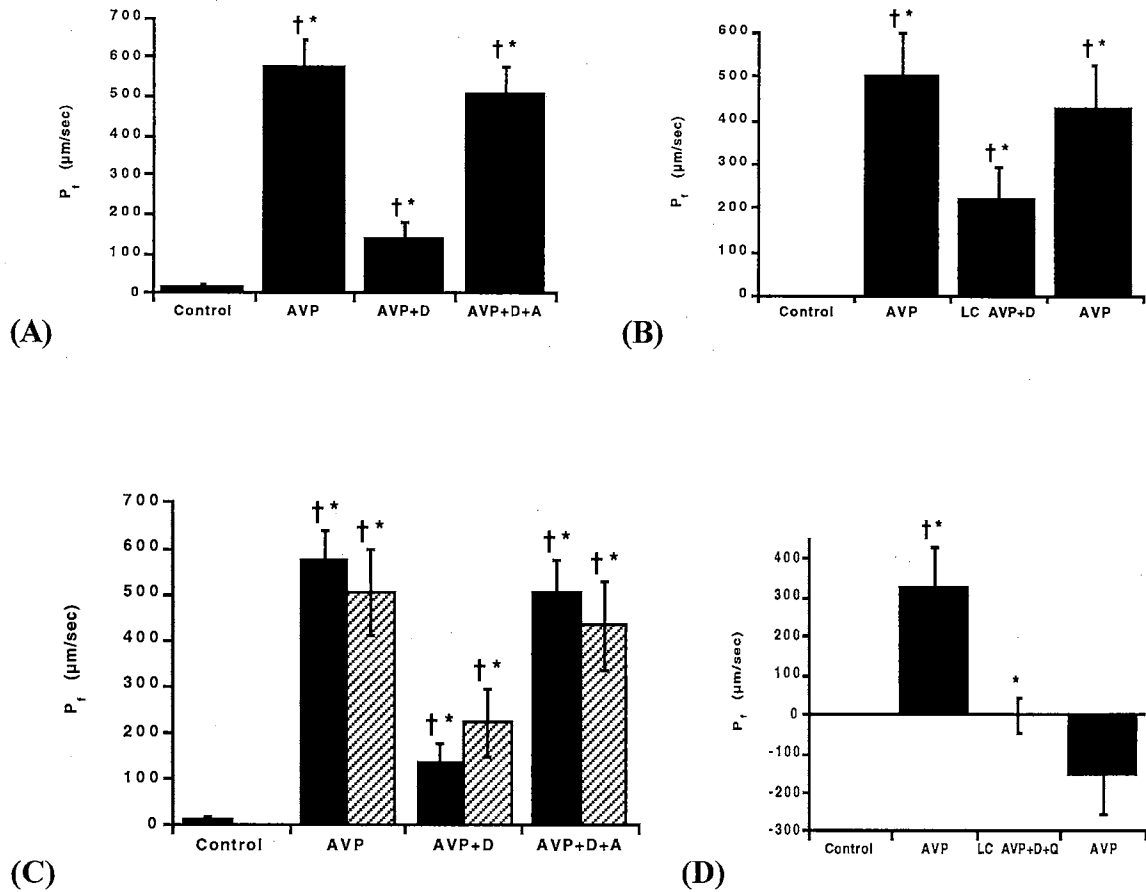


**Figure 2.** Dexmedetomidine-induced inhibition of  $P_f$  under standard and low calcium conditions. **(A)** Dexmedetomidine inhibits AVP-stimulated  $P_f$ . AVP-stimulated  $P_f$  is inhibited with dexmedetomidine ( $p < .01$ ) and this effect is reversed with atipamezole ( $p < .05$ ).  $n = 4$ . **(B)** Low calcium bath does not affect dexmedetomidine-induced inhibition of AVP-stimulated  $P_f$ . AVP stimulates  $P_f$  ( $p < .05$ ) and dexmedetomidine inhibits  $P_f$  ( $p < .01$ ).  $n = 5$ . **(C)** Standard bath vs low calcium bath. Comparison of two studies shows no difference between normal calcium (1.5 mM) and low calcium conditions in any period. Solid bars represent protocol 3 and hatched bars represent protocol 4. **(D)** Low calcium bath with Quin-2 AM. The combination of low calcium bath, calcium chelator, AVP, and dexmedetomidine resulted in a  $P_f$  less than control.  $P_f$  continued to decline after removal of chelator and dexmedetomidine and return to normal 1.5  $\mu\text{M}$  calcium bath indicating irreversible tissue damage.  $n = 3$ .

D, 1  $\mu\text{M}$  dexmedetomidine; A, 1  $\mu\text{M}$  atipamezole; Q= 65  $\mu\text{M}$ .

† = different from control period. \* = different from previous period.

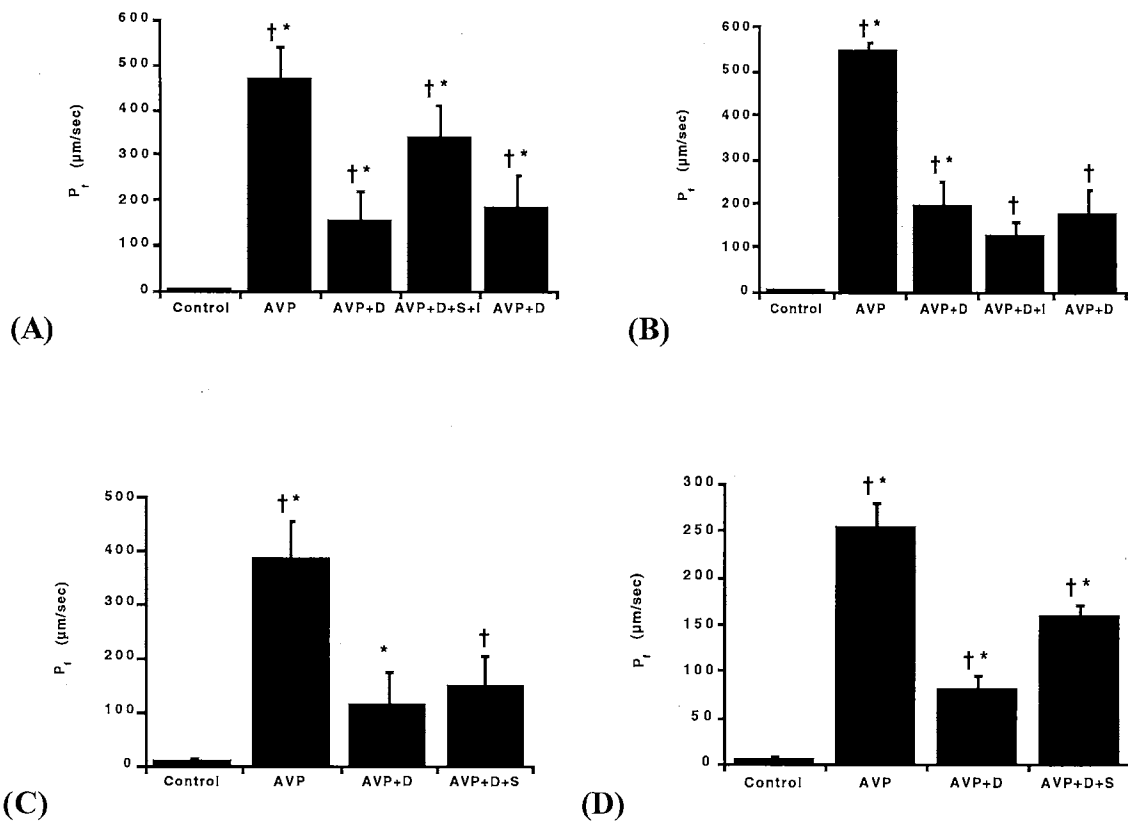


**Figure 3.** Effects of staurosporine and indomethacin. **(A)** Staurosporine and indomethacin reverse dexmedetomidine-induced inhibition of AVP-stimulated  $P_f$ . AVP increased  $P_f$  ( $p < .001$ ) and dexmedetomidine inhibited  $P_f$  ( $p < .05$ ). Addition of 5  $\mu\text{M}$  indomethacin and 10 nM staurosporine reversed the inhibition ( $p < .05$ ), and removal of these agents restored the inhibition ( $p < .05$ ).  $n=4$ . **(B)** Indomethacin does not affect  $P_f$ . Indomethacin at 5  $\mu\text{M}$  does not reverse dexmedetomidine-induced inhibition of AVP-stimulated  $P_f$ .  $n=4$ . **(C)** Low dose staurosporine does not affect  $P_f$ . Staurosporine at 10 nM does not reverse dexmedetomidine-induced inhibition of AVP-stimulated  $P_f$ .  $n=4$ . **(D)** High dose staurosporine reverses dexmedetomidine-induced inhibition of AVP-stimulated  $P_f$ . Dexmedetomidine inhibits AVP-stimulated  $P_f$  and this effect is reversed with 100 nM staurosporine ( $p < .05$ ).  $n=5$ . D, Dexmedetomidine; S, Staurosporine; I, Indomethacin.

$\dagger$  = different from control period. \* = different from previous period.

In the first electrophysiology experiment, AVP hyperpolarized transepithelial voltage ( $V_t$ ) and decreased transepithelial resistance ( $R_t$ ) indicating an increase in sodium reabsorption. The exchange of the 1.5 mM calcium-containing bath for the low calcium condition of 0.1 mM calcium did not significantly effect  $V_t$  or  $R_t$  (figures 4A and 4B). In the second electrophysiology study, AVP once again hyperpolarized  $V_t$  and decreased  $R_t$ . The addition of the dexmedetomidine depolarized  $V_t$  and increased  $R_t$  *via* its inhibitory action on AVP-stimulated transport. The addition of the PKC synthesis inhibitor indomethacin and the PG synthesis inhibitor staurosporine caused a slight reversal of dexmedetomidine's effects, but this was not significant (figures 5A and 5B).

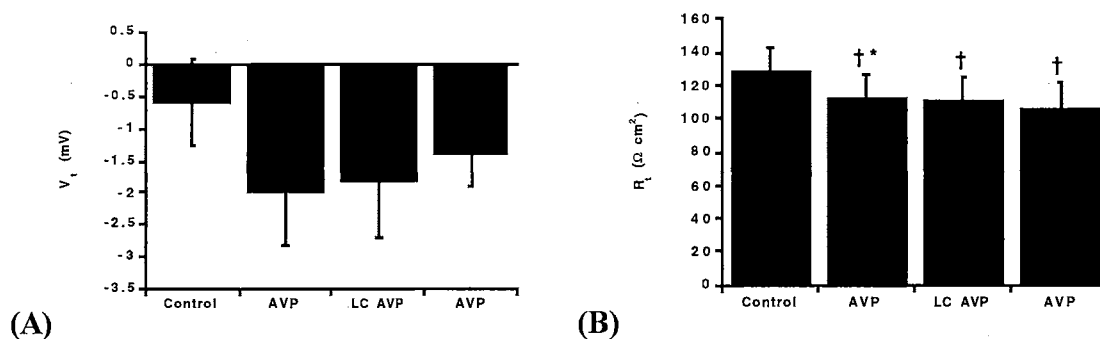


**Figure 4.** Electrophysiological effects of low calcium bath. **(A)** Low calcium bath does not affect  $V_t$ . AVP (220 pM) hyperpolarized  $V_t$  and switching to a low calcium bath had no significant effect. **(B)** Low calcium bath does not affect  $R_t$ . AVP decreased  $R_t$  ( $p < .05$ ) and the low calcium bath had no effect.  $n=5$ .

LC, 0.1  $\mu\text{M}$  calcium bath.

<sup>†</sup> = different from control period. \* = different from previous period.

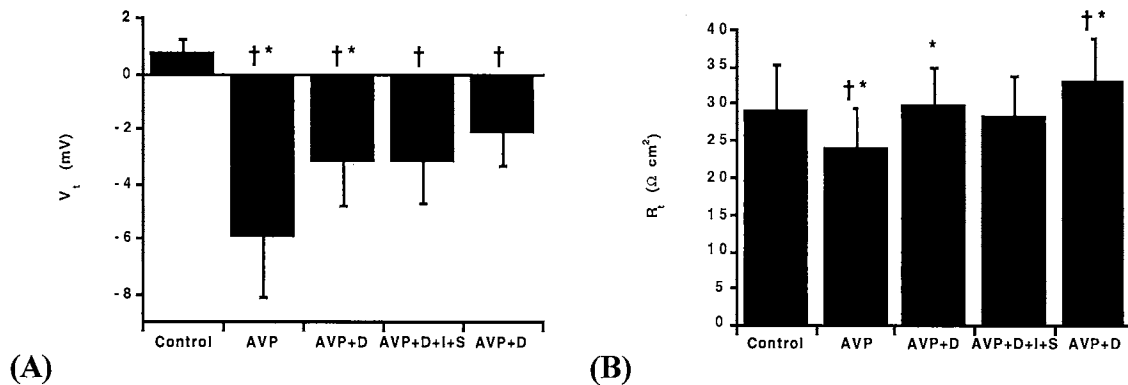


**Figure 5.** Electrophysiological effects of staurosporine and indomethacin. **(A)** AVP (220 pM) hyperpolarized  $V_t$  ( $p < .001$ ) and dexmedetomidine (1  $\mu$ M) depolarized  $V_t$  ( $p < .05$ ). There was no significant reversal of the dexmedetomidine effects seen with the addition of 5  $\mu$ M indomethacin and 10 nM staurosporine. **(B)** Staurosporine and indomethacin do not affect  $R_t$ . AVP decreased  $R_t$  ( $p < .05$ ) and dexmedetomidine increased  $R_t$  ( $p < .05$ ). There was no significant reversal of the dexmedetomidine effects seen with the addition of indomethacin and staurosporine, however there was a difference seen with the removal of the experimental agents ( $p < .05$ ).  $n=5$ . D, Dexmedetomidine; S, Staurosporine; I, Indomethacin. † = different from control period. \* = different from previous period.

A final flux protocol was added to the study in which indomethacin was added to the bath before staurosporine to determine if there is an order effect of these inhibitors. Results are shown in figure 6. Indomethacin alone had no effect on dexmedetomidine-induced inhibition of AVP-stimulated  $P_f$ , but the subsequent addition of staurosporine caused a significant ( $p < .05$ ) decrease that was not reversible (figure 6).

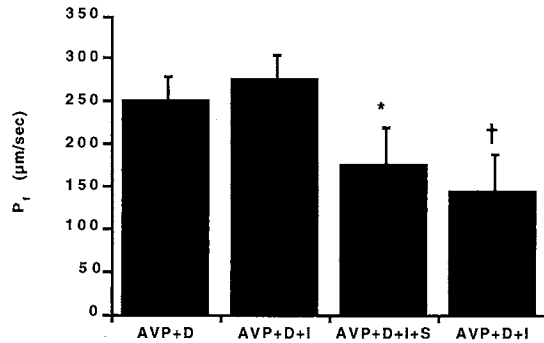


**Figure 6.** Effect of administration order of PG and PKC inhibitors on dexmedetomidine-induced inhibition of  $P_f$ . Indomethacin ( $5 \mu\text{M}$ ) had no significant effect on dexmedetomidine-induced inhibition, but addition of staurosporine decreased  $P_f$  ( $p < .05$ ). Removal of staurosporine from the bath had no effect.  $n=8$ .

D, Dexmedetomidine; S, Staurosporine; I, Indomethacin.

\* = different from previous period.

#### 4.5 Discussion

The activation of PKC, elevation of intracellular calcium, and prostaglandin synthesis are major signal transduction pathways generated by phospholipase C and phosphatidylinositol hydrolysis. The individual roles of each of these components and their complex interactions in regulating cell function is being extensively studied in different tissues. These intracellular messengers have also been shown to influence several signalling pathways and may be additive or antagonistic in their cellular response [355]. In the mammalian nephron, investigation of these pathways is of great interest because evidence

has linked them to the  $\alpha_2$ -mediated inhibitory action on sodium and water transport, particularly in the distal segments.

Ishikawa *et al* [356] showed that AVP increased intracellular free calcium concentration in rat papillary collecting tubule cultured cells, and this response was increased in the presence of a calcium-free medium. Other investigators have also demonstrated a coupling of the AVP response to intracellular and extracellular calcium levels [357, 358]. Other studies concluded that the increased cytosolic calcium occurs not by a direct inhibition of adenylyl cyclase *via* a  $G_i$  protein, but rather by AVP stimulation of PLC. PLC stimulation in turn activates PKC, which then inhibits cAMP formation in rat IMCD cells [341]. Similar results were obtained in the rabbit CCD [339, 359].

Studies in the isolated rat IMCD segments concluded that calcium increases in response to AVP are associated with the  $V_2$  receptor and are linked to adenylyl cyclase [338]. In contrast, studies in the isolated rat CCD have indicated the  $V_1$  receptor rather than the  $V_2$  receptor as mediating the intracellular calcium response [360]. In addition, calcium receptor proteins (CaRs) have now been reported in the rat IMCD [361]. These CaRs sense and respond to alterations in extracellular calcium concentrations and specifically reduce AVP-induced osmotic water permeability when luminal calcium rises. Purified IMCD endosomes have been shown to contain aquaporin-2 [54], CaRs, specific stimulatory and inhibitory GTP binding proteins previously reported to interact with CaRs [362], and isoforms of PKC [361]. Whether or not a CaR is located in the rat CCD is not yet known.

Dillingham *et al* [339] observed that a pronounced reduction in extracellular calcium concentration reduced the hydraulic conductivity ( $L_p$ ) response of isolated rabbit CCDs to AVP and cAMP, and the addition of calcium ionophore A23187 had a stimulatory effect. Jones *et al* [340] investigated the effects of varying extracellular and intracellular calcium concentrations on the development of the hydrosmotic response of rabbit CCDs to AVP or cAMP. In that study, the investigators found that the AVP response was enhanced by lowering the extracellular calcium concentration from 1.0 to 0.1 mM, but was not altered by increasing it. Exposing the tubules to the lower calcium bath with the addition of the calcium chelator quin 2-AM inhibited the AVP response by 68%. Interestingly, addition of the quin 2-AM after AVP enhanced the AVP response and addition of the calcium ionophore ionomycin decreased the AVP response. Those results are consistent with the view that transient changes in intracellular calcium levels are required for the development of the AVP response but that sustained increases inhibit the development and the maintenance of the AVP-induced hydrosmotic response. Although obtained under different experimental conditions and in a different species, these findings raise doubts about the specific role of intracellular and extracellular calcium concentrations in AVP-induced water permeability in the CCD.

With this in mind, the present study was undertaken to determine the effect of decreased calcium concentrations on the  $\alpha_2$ -mediated inhibition of AVP-stimulated water transport in the rat CCD. Results indicate that transient decreased extracellular calcium concentrations do not affect AVP-induced water permeability (figure 2B) as compared to an AVP time-control study (figures 2A and 2C). This is in contrast with previous work

in the rabbit CCD [340] and in the rat medullary collecting tubule [363] where removal of calcium from the bath resulted in an increased AVP response while an increase in calcium was inhibitory. The inhibitory effect of extracellular calcium may be due to calcium influx into the cytosol where it increases the activity of cAMP-phosphodiesterase, and thus cAMP breakdown, while decreased calcium has the opposite effect where calcium moves out of the cytosol and thus decreases the activity of the cAMP-phosphodiesterase [363]. This response is species specific however, because increased cytosolic calcium concentrations and PKC activation do not inhibit water transport in the CCD of the rat [364]. Since the interest in the present study lies not with what calcium does to the AVP response so much as what influence calcium has on the  $\alpha_2$ -mediated inhibition of the AVP response, the  $\alpha_2$  agonist dexmedetomidine was studied in the low calcium condition. Results indicate that dexmedetomidine is effective in inhibiting the AVP hydrosмотic response (figure 2D) and that a transient decrease in extracellular calcium does not limit the action of the  $\alpha_2$  agonist (figures 2E and 2F).

Gesek [353] showed that  $\alpha_2$  receptors activate PLC and increase PKC activity in cultured distal convoluted tubule cells. Nadler *et al* [307] report that PGE<sub>2</sub> reversibly inhibits AVP- and cAMP-stimulated P<sub>f</sub> in the isolated rat IMCD and that 10 nM staurosporine prevents this inhibition. Ando *et al* [365] demonstrated that PKC activators suppress AVP-induced water transport at a step distal to cAMP generation in the rabbit CCD. Hébert *et al* [306] report that PGE<sub>2</sub> inhibits AVP-induced water flow *via* PKC activation and Holt and Luchene [366] and Hébert *et al* [352] found that PGE<sub>2</sub>

inhibits sodium transport in the rabbit CCD. Rouch and Kudo [30] report that PKC and prostaglandins are involved in the  $\alpha_2$  mechanism, and that staurosporine and indomethacin-sensitive cellular mediators modulate  $P_f$  in the rat IMCD, but Rouch *et al* [364] also concluded that intracellular calcium concentrations and PKC activation do not inhibit sodium and water transport in the rat CCD. With those previous findings in mind, the goal of this part of the present study was to determine if intracellular prostaglandin production and PKC do indeed play a role in  $\alpha_2$ -mediated inhibition, and if the respective pathways are independent of each other in the rat CCD.

To test the involvement of prostaglandins and PKC, the cyclooxygenase inhibitor indomethacin was used at 5  $\mu$ M the PKC inhibitor staurosporine was used at 10 nM. When used together, these inhibitors reversed dexmedetomidine-induced inhibition of AVP-stimulated water permeability (figure 3A). In addition, the  $\alpha_2$  inhibition returned upon removal of indomethacin and staurosporine from the bathing solution, indicating that the effects are reversible. Since it was not known whether one of these agents or both were required to cause this effect, they were then examined separately. Indomethacin alone at 5 $\mu$ M and staurosporine alone at 10 nM failed to reverse dexmedetomidine's effects (figures 3B and 3C, respectively). Staurosporine at 100 nM was sufficient, however, to reverse the  $\alpha_2$ -mediated inhibition (figure 3D). These data suggest that PKC may be involved as part of a signalling pathway in the  $\alpha_2$ -mediated inhibition of AVP-induced  $P_f$  in the rat CCD. In the final flux protocol, addition of the inhibitors was separated, with indomethacin being added to the bath a period before staurosporine. The

purpose of that protocol was to determine if the order of administration had an effect on the final outcome. Results do not indicate an order effect (figure 6).

The application of electrophysiologic principles to the study of the collecting duct has been well studied and provide valuable information about sodium transport [5, 39, 42, 367, 368]. The application of cable analysis to isolated, perfused tubules allows for the measurement of transepithelial voltage and transepithelial resistance [346, 369]. In the rat CCD, AVP causes a sustained increase in sodium transport [2, 39, 142] thought to be the result of recruitment of epithelial sodium channels from cytoplasmic vesicles to the apical plasma membrane [45, 81, 146]. Increased sodium channel activity in the apical membrane depolarizes  $V_t$ , and decreases  $R_t$  [370].

The effect of increased intracellular calcium concentrations has been studied in the rabbit CCD where investigators found that it inhibits AVP-stimulated depolarization of  $V_t$  and decreases  $R_t$  [371, 372]. The view of that study is that increased intracellular calcium concentrations reduce sodium transport by inhibiting the rate of sodium entry across the apical membrane [372]. To date, no other electrophysiological studies in the rat CCD have been done to determine if low extracellular calcium concentrations would effect the AVP-mediated response. Results of the present study indicate that decreased extracellular calcium does not effect sodium transport initiated by AVP (figures 4A and 4B). Accordingly, results of the second electrophysiology study indicate that although there was an apparent reversal of the effects of dexmedetomidine with PKC and prostaglandin inhibition, the effect was statistically insignificant (figures 5A and 5B). The low n values as well as the high variability of these measurements make achieving

statistical significance difficult, and it is possible that an effect will be seen with further experiments.

## Chapter V

# EFFECT OF OXYMETAZOLINE, ARC-239, AND WB4101 ON SODIUM AND WATER TRANSPORT IN THE RAT CCD

### 5.1 Introduction

Arginine vasopressin (AVP) stimulates water and sodium transport in the collecting duct of the rat and this response is inhibited by alpha-2 ( $\alpha_2$ ) agonists. There are at least three subtypes of the  $\alpha_2$  adrenoceptor ( $\alpha_{2A}$ ,  $\alpha_{2B}$ , and  $\alpha_{2C}$ ), all of which are activated nonselectively by epinephrine and norepinephrine [233, 236-240]. One of these agonists is oxymetazoline, which has a binding preference for the  $\alpha_{2A}$  subtype [233, 237, 239, 373]. There are currently no subtype-selective agonists for the  $\alpha_{2B}$ , and  $\alpha_{2C}$  subtypes, but antagonists that are  $\alpha_2$  subtype-preferring are available. These include ARC-239, which has a high affinity for the  $\alpha_{2B}$  subtype [233, 237, 239, 373] and WB4101 which has a high affinity for the  $\alpha_{2C}$  subtype [239, 373]. The inhibitory mechanism of the  $\alpha_2$  agonists is attributed to the reduction of intracellular cAMP through activation of an inhibitory G protein. Other studies have shown however, that  $\alpha_2$  agonists inhibit water permeability even in the presence of nonhydrolyzable analogs of cAMP [29].

In order to characterize the response of the rat CCD to the  $\alpha_{2A}$  agonist oxymetazoline, flux experiments were performed to determine osmotic water permeability ( $P_f$ ) and electrophysiological experiments were performed to determine transepithelial

voltage ( $V_t$ ) and transepithelial resistance ( $R_t$ ) as an indicator of sodium transport. Electrophysiological experiments were conducted in controls, rats implanted with deoxycorticosterone (DOC) pellets, and rats fed a low salt diet. In the group fed a low salt diet, intracellular impalements were made to determine voltage across the basolateral membrane ( $V_{bl}$ ) and fractional resistance of the apical membrane ( $fR_{ap}$ ). Additional flux experiments were done using a nonhydrolyzable cAMP analog instead of AVP to stimulate transport in order to determine if cAMP is a required second messenger for the  $\alpha_2$ -mediated response.

The  $\alpha_{2B}$  antagonist ARC-239 and the  $\alpha_{2C}$  antagonist WB4101 were also tested in flux studies where dexmedetomidine was used as the  $\alpha_2$  non-selective agonist in order to inhibit AVP-stimulated water permeability.

## 5.2 Methods

After dissection, CCDs were mounted on concentric pipettes and a control period was initiated as described previously (see chapter 3). AVP (220 pM) or 8CPTcAMP (100  $\mu$ M) was used to stimulate  $P_f$  and either oxymetazoline (1  $\mu$ M) or dexmedetomidine (1  $\mu$ M) was used as the inhibitor. ARC-239 (1  $\mu$ M) and WB4101 (1  $\mu$ M) were used as  $\alpha_2$  antagonists. All agents were added to the bath and experiments were conducted at 37°C.

### 5.3 Source of Biochemicals

AVP, 8CPTcAMP, ARC-239, and WB4101 were purchased from Sigma Chemical Co. (St. Louis, MO). Dexmedetomidine and atipamezole were obtained from Orion Pharma (Turku, Finland) and  $^3\text{H}$ -inulin was purchased from New England Nuclear (Boston, MA).

### 5.4 Results

#### *5.4.1 Effect of Oxymetazoline on AVP- and cAMP-Stimulated $P_f$*

Figure 7 shows that 1  $\mu\text{M}$  oxymetazoline decreased AVP-stimulated  $P_f$  from  $768 \pm 80$  to  $194 \pm 35$   $\mu\text{m}/\text{sec}$  ( $p < .001$ ) constituting an inhibition of 71 %. Atipamezole at 1  $\mu\text{M}$  completely reversed the inhibition ( $p < .001$ ) (figure 7A). In another protocol, oxymetazoline was added after the control period and  $P_f$  increased slightly, but not significantly, indicating that oxymetazoline does not effect basal  $P_f$  in the absence of AVP.  $P_f$  increased dramatically upon addition of AVP and atipamezole from  $51 \pm 30$  to  $507 \pm 92$   $\mu\text{m}/\text{sec}$  ( $p < .001$ ) and was once again inhibited in the absence of atipamezole ( $p < .05$ ) (figure 7B). Figure 7C shows that the non-hydrolyzable cAMP analog 8CPT-cAMP increased  $P_f$  from  $6 \pm 3$  to  $435 \pm 77$   $\mu\text{m}/\text{sec}$  ( $p < .001$ ) and that oxymetazoline is unable to inhibit this (figure 7C).

#### 5.4.2 Effect of Oxymetazoline on $V_t$ , $R_t$ , $V_{bl}$ and $fR_a$

Figure 8A shows that in control animals, oxymetazoline depolarized the AVP-stimulated hyperpolarization in  $V_t$  from  $-8\pm 1$  to  $-7\pm 1$  mV ( $p < .01$ ) and the effect was completely reversible. Oxymetazoline also inhibited the AVP-induced reduction in  $R_t$ , increasing it from  $26\pm 9$  to  $29\pm 10$   $\Omega\cdot\text{cm}^2$  ( $p < .05$ ) (figure 8B). Figure 8C shows that oxymetazoline depolarized the AVP-stimulated hyperpolarization in  $V_t$  ( $p < .01$ ) in DOC-treated animals and the effect was again reversible. Oxymetazoline also inhibited the AVP-induced reduction in  $R_t$  in the DOC-treated group ( $p < .05$ ) (figure 8D). Figure 8E shows that in animals fed a low salt diet for 4 or more days, oxymetazoline depolarized the AVP-stimulated hyperpolarization in  $V_t$  ( $p < .01$ ) and inhibited the AVP-induced reduction in  $R_t$  ( $p < .05$ ) (figure 8F). Principal cell impalements made on CCDs from low salt diet animals show that oxymetazoline inhibits  $V_{bl}$  (figure 8G) and  $fR_{ap}$  (figure 8H).

Comparisons between the three groups (control, DOC-treated, low salt diet) in the electrophysiology studies shows that  $V_t$  was enhanced markedly in the DOC-treated and low salt diet groups (table IV). In the presence of AVP, there was a 38% increase in  $V_t$  in the control group (from  $-5.8\pm 0.6$  to  $-8.0\pm 1.0$  mV) and a 13% decrease with the addition of oxymetazoline (from  $-8.0\pm 1.0$  to  $-7.0\pm 1.0$  mV). In the DOC-treated and low salt groups, the increases in  $V_t$  with AVP were 77% and 91%, respectively (from  $-4.8\pm 0.9$  to  $-8.5\pm 1.5$  and  $-4.5\pm 1.3$  to  $-8.6\pm 1.9$  mV). With the addition of oxymetazoline,  $V_t$  decreased by 32% and 21%, respectively (from  $-8.5\pm 1.5$  to  $-5.8\pm 1.0$  and  $-8.6\pm 1.9$  to  $-6.8\pm 1.8$  mV). There was a 13% decrease in  $R_t$  in the control group in the presence of AVP (from  $40.9\pm 12.9$  to

35.6±12.5  $\Omega \text{ cm}^2$ ) and an 11% increase with the addition of oxymetazoline (from 35.6±12.5 to 39.5±11.7  $\Omega \cdot \text{cm}^2$ ). In the DOC-treated and low salt groups, the decreases in  $R_t$  with AVP were 12% and 25%, respectively (from 25.7±13.5 to 22.7±12.1 and 46.8±5.0 to 34.9±5.9  $\Omega \cdot \text{cm}^2$ ). With the addition of oxymetazoline,  $R_t$  increased by 13% and 24%, respectively (from 22.7±12.1 to 25.6±13.5 and 34.9±5.9 to 43.4±6.0  $\Omega \cdot \text{cm}^2$ ). In the low salt group,  $V_{bl}$  decreased and  $fR_{ap}$  increased with oxymetazoline and this effect was reversible. This data is summarized in table IV.

<b>Vt (mV)</b>	<b>Control</b>	<b>AVP</b>	<b>AVP+Oxy</b>	<b>AVP</b>
<b>Control Diet</b>	-5.8±0.6	-8.0±1.0*	-7.0±1.0*	-8.0±1.0* n=3
<b>Low Na Diet</b>	-4.5±1.3	-8.6±1.9*	-6.8±1.8*	-7.9±1.8 n=8
<b>DOC Pellet</b>	-4.8±0.9	-8.5±1.5*	-5.8±1.0*	-7.3±1.0* n=4

<b>Rt (<math>\Omega \cdot \text{cm}^2</math>)</b>	<b>Control</b>	<b>AVP</b>	<b>AVP+Oxy</b>	<b>AVP</b>
<b>Control Diet</b>	40.9±12.9	35.6±12.5*	39.5±11.7*	36.3±11.4 n=4
<b>Low Na Diet</b>	46.8±5.0	34.9±5.9*	43.4±6.0*	40.6±6.6 n=8
<b>DOC Pellet</b>	25.7±13.5	22.7±12.1*	25.6±13.5*	25.0±13.8 n=3

<b>Low Sodium</b>	<b>AVP</b>	<b>AVP+Oxy</b>	<b>AVP</b>
<b>Vbl (mV)</b>	-86.0±1.4	-87.9±1.4*	-86.6±0.9 n=4
<b>fRap</b>	.918±.020	.933±.017	.920±.020 n=4

**Table IV.** Electrophysiological Data for Oxymetazoline. Summary for control, DOC-treated, and rats fed a low sodium diet. See text for definitions.  
\* Different from previous period

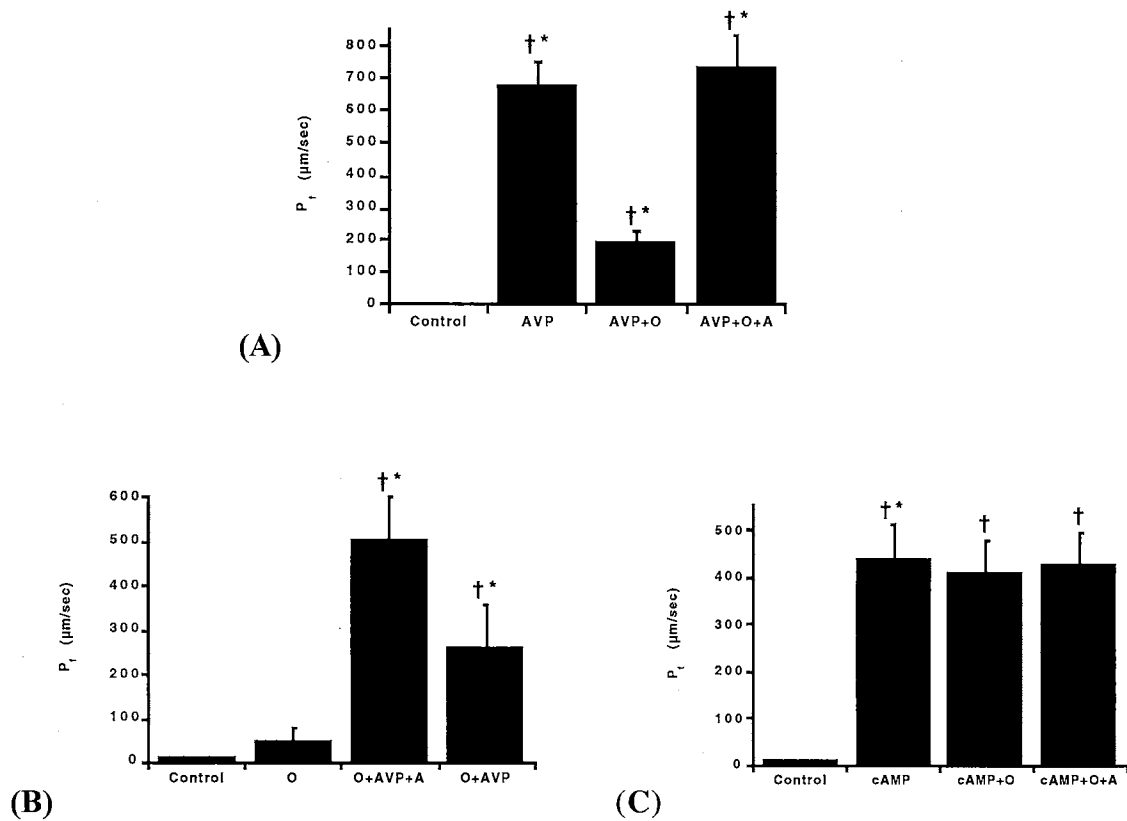


**Figure 7.** Effects of oxymetazoline on AVP- and cAMP-stimulated  $P_f$ . **(A)** Oxymetazoline inhibits AVP-stimulated  $P_f$ . AVP stimulates  $P_f$  ( $p < .001$ ) and oxymetazoline inhibits AVP-stimulated  $P_f$  ( $p < .001$ ). Atipamezole reverses oxymetazoline inhibition ( $p < .001$ ).  $n = 10$ . **(B)** Oxymetazoline does not effect basal  $P_f$ . Addition of AVP and atipamezole to the bath increases  $P_f$  ( $p < .001$ ) and removal of atipamezole reduces  $P_f$  ( $p < .05$ ).  $n = 4$ . **(C)** Oxymetazoline does not affect cAMP-stimulated  $P_f$ . cAMP stimulates  $P_f$  ( $p < .001$ ) and the addition of oxymetazoline and oxymetazoline + atipamezole have no effect.  $n = 5$ .

AVP, arginine vasopressin (220 pM); O, 1 µM Oxymetazoline; A, 1 µM Atipamezole; cAMP, 100 µM 8-(4-chlorophenylthio)-Cyclic Adenosine Monophosphate.

† = different from control period. \* = different from previous period.

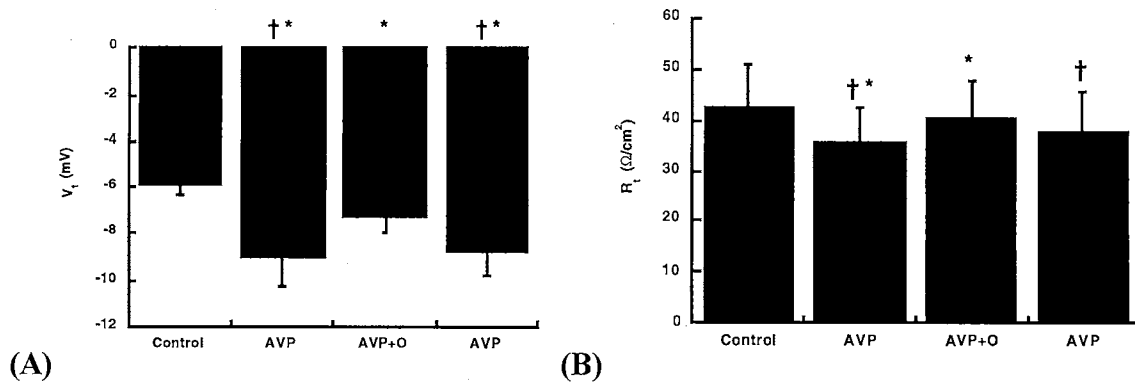


**Figure 8 (A and B).** Electrophysiological effects of oxymetazoline. **(A)** Oxymetazoline depolarizes  $V_t$  in control rats. AVP hyperpolarizes  $V_t$  ( $p < .001$ ) and addition of oxymetazoline to the bath depolarizes  $V_t$  ( $p < .05$ ). This effect is reversed with removal of oxymetazoline ( $p < .05$ ). **(B)** Oxymetazoline increases  $R_t$  in control rats. AVP reduces  $R_t$  ( $p < .05$ ) and addition of oxymetazoline to the bath increases  $R_t$  ( $p < .05$ ).  $n=4$ .  
 † = different from control period. \* = different from previous period.

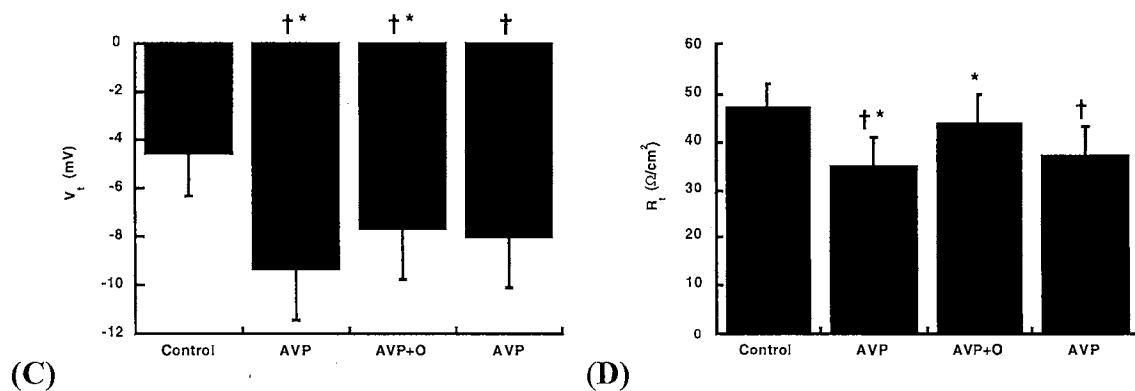


**Figure 8 (C and D).** Electrophysiological effects of oxymetazoline. **(C)** Oxymetazoline depolarizes  $V_t$  in low salt diet rats. AVP hyperpolarizes  $V_t$  ( $p < .001$ ) and addition of oxymetazoline to the bath depolarizes  $V_t$  ( $p < .01$ ). This effect is reversed with removal of oxymetazoline ( $p < .05$ ).  $n=6$ . **(D)** Oxymetazoline increases  $R_t$  in low salt diet rats. AVP reduces  $R_t$  ( $p < .05$ ) and addition of oxymetazoline to the bath increases  $R_t$  ( $p < .05$ ).  $n=8$ .  
 † = different from control period. \* = different from previous period.

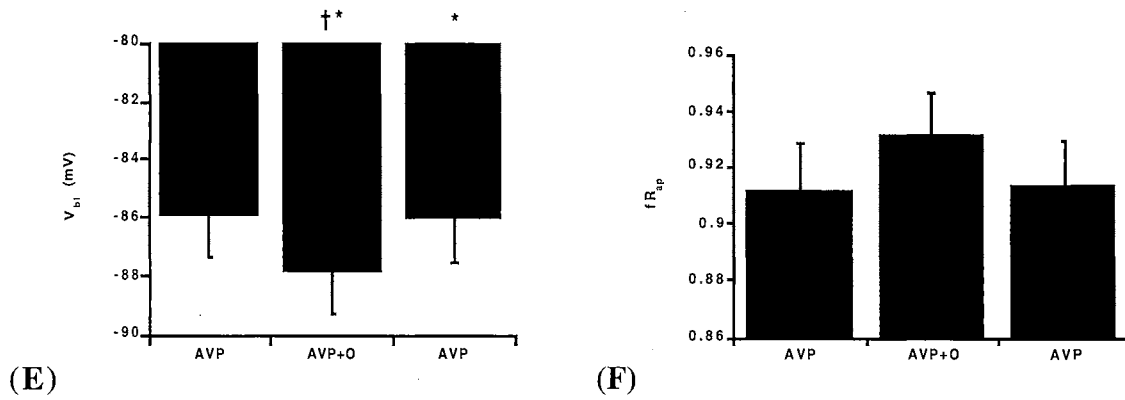


**Figure 8 (E and F).** Electrophysiological effects of oxymetazoline. **(E)** Oxymetazoline depolarizes  $V_{bl}$  in low salt diet rats. Addition of oxymetazoline to the bath depolarizes  $V_{bl}$  ( $p < .01$ ) and this effect is reversed with removal of oxymetazoline ( $p < .05$ ).  $n = 4$ . **(F)** Oxymetazoline increases  $fR_{ap}$  in low salt diet rats. Addition of oxymetazoline to the bath increases  $fR_{ap}$  and this effect is reversed with removal of oxymetazoline.  $n = 5$ .  
 † = different from initial AVP period. \* = different from previous period.

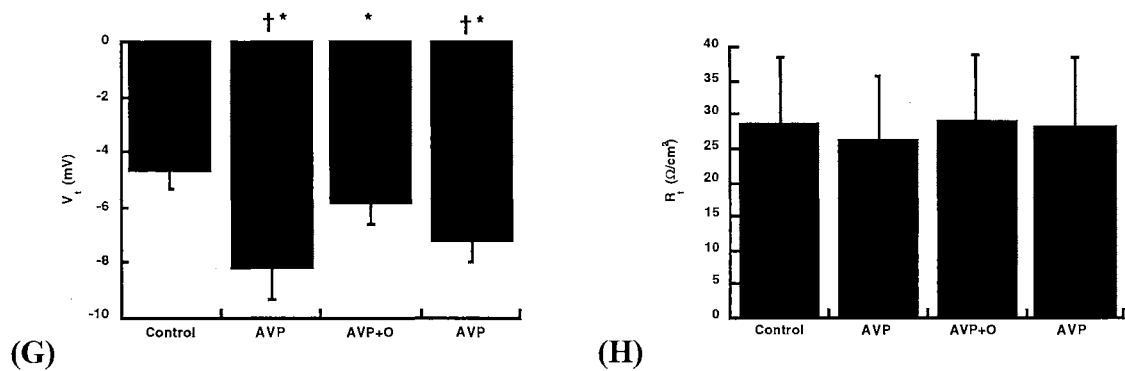


**Figure 8 (G and H).** Electrophysiological effects of oxymetazoline. **(G)** Oxymetazoline depolarizes  $V_t$  in DOC-treated rats. AVP hyperpolarizes  $V_t$  ( $p < .001$ ) and addition of oxymetazoline to the bath depolarizes  $V_t$  ( $p < .001$ ). This effect is reversed with removal of oxymetazoline ( $p < .05$ ).  $n = 5$ . **(H)** Oxymetazoline increases  $R_t$  in DOC-treated rats. AVP reduces  $R_t$  and addition of oxymetazoline to the bath increases  $R_t$ .  $n = 4$ .  
 † = different from control period. \* = different from previous period.

### 5.4.3 Effect of ARC-239 on AVP-stimulated $P_f$

Figure 9 shows the results of the ARC-239 study. Dexmedetomidine at 1  $\mu$ M inhibited AVP-stimulated  $P_f$  by 51% ( $p < .05$ ). ARC-239 reversed this inhibition by 39% ( $p < .05$ ) (figure 9A). In another set of experiments, the experimental periods were reversed and ARC-239 still significantly blocked dexmedetomidine-mediated inhibition by 50% ( $p < .05$ ) (figure 9B). In both studies, there was no significant difference between the AVP period and the AVP + D + ARC period.

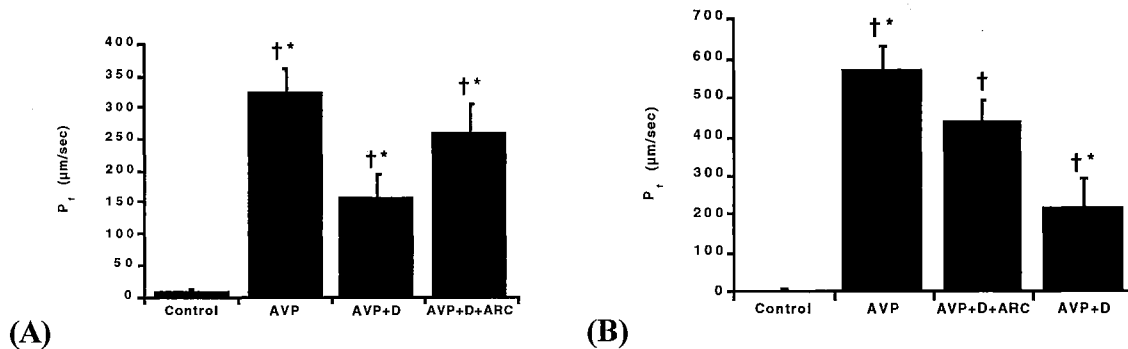


**Figure 9.** Effect of ARC-239 on dexmedetomidene-induced inhibition of  $P_f$ . (A) ARC-239 reverses dexmedetomidine-induced inhibition of  $P_f$ . After the control period, 220 pM AVP was added to the bath and  $P_f$  increased ( $p < .001$ ). Addition of 1  $\mu$ M dexmedetomidine inhibited  $P_f$  and 1  $\mu$ M ARC-239 reversed the inhibition.  $n=4$ . (B) Effects of ARC-239 are reversible.  $n=4$ .

AVP, arginine vasopressin; D, dexmedetomidine; ARC, ARC-239.

† = different from control period. \* = different from previous period.

#### 5.4.4 Effect of WB4101 on AVP-stimulated $P_f$

Figure 10 shows the results of the WB4101 study. Dexmedetomidine at 1  $\mu$ M inhibited AVP-stimulated  $P_f$  ( $p < .01$ ) and WB4101 reversed this inhibition by 66% ( $p < .01$ ) (figure 10A). In another set of experiments, the experimental periods were reversed and WB4101 still blocked dexmedetomidine-mediated inhibition by 65% ( $p < .01$ ) (figure 10B).

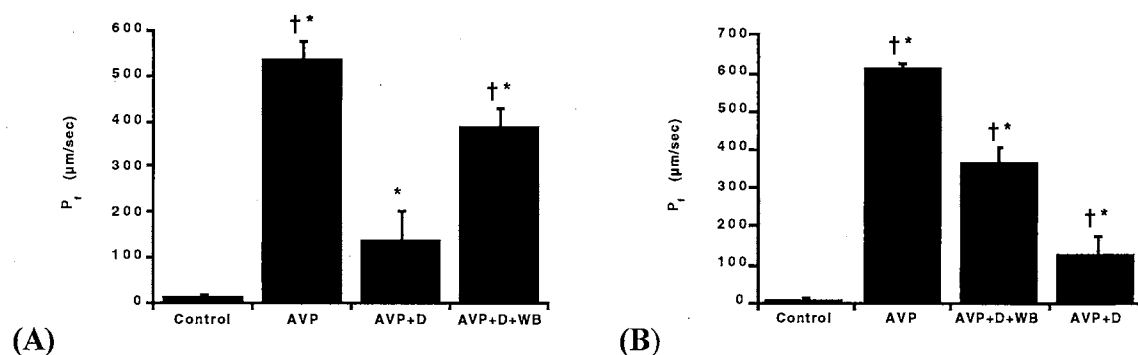


**Figure 10.** Effect of WB4101 on dexmedetomidene-induced inhibition of  $P_f$ . (A) WB4101 reverses dexmedetomidene-induced inhibition of  $P_f$ . After the control period, 220 pM AVP was added to the bath and  $P_f$  increased ( $p < .001$ ). Addition of 1  $\mu$ M dexmedetomidine inhibited  $P_f$  and 1  $\mu$ M WB4101 reversed the inhibition.  $n=5$ . (B) Effects of WB4101 are reversible.  $n=4$ .

AVP, Arginine vasopressin; D, Dexmedetomidine; WB, WB4101.

† = different from control period. \* = different from previous period.

## 5.5 Discussion

The major findings of this study are that the  $\alpha_{2A}$ -preferring agonist oxymetazoline inhibits AVP-stimulated  $P_f$  but not cAMP-stimulated  $P_f$ , and inhibits all of the measured

electrophysiological parameters. Overall these results suggest that oxymetazoline inhibits AVP-stimulated sodium and water reabsorption in the rat CCD *via* a cAMP-dependent mechanism. The finding that oxymetazoline alone did not affect  $P_f$  (figure 7B) supports previous studies indicating the requirement of AVP in the  $\alpha_2$  effect [8].

It is known that  $\alpha_2$  adrenergic receptors induce diuresis at two separate sites, one is AVP dependent while the other is non-AVP dependent [374, 375]. The AVP-dependent site occurs in the rat CCD and plays a critical role in the regulation of sodium and water balance [11, 47, 133, 141]. The effect of  $\alpha_2$  agonists on sodium and water transport in the CCD has been extensively studied. Studies by Krothapalli *et al* [19, 20] indicate that the adrenergic-induced inhibition of AVP-stimulated  $P_f$  in the rabbit CCD occurs *via* a pre-cAMP event related to adenylyl cyclase inhibition. In 1984, Chabardés *et al* [376] showed that the  $\alpha_2$  agonist clonidine reduces AVP-stimulated cellular cAMP increases in the rat CCD. Those findings were supported in 1985 by Umemura *et al* [160] who report that epinephrine inhibits AVP-stimulated cAMP accumulation in the rat CCD and IMCD and that the  $\alpha_2$  antagonist yohimbine reverses the effects, suggesting an  $\alpha_2$ -mediated mechanism. In 1991, Chen *et al* [6] showed that clonidine inhibited  $P_f$  and  $V_t$ , and in 1994 Rouch and Kudo [7] showed that the  $\alpha_2$  agonist dexmedetomidine inhibits  $P_f$ ,  $V_t$  and  $R_t$  in the rat CCD. These findings were further supported by Rouch *et al* [8] when it was shown that the  $\alpha_2$  antagonist atipamezole reverses those effects.

Evidence suggesting that a signal pathway other than cAMP may be involved in the  $\alpha_2$  mechanism stemmed from a study by Hawk *et al* [29] in which the transport

properties of CCDs from Sprague-Dawley, Dahl salt-sensitive and salt-resistant rats were studied. In these studies rats were treated with DOC, which increases sodium reabsorption *via* mineralocorticoid actions, and epinephrine was found to inhibit AVP-stimulated as well as cAMP-stimulated  $P_f$ . Therefore epinephrine inhibits both the cAMP-dependent flux produced by AVP and the cAMP-independent flux produced by DOC. They also showed that epinephrine inhibits  $P_f$  stimulated by the non-hydrolyzable cAMP analog 8-bromo-adenosine, indicating that this inhibition occurs even in the presence of constant levels of intracellular cAMP.

In the present study, the  $\alpha_{2A}$  agonist oxymetazoline was studied in the isolated perfused rat CCD. Oxymetazoline significantly inhibited AVP-stimulated  $P_f$  (figure 7A) but did not inhibit  $P_f$  stimulated by the non-hydrolyzable cAMP analog 8CPT-cAMP (figure 7C). 8CPT-cAMP was used in this study because it is resistant to the actions of phosphodiesterase and because Snyder *et al* [18] showed that this analog is a potent activator of protein kinase A in CCD cells and suggested that it be the cAMP analog of choice in functional studies of isolated perfused tubules.

The electrophysiological parameters of  $V_t$ ,  $R_t$ ,  $V_{bl}$ , and  $fR_{ap}$  are used as an indicator of sodium transport, and figure 8 (A through H) illustrates that oxymetazoline inhibits the AVP-stimulated effects and is consistent with  $\alpha_2$ -mediated inhibition of sodium reabsorption. Schafer and Troutman [40] showed that AVP increases sodium transport in the CCD by stimulating adenylyl cyclase and increasing cAMP levels. The increase in cAMP stimulates protein kinase A (PKA) and the subsequent phosphorylation of proteins leads to the insertion of sodium channels into the membrane from cytoplasmic

vesicles [146, 377]. In addition to AVP, aldosterone also increases sodium transport in the CCD, but this is thought to occur by a different mechanism. Aldosterone-stimulated sodium transport results from the opening of silent (cryptic) sodium channels already present in the membrane, protein synthesis of new sodium channels, and stimulation of the basolateral Na/K-ATPase [146, 148, 377]. Interestingly, oxymetazoline inhibited AVP-stimulated sodium transport even in DOC-treated rats and rats fed a low salt diet. Of further interest is the finding that while the DOC-treated and low salt diet rats had a more pronounced  $V_t$  response to both AVP and oxymetazoline (table IV), only the low salt group had an enhanced effect in  $R_t$ . In impaired principal cells,  $V_{bl}$  was hyperpolarized and  $fR_{ap}$  increased in the presence of oxymetazoline and these effects were reversed when oxymetazoline was removed from the bathing solution (Table III).

Wilborn *et al* [378] showed that the  $\alpha_{2A}$  adrenoceptor subtype is located in the cortical collecting duct of the rat, and concluded in 1998 [161] that the primary adrenoceptor involved in the regulation of sodium and water in the CCD is either an  $\alpha_{2A}$  or  $\alpha_{2B}$  based on isoform expression. Bylund *et al* [233] conducted an extensive study on the binding affinities of various drugs to  $\alpha_{2A}$  and  $\alpha_{2B}$  adrenergic receptor subtypes and determined that oxymetazoline binds with high affinity to the  $\alpha_{2A}$  subtype while ARC-239 binds with highest affinity to the  $\alpha_{2B}$  subtype. In 1991, Uhlén *et al* [237, 373] supported those findings with binding studies showing a  $K_d$  (in nM) for oxymetazoline of 13 at the  $\alpha_{2A}$  receptor whereas the  $K_d$  at the  $\alpha_{2B}$  receptor was 860 and the  $K_d$  was 120 at the  $\alpha_{2C}$  receptor, indicating a high selectivity of oxymetazoline for the  $\alpha_{2A}$  subtype. The

same set of studies also determined the  $K_d$  for ARC-239 to be 8.8 at the  $\alpha_{2B}$  receptor, and 760 and 46 at the  $\alpha_{2A}$  and  $\alpha_{2C}$  receptors respectively. WB4101 was found to have a  $K_d$  of 4.5 at the  $\alpha_{2C}$  receptor with  $K_d$ s of 140 and 26 at the  $\alpha_{2A}$  and  $\alpha_{2B}$  receptors respectively [373].

In summary, this study indicates that the  $\alpha_{2A}$  subtype-preferring agonist oxymetazoline has an effect in the rat CCD where it inhibits AVP-stimulated salt and water reabsorption. In addition, these findings indicate that the intracellular signalling pathway of oxymetazoline is indeed coupled to the inhibition of adenylyl cyclase and thus inhibition of cAMP accumulation within the principal cell. In the present studies, the inhibition afforded by dexmedetomidine was an average of 67% and the inhibition by oxymetazoline was 60% which is not significantly different. This is of interest because dexmedetomidine is non-selective for the  $\alpha_2$  subtype and has been shown to inhibit AVP-stimulated  $P_f$  by cAMP inhibition and some other mechanism such as PKC inhibition as shown in the previous chapter (Chapter IV). This study also shows an effect with the  $\alpha_{2B}$  and  $\alpha_{2C}$  subtype-preferring antagonists in the rat CCD. ARC-239 reversed dexmedetomidine-induced inhibition by 45% and WB4101 reversed it by 66%. The non-selective  $\alpha_2$  antagonist atipamezole reversed oxymetazoline-induced inhibition by 62%. This is of interest because all of the selected agents affected (inhibited or reversed inhibition)  $P_f$  by 60-67% except for ARC-239, which was less effective. It can not be suggested however, that ARC-239 is acting *via* a different receptor subtype than WB4101 or any other agents since all agents were used at the relatively high concentration

of 1  $\mu\text{M}$ . Further experiments, including dose response studies, will need to be carried out in order to determine if these subtypes are truly functional in this nephron segment.

## Chapter VI

### EFFECT OF AGMATINE ON WATER TRANSPORT

#### IN THE RAT CCD

##### 6.1 Introduction

Some of the biological effects previously thought to be mediated by  $\alpha_2$  agonists are now known to be due to stimulation of a novel class of receptors called imidazoline receptors (I receptors or IR) [21, 379, 380]. These I receptors have a high preference for compounds with the imidazoline moiety such as clonidine and idazoxan [21, 246]. There are two main types of I receptors,  $I_1$  and  $I_2$ . The  $I_1$  receptor has a higher affinity for clonidine and the  $I_2$  receptor has a higher affinity for idazoxan [246, 381]. Both subtypes have been shown that exist in the rat kidney [15, 16, 22, 382]. A number of differences have been demonstrated between  $\alpha_2$ -adrenergic receptors and I receptors in the rat kidney. Stimulation of either receptor leads to diuresis in the rat, but the increase after  $\alpha_2$ -adrenergic stimulation is secondary to free water clearance [383] whereas the increase after  $I_1$  stimulation is secondary to an increase in osmolar clearance [380] indicating that salt and water excretion may or may not be coupled in the rat CCD. Free water clearance is movement of water that is not dependent on sodium transport, and is characteristic of the collecting duct. In addition, the effects of  $\alpha_2$  stimulation are dependent on vasopressin while the effects of IR stimulation are not [380, 383]. Binding studies have

shown a 5-fold selectivity of idazoxan for  $I_2$  sites over  $\alpha_2$  sites ( $K_d = 10.6$  vs.  $55.4$  nM, respectively) [384].

The endogenous ligand for these IRs remained a mystery until 1984 when a substance of unknown structure was isolated from human brain that bound with high affinity to imidazoline sites [260]. This substance was capable of displacing clonidine, which binds to  $\alpha_2$  and I receptors and was thus called clonidine-displacing substance (CDS) [22]. In 1994, a CDS from bovine brain was isolated and its structure identified [261, 262]. It was determined to be a product of arginine metabolism and named agmatine.

Arginine is metabolized to agmatine in the presence of arginine decarboxylase (ADC) [261, 269, 385]. Recent studies in the kidney have shown measurable agmatine levels and ADC activity, as well as diamine oxidase activity, an enzyme that metabolizes agmatine [269, 385]. Agmatine has been reported to bind with high affinity to  $\alpha_2$ ,  $I_1$  and  $I_2$  receptors making it the first endogenous imidazoline receptor ligand of known structure [261, 262]. Further studies have found that agmatine displays preferential affinity for the  $I_1$  binding site [263-265]. In human platelets the affinity of agmatine for the  $I_1$  receptor subtype is 2200-fold greater than that of the  $I_2$  subtype, 1400-fold greater than that of the  $\alpha_{2A}$  adrenoceptors, 5000-fold greater than the  $\alpha_{2B}$  adrenoceptors, and 800-fold over the  $\alpha_{2C}$  adrenoceptors [264].

Much research is being conducted in order to determine the physiological roles of agmatine. It is a cation and has been shown to open up some ion channels by activation

of nicotinic acetylcholine receptors [271]. Agmatine may also have a role in insulin-glucose metabolism since it was shown to facilitate the release of insulin from pancreatic cells exposed to glucose [272]. Functional studies of agmatine in the kidney have shown that in rats, microperfusion of agmatine into renal interstitium and the urinary space of the surface glomeruli produces reversible increases in the single nephron filtration rate (SNFR) and absolute proximal reabsorption (APR). Yohimbine (an  $\alpha_2$  antagonist) produces the opposite effects and BU-224 (an  $I_2$  agonist) mimics agmatine's effects on SNFR but does not effect APR [269]. Further studies show that agmatine's effects on SNFR can be blocked with N-monomethyl-arginine (NMMA), a nitric oxide synthase (NOS) inhibitor, and incubation of glomeruli with agmatine produces significant increases in cGMP formation which are not blocked with yohimbine [386]. Thus it remains unclear whether agmatine acts by binding to  $\alpha_2$ -adrenoceptors, imidazoline receptors, or by a separate mechanism. The purpose of this study was to determine the effect of agmatine on AVP-stimulated  $P_f$  in the rat CCD. The hypothesis is that agmatine will inhibit  $P_f$  in a manner not linked to  $\alpha_2$  adrenergic receptors.

## 6.2 Methods

After dissection, CCDs were mounted on concentric pipettes and a control period was initiated as described previously (see chapter 3). In one set of experiments, AVP (220 pM) was used to stimulate  $P_f$ , dexmedetomidine (1  $\mu$ M) was used as the  $\alpha_2$  agonist, and idazoxan (1  $\mu$ M) was used as the antagonist. In the other studies, AVP (220 pM) or

8CPTcAMP (100  $\mu$ M) was used to stimulate  $P_f$ . In those experiments, agmatine, yohimbine, and idazoxan were all used at 1  $\mu$ M. All agents were added to the bath and experiments were conducted at 37°C. The experimental protocols are shown in table V.

Protocol	Period			
	1	2	3	4
1	Control	AVP	AVP+D	AVP+D+I
2	Control	AVP	AVP+Ag	AVP
3	Control	AVP	AVP+Ag	AVP+Ag+Y
4	Control	cAMP	cAMP+Ag	cAMP+Ag+I

**Table V.** Protocols to Investigate Agmatine.

AVP, Arginine Vasopressin; Ag, Agmatine; cAMP, 8CPT-cAMP; D, Dexmedetomidine; I, Idazoxan; Y, Yohimbine.

### 6.3 Source of Biochemicals

AVP and CPT-cAMP were purchased from Sigma Chemical Co. (St. Louis, MO). Idazoxan was purchased from Research Biochemicals International (Natick, MA). Agmatine sulfate was purchased from Tocris Cookson (Ballwin, MO). Yohimbine was kindly provided by Boehringer Ingelheim (Ridgefield, CT), and  $^3$ H-inulin was purchased from New England Nuclear (Boston, MA).

## 6.4 Results

Figure 11A shows the results of protocol 1 using idazoxan with the  $\alpha_2$  adrenergic agonist dexmedetomidine. Dexmedetomidine inhibited AVP-stimulated  $P_f$  ( $p < .001$ ) and this inhibition was reversed with idazoxan ( $p < .01$ ). This blockade of  $\alpha_2$  effects was partial, reaching approximately 50% of maximal AVP stimulation ( $508 \pm 48$  compared to  $252 \pm 48$   $\mu\text{m}/\text{sec}$ ). In protocol 2, AVP was used to stimulate  $P_f$  and agmatine inhibited this effect (figure 11B) ( $p < .05$ ). The removal of agmatine from the bath allowed  $P_f$  to increase again ( $p < .05$ ). In protocol 3, the  $\alpha_2$  antagonist yohimbine failed to reverse the agmatine-induced inhibition of AVP-stimulated  $P_f$  (figure 11C). In the fourth protocol,  $P_f$  was stimulated with 8CPT-cAMP and agmatine inhibited this effect ( $p < .05$ ). The  $I_2$  and  $\alpha_2$  antagonist idazoxan failed to reverse the effect (figure 11D).

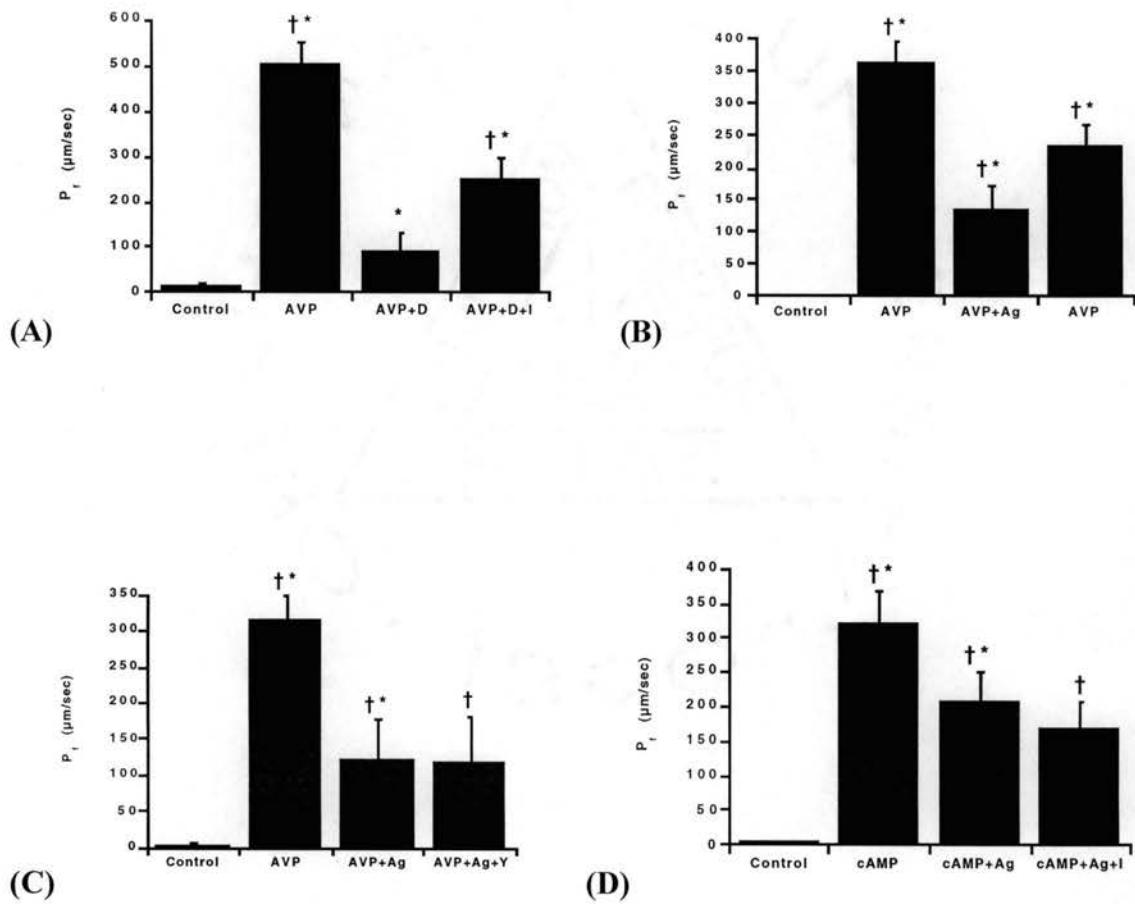


**Figure 11.** Effect of idazoxan and agmatine on  $P_f$ . **(A)** Idazoxan reverses dexmedetomidine-induced inhibition of  $P_f$ . After the control period, 220 pM AVP was added to the bath and  $P_f$  increased ( $p < .001$ ). Addition of 1 µM dexmedetomidine inhibited  $P_f$  ( $p < .001$ ) and 1 µM idazoxan reversed the inhibition ( $p < .05$ ).  $n = 7$ . **(B)** Agmatine inhibits AVP-stimulated  $P_f$ . Agmatine (1 µM) inhibits AVP-stimulated  $P_f$  ( $p < .05$ ) and the effect is reversible ( $p < .05$ ).  $n = 4$ . **(C)** Yohimbine does not reverse agmatine-induced inhibition of  $P_f$ . Agmatine inhibited AVP-stimulated  $P_f$  ( $p < .05$ ) and yohimbine had no effect.  $n = 4$ . **(D)** Agmatine inhibits cAMP-stimulated  $P_f$  and is not reversed with idazoxan. 100 µM cAMP stimulates  $P_f$  ( $p < .001$ ) and agmatine inhibits this effect ( $p < .05$ ). Idazoxan failed to reverse this inhibition.  $n = 6$ . AVP, Arginine vasopressin; D, Dexmedetomidine; I, Idazoxan; Ag, Agmatine; Y, Yohimbine.

† = different from control period. \* = different from previous period.

## 6.5 Discussion

One of the known effects of  $\alpha_2$  adrenergic agonists is their ability to lower blood pressure centrally [247, 248, 387]. This hypotensive effect is now accepted as being due to action on  $\alpha_2$  adrenergic receptors as well as nonadrenergic I receptors [387]. These I receptors are present in a range of mammalian tissues and are distinct from  $\alpha_2$  receptors in that they are insensitive to the catecholamines epinephrine and norepinephrine [264, 388]. The binding sites have been classified into two groups,  $I_1$  and  $I_2$  with the  $I_2$  subtype being preferential for idazoxan [270]. The  $I_2$  receptor has been suggested to play a role in protein activation in the brain, produce hyperalgesia in rats, and alter sodium uptake in rabbit kidney [384, 389, 390]. A number of studies indicate that  $I_2$  binding sites are associated with the monoamine oxidase system (MAO) enzymes [259, 391-394].

The substrate for the production of agmatine is arginine, which enters the cell by facilitated transport and is converted by the enzymatic action of ADC on the mitochondrial membrane [269] (see section 2.5.3 and diagram 7). Once synthesized, agmatine can bind to  $I_2$  receptors on the mitochondrion or to  $\alpha_2$  adrenergic, and possibly  $I_1$  receptors on the plasma membrane. It may also be released extracellularly since agmatine has been found in plasma. The synthesis of agmatine is thought to be regulated by feedback inhibition of ADC within the cell [270].

Although it was previously known to occur in plants, bacteria, and lower life forms, the discovery of ADC in rat brain indicates that the source of agmatine is endogenous since ADC is the enzyme involved in the rate-limiting step in agmatine biosynthesis. Of

additional interest is the localization of ADC to mitochondrial membranes since that is also the location of I<sub>2</sub> receptors [261]. Agmatine has been shown to be widely distributed in the body with its rank order of concentration being stomach > small intestine >> adrenal > heart > brain > plasma [262]. ADC activity has been identified in the renal cortex and medulla and diamine oxidase has been localized to the glomeruli [269], suggesting a functional role for agmatine in the kidney.

The purpose of this study was two-fold. First, to test the effect of idazoxan on  $\alpha_2$ -mediated inhibition of AVP-stimulated P<sub>f</sub> in the rat CCD. Second, to determine if agmatine would have an effect on AVP-stimulated P<sub>f</sub> in the rat CCD and if this effect was cAMP-mediated as well as whether or not it could be inhibited by  $\alpha_2$  or I<sub>2</sub> receptor antagonists. With the first protocol, we found that dexmedetomidine inhibited AVP-stimulated P<sub>f</sub> by 81.3% and idazoxan reversed the inhibition by 32% (figure 11A). Agmatine inhibited AVP-stimulated P<sub>f</sub> by 60% and inhibited cAMP-stimulated P<sub>f</sub> by 35%. Yohimbine reversed agmatine inhibition of AVP-stimulated P<sub>f</sub> by only 4%, which was not significant and idazoxan failed to reverse agmatine inhibition of cAMP-mediated P<sub>f</sub> (figures 11C and 11D, respectively). In summary, the key findings are that idazoxan can reverse  $\alpha_2$ -mediated inhibition and this may occur through  $\alpha_2$  receptor antagonism or at a separate I receptor site, and that agmatine partially inhibits AVP- and cAMP-stimulated P<sub>f</sub> through a site distinct from the  $\alpha_2$  and I<sub>2</sub> receptors. Agmatine may therefore represent a novel endogenous regulatory pathway for water reabsorption in the distal nephron.

The specific binding site for agmatine has not been identified, but Pinthong *et al* [395] found that while agmatine inhibits clonidine binding, it does not activate  $\alpha_2$  receptors or inhibit  $\alpha_2$ -mediated responses in several rat tissues studied. Conversely, Molderings *et al* [396] report that in the rat vena cava, agmatine is a positive modulator at an allosteric  $\alpha_2$  binding site and an antagonist at the ligand recognition site of  $\alpha_2$  adrenoceptors. In that study, agmatine increased clonidine affinity for  $\alpha_2$ -adrenoceptors by 7 fold. It should be noted, however, that agmatine concentrations as high as 100  $\mu\text{M}$  were required to initiate the effect. Interestingly, radioligand-labelled agmatine is not displaced by rauwolscine ( $\alpha_2$  antagonist), moxonidine ( $\alpha_2$  and  $\text{I}_1$  agonist), or cirazoline ( $\alpha_1$  and  $\text{I}_2$  agonist) supporting the role of another receptor for agmatine.

## Chapter VII

### EFFECT OF PEPTIDE YY ON AVP-STIMULATED SODIUM AND WATER

#### TRANSPORT IN THE RAT CCD

##### 7.1 Introduction

Peptide YY (PYY) is a member of the pancreatic polypeptide family and is released from the endocrine cells of the gut in response to food [273]. In humans, plasma levels of PYY increase postprandially and during diarrheal illness and cause a decrease in glomerular filtration rate (GFR), plasma renin activity, and aldosterone levels while increasing sodium excretion [13]. PYY shares 70% sequence homology with neuropeptide Y (NPY) and both bind with varied affinity to Y receptors (Y1 - Y5) which have been identified in brain, heart, gut, blood vessels, and kidney of several species [285].

PYY and NPY bind with equal affinities to both the Y1 and Y2 receptors and although most studies of PYY action have focused on the gastrointestinal system, Y1 and Y2 receptors have been demonstrated in the kidney and shown to reduce renal blood flow (RBF) and lead to diuresis and natriuresis in the rat [14] [32]. Evidence suggests that the decrease in RBF is mediated *via* the Y1 receptor whereas diuresis and natriuresis is mediated *via* the Y2 receptor [32]. Evidence also suggests that the Y2 receptor is coupled to a pertussis-toxin sensitive G protein and it has been proposed that NPY acts directly through an  $\alpha_2$ -adrenergic receptor in the rat CCD [26]. In the present studies, the specific Y2 receptor agonist PYY<sub>3-36</sub> was used to determine if the diuretic and natriuretic effects of

PYY are mediated by the Y2 receptor subtype in the rat CCD and yohimbine was used to determine if the effects are mediated by an alpha-2 mechanism.

## 7.2 Methods

After dissection, CCDs were mounted on concentric pipettes and a control period was initiated as described previously (see chapter 3). AVP (220 pM) was used to stimulate  $P_f$  and PYY<sub>3-36</sub> was used at 10 nM in one set of experiments and 100 nM in another set of experiments. All agents were added to the bath and experiments were conducted at 37°C. All rats were maintained on a low salt diet to maximize sodium transport.

## 7.3 Source of Biochemicals

AVP was purchased from Sigma Chemical Co. (St. Louis, MO). PYY<sub>3-36</sub> was purchased from Peninsula Laboratories (CA) and idazoxan was purchased from Research Biochemicals International (Natick, MA). Yohimbine was kindly provided by Boehringer Ingelheim (Ridgefield, CT), and <sup>3</sup>H-inulin was purchased from New England Nuclear (Boston, MA).

## 7.4 Results

### 7.4.1 Effect of PYY<sub>3-36</sub> on AVP-Stimulated P<sub>f</sub>

The data from the flux experiments show that in the rat CCD, P<sub>f</sub> is near zero during the control period. With the addition of 220 pM AVP, P<sub>f</sub> increases from 4±1 to 499±59 μm/sec in the first set of experiments, and the subsequent addition of PYY<sub>3-36</sub> at 10 nM reduced P<sub>f</sub> to 392±66 μm/sec which is not a significant effect (figure 12A). In the second set of experiments, AVP increased P<sub>f</sub> to 395±48 μm/sec and PYY<sub>3-36</sub> at 100 nM significantly reduced AVP-stimulated P<sub>f</sub> by 55.5% to 175±40 μm/sec (p<.05)(figure 12B). In the third study, the α<sub>2</sub> adrenergic antagonist yohimbine was used at 1 μM in the final experimental period. In those experiments, 100 nM PYY<sub>3-36</sub> reduced P<sub>f</sub> from 484±50 to 311±22 μm/sec and yohimbine not only failed to reverse the PYY-mediated inhibition of P<sub>f</sub>, but significantly reduced it further to 129±48 μm/sec (p<.05)(figure 12C).

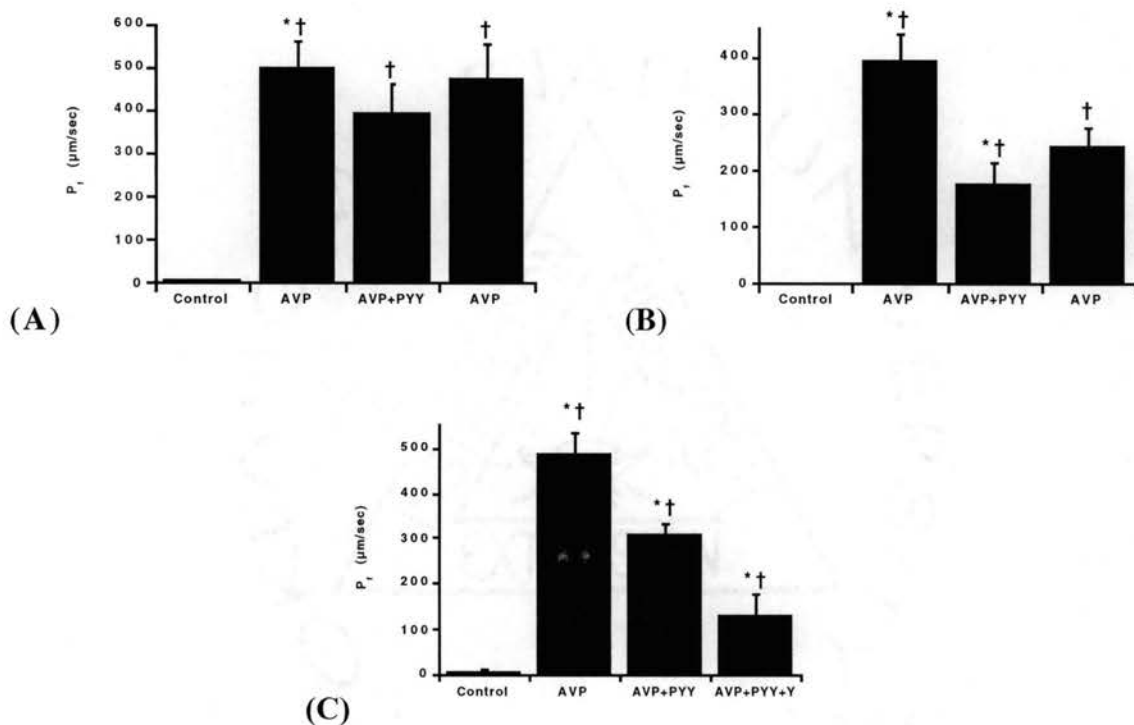


**Figure 12.** Effect of 10 nM PYY<sub>3-36</sub> on AVP-stimulated P<sub>f</sub>. **(A)** 10 nM PYY<sub>3-36</sub> does not affect AVP-stimulated P<sub>f</sub>. After the control period, 220 pM AVP was added to the bath and P<sub>f</sub> increased (p<.001). Addition of 10 nM PYY<sub>3-36</sub> failed to significantly inhibit the AVP response. n=4. **(B)** 100 nM PYY<sub>3-36</sub> inhibits AVP-stimulated P<sub>f</sub> (p<.001). n=5. **(C)** Effects of 100 nM PYY<sub>3-36</sub> are enhanced with 1 μM yohimbine. n=5. AVP, Arginine Vasopressin; PYY, PYY<sub>3-36</sub>; Y, Yohimbine. † = different from control period. \* = different from previous period.

#### 7.4.2 Effect of PYY<sub>3-36</sub> on V<sub>t</sub> and R<sub>t</sub>

In the electrophysiology experiments, the initial control period V<sub>t</sub> was -3.1±1.2 mV and this was hyperpolarized to -6.8±0.7 mV in the presence of AVP. V<sub>t</sub> was inhibited by 10 nM PYY<sub>3-36</sub> to -5.5±0.8 mV (p<.05) (figure 13A). This effect was reversed when PYY<sub>3-36</sub> was removed from the bathing solution and V<sub>t</sub> hyperpolarized again to -7.1±0.5

mV ( $p < .05$ ).  $V_t$  depolarized in the final control period to  $-5 \pm 1.0$  mV ( $p < .05$ ). The control  $R_t$  was  $167 \pm 32 \Omega \cdot \text{cm}^2$  and was reduced with AVP to  $130 \pm 20 \Omega \cdot \text{cm}^2$  ( $p < .05$ ). PYY<sub>3-36</sub> increased  $R_t$  to  $142 \pm 19 \Omega \cdot \text{cm}^2$  although this was not statistically significant. Removal of PYY<sub>3-36</sub> from the bath decreased  $R_t$  to  $133 \pm 18 \Omega \cdot \text{cm}^2$  and returning to control conditions increased  $R_t$  to  $142 \pm 19 \Omega \cdot \text{cm}^2$  (figure 13B).

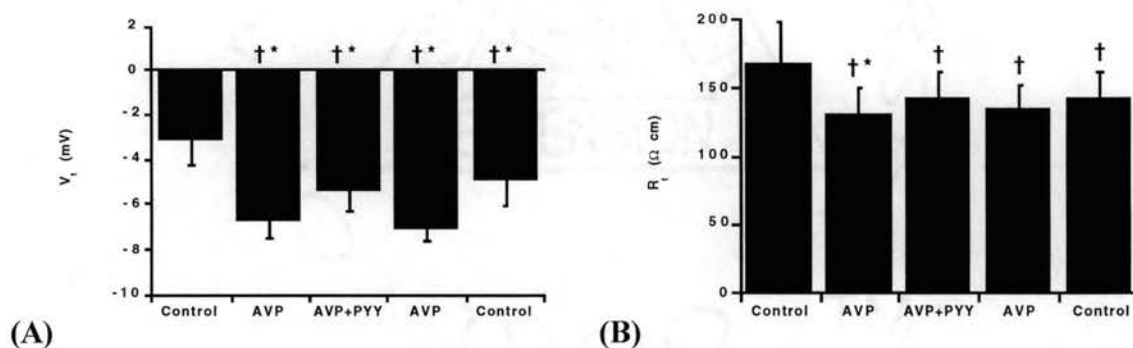


**Figure 13.** Electrophysiological effects of PYY<sub>3-36</sub>. **(A)** PYY<sub>3-36</sub> depolarizes  $V_t$ . After the control period, 220 pM AVP was added to the bath and  $V_t$  hyperpolarized ( $p < .001$ ). Addition of PYY<sub>3-36</sub> resulted in a depolarization ( $p < .05$ ) that was reversible ( $p < .05$ ). **(B)** PYY<sub>3-36</sub> increases  $R_t$ . PYY<sub>3-36</sub> reversed the decrease in  $R_t$  initiated by AVP, but this was not statistically significant.  $n=8$ .

† = different from control period. \* = different from previous period.

## 7.5 Discussion

The goal of this study was to determine if PYY acting through the  $Y_2$  receptor would affect AVP-stimulated sodium and water permeability in the rat CCD. All Y receptor subtypes belong to the family of G protein-coupled receptors [275, 284]. They preferentially act through  $G_o$  or  $G_i$  and are therefore coupled to the inhibition of adenylyl cyclase [275]. Although other signalling pathways have been indicated, such as the mobilization of calcium secondary to  $IP_3$  production [397], renal  $Y_2$  receptors are believed to be negatively coupled to the cAMP pathway in the manner of  $\alpha_2$  adrenergic receptors [278, 284, 290]. At the protein level, studies have identified Y receptor sites in rabbit kidney and identified them as predominantly of the  $Y_2$  subtype [290, 398, 399]. Few Y receptors have been detected in rat kidney by molecular biology techniques [14, 400], but this may be due to rapid radioligand degradation by endopeptidase-2 [401]. Functional experiments in isolated proximal tubules and isolated whole kidney however, have demonstrated that rat kidney does express Y receptors [33, 277].

Wahlestedt *et al* [402] determined that  $Y_1$  receptors require the intact PYY or NPY molecule for binding while the  $Y_2$  receptor requires only the carboxyl terminal fragment of either peptide for binding. Competitive binding experiments have shown differences between rabbit and rat Y receptor subtypes [13]. NPY competed effectively with radioactive PYY ( $^{125}I$ -PYY) in both species, but the  $Y_2$  and  $Y_4$  agonists had no effect in the rat, and the  $Y_1$  agonist had no effect in the rabbit [13]. On the other hand, Sheikh *et al* [399] demonstrated that rabbit proximal tubule PYY receptors are of the  $Y_2$  subtype, and

Ohtomo *et al* [277] found the rat proximal tubule NPY receptors also to be of the  $Y_2$  subtype.

Previous studies show a  $K_d$  value for PYY in the rat papilla of 0.7 nM which is only 25 times the fasting concentration in rat plasma (28 pM) [403] and is consistent with receptor activation after postprandial increases of PYY. This  $K_d$  agrees with the value from binding studies of PYY in intestinal crypt cells [404], and thus supports a physiological role for PYY on renal receptors. There are two possible explanations for why PYY<sub>3-36</sub> at a concentration of 10 nM did not have an appreciable effect on water transport in the flux studies. First, it has been noted that PYY binds strongly to glass and the flux and electrophysiology experiments utilize solution reservoirs made of glass as well as glass pipettes suspending the tubules. It is therefore possible that the PYY<sub>3-36</sub> concentration delivered to the tubule was much less than the original 10 nM. Second, it has been shown that the closely related peptide, NPY, is more effective *in vivo* than *in vitro* [276]. This may be due to the presence of tonic adrenergic and/or other stimuli *in vivo*, and the absence of such stimuli *in vitro*. Increasing the PYY<sub>3-36</sub> concentration to 100 nM did have a significant effect on the isolated rat CCD, however the exact delivered concentration was not determined.

Infusion of PYY or NPY causes a reduction in renal blood flow [31] and thus it could be expected that PYY would inhibit sodium and water excretion. Studies in anaesthetized rats however, have reported an increase in urine flow after NPY administration [25, 31]. Diuresis has also been reported in humans after administration of PYY doses corresponding to physiological postprandial plasma levels [405]. Studies by Blaze *et al*

[13] and Bischoff *et al* [31] concluded that physiologic doses of NPY and PYY are natriuretic. This supports the present studies which demonstrate that PYY<sub>3-36</sub> is capable of hyperpolarizing transepithelial voltage and increasing transepithelial resistance in the principal cell (figures 13A and 13B) although the effects on  $R_t$  were not statistically significant. This  $V_t$  data is in accordance with the flux data presented in the current study showing that AVP-induced water permeability is inhibited with PYY<sub>3-36</sub> (figure 12B).

In renal vasculature, PYY and NPY have been shown to potentiate the vasoconstricting effects of other drugs [275, 276, 282, 406, 407]. Indeed, NPY has been shown to be stored and released with norepinephrine from sympathetic nerves [274]. Pernow and Lundberg [282] found that NPY and  $\alpha_2$  agonists inhibit norepinephrine release in parallel, and the  $\alpha_2$  antagonist yohimbine enhances NPY and norepinephrine release, indicating an  $\alpha_2$ -mediated inhibition of release in pig sympathetic neurons. Interestingly, the present study indicated that yohimbine enhanced PYY-mediated inhibition of AVP-stimulated  $P_f$  (figure 12C). This is in contrast the study by Dillingham and Anderson [26] in which the authors concluded that NPY actions occur *via* an  $\alpha_2$  receptor in the rat CCD. In addition, Harfstrand and Fuxe [408] report that the hypotensive effect of NPY is enhanced after central blockade of the  $\alpha_2$ -adrenoceptor using idazoxan in rat brain. Although the relationship between  $\alpha_2$ -adrenergic receptors and Y receptors is still unclear, receptor interaction may exist at the coupling unit and/or at the recognition site proteins. In conclusion, the present study shows that PYY inhibits

AVP-stimulated water and salt transport through the  $Y_2$  receptor subtype in a manner that may be influenced by  $\alpha_2$  adrenergic receptors in the rat CCD.

## Chapter VIII

### SUMMARY AND CONCLUSIONS

The data obtained in these studies leads to the following conclusions concerning sodium and water transport in the isolated, perfused rat CCD:

1. Decreased extracellular and luminal calcium concentrations do not affect AVP-stimulated  $P_f$ ,  $V_t$ , or  $R_t$ , or  $\alpha_2$ -mediated inhibition of AVP-stimulated  $P_f$ .
2. PKC inhibition reverses  $\alpha_2$ -mediated inhibition of AVP-stimulated  $P_f$ .
3. The  $\alpha_{2A}$ -preferring agonist oxymetazoline inhibits AVP- but not cAMP-stimulated  $P_f$ , depolarizes  $V_t$ , and increases  $R_t$  in rats fed normal or low salt diets, and in rats treated with DOC.
4. The  $\alpha_{2B}$ -preferring antagonist ARC-239 reverses  $\alpha_2$ -mediated inhibition of AVP-stimulated  $P_f$ .
5. The  $\alpha_{2C}$ -preferring antagonist WB4101 reverses  $\alpha_2$ -mediated inhibition of AVP-stimulated  $P_f$ .
6. The  $\alpha_2$ - and  $I_2$ -preferring antagonist idazoxan reverses  $\alpha_2$ -mediated inhibition of AVP-stimulated  $P_f$ .
7. Agmatine, the putative endogenous imidazoline ligand, inhibits AVP- and cAMP-stimulated  $P_f$  and is not reversed with  $\alpha_2$ - or  $I_2$ - receptor antagonists.
8. The  $Y_2$ -preferring agonist PYY<sub>3-36</sub> inhibits AVP-stimulated  $P_f$ , depolarizes  $V_t$  and increases  $R_t$ .

The mechanism of AVP stimulated water and sodium permeability in the principal cell of the CCD occurs through the activation of a  $V_2$  adrenergic receptor coupled to a stimulatory G protein that activates adenylyl cyclase and leads to an increase in intracellular cAMP levels. The mechanism of  $\alpha_2$  adrenergic inhibition of AVP-stimulated permeability involves inhibition of the cAMP increase through the  $\alpha_2$  adrenergic receptor coupled to an inhibitory G protein. The discovery in 1993 by Hawk *et al* [29] showing that another signalling pathway is also present has led to much interest in second messengers and receptor subtypes. Studies investigating second messengers have already shown that  $\alpha_2$  adrenergic receptors activate PLC and increase PKC activity in cultured distal convoluted tubule cells [353] and that  $PGE_2$  reversibly inhibits AVP- and cAMP-stimulated  $P_f$  in the isolated rat IMCD [307]. Those reports raised the question of whether or not  $\alpha_2$  adrenergic receptors in the rat CCD rely on the PLC/PKC pathway or generation of prostaglandins in addition to cAMP inhibition to produce their inhibitory effect on AVP-stimulated salt and water permeability.

The present investigations conclude that extracellular calcium and intracellular prostaglandin production are not required for the inhibitory effect of the  $\alpha_2$  adrenergic receptors. Furthermore, PKC is indicated as a second messenger involved in the  $\alpha_2$  inhibition of AVP-stimulated water permeability in the rat CCD. Of additional importance is the finding that oxymetazoline inhibits AVP-stimulated, but not cAMP-stimulated water permeability, from which it is concluded that the  $\alpha_{2A}$ -subtype relies on inhibition of adenylyl cyclase as its mode of action. It is further concluded that agmatine

inhibits AVP-stimulated water permeability in the rat CCD *via* a receptor distinct from  $\alpha_2$ -adrenergic and imidazoline receptors. Finally, it is concluded that PYY inhibits AVP-stimulated salt and water permeability in the rat CCD not through an  $\alpha_2$  receptor, but through a  $Y_2$  receptor that may be influenced or coupled to the  $\alpha_2$  receptor.

All of the above conclusions constitute a basis for future studies. These studies were designed to provide new information on the possible signalling pathways and second messengers involved in the  $\alpha_2$ -mediated mechanism of inhibition, and to provide some insight to the actions of agmatine and PYY as they relate to  $\alpha_2$ -mediated inhibition of salt and water permeability in the rat CCD. Certainly more in-depth investigation is required, including establishment of dose-response curves and assays for specific second messengers. Utilization of other techniques such as immunohistochemistry to visualize specific receptors, and patch-clamping to characterize ion movement will be needed to provide a better understanding of the  $\alpha_2$ -mediated mechanism. It is also important to remember that these studies have been carried out *in vitro*, without the many possible influences from other endogenous neurotransmitters and hormones.

In the CCD *in vivo*, circulating AVP and aldosterone lead to increased reabsorption of sodium and water by the principal cell while epinephrine and norepinephrine counteract this effect through the  $\alpha_2$  adrenergic receptor. Renal dopamine produced in the proximal tubule binds to luminal receptors in the CCD and acts to inhibit AVP-induced sodium and water permeability. Renal serotonin is also produced by proximal tubule cells but has the opposite effect as dopamine in that it promotes natriuresis and diuresis. ANP

influences CCD function by modulating renin and aldosterone secretion, and may have a direct stimulatory effect on sodium and water excretion in the principal cell. Another natriuretic hormone, urodilatin, is synthesized in the kidney and its effect on the principal cell is still unknown. Endothelin produced in the kidney acts as a tonic modulator of sodium transport and has yet undetermined effects in the CCD. These hormones and other endocrine, neurocrine, and paracrine substances that regulate principal cell sodium and water permeability dictate an appreciation for the complexity of renal sodium and water homeostasis. Dissecting individual signalling pathways and receptor interactions is required to better understand these mechanisms and ultimately lead to improved treatments for hypertension and diseases of sodium imbalance.

## REFERENCES

1. Schwartz, G.J. and M.B. Burg, *Mineralocorticoid effects on cation transport by cortical collecting tubules in vitro*. Am. J. Physiol, 1978. **235**: p. F576-F585.
2. Reif, M.C., S.L. Troutman, and J.A. Schafer, *Sodium transport by the rat cortical collecting tubule. Effects of vasopressin and deoxycorticosterone*. J. Clin. Invest, 1986. **77**: p. 1291-1298.
3. Harris, H.W., Jr., K. Strange, and M.L. Zeidel, *Current understanding of the cellular biology and molecular structure of the antidiuretic hormone-stimulated water transport pathway*. J. Clin. Invest, 1991. **88**: p. 1-8.
4. Nielson, S., et al., *Vasopressin increases water permeability of kidney collecting duct by inducing translocation of aquaporin-CD water channels to plasma membrane*. Proc. Natl. Acad. Sci., 1995. **92**(February): p. 1013-1017.
5. Eaton, D.C., et al., *Renal sodium channels: Regulation and single channel properties*. Kidney International, 1995. **48**: p. 941-949.
6. Chen, L., M.C. Reif, and J.A. Schafer, *Clonidine and PGE<sub>2</sub> have different effects on Na<sup>+</sup> and water transport in the rat and rabbit CCD*. Am. J. Physiol, 1991. **261**(Renal Fluid Electrolyte Physiol. **30**): p. F126-F136.
7. Rouch, A.J. and L.H. Kudo, *Dexmedetomidine inhibits arginine vasopressin-stimulated water permeability, transepithelial resistance and voltage in rat CCD*. FASEB J, 1994. **8**: p. A551.
8. Rouch, A.J., L.H. Kudo, and C. Hébert, *Dexmedetomidine inhibits osmotic water permeability in the rat cortical collecting duct*. J. Pharmacol. Exp. Ther, 1997. **281**: p. 62-69.
9. Nonoguchi, H., J.M. Sands, and M.A. Knepper, *ANF inhibits NaCl and fluid absorption in cortical collecting duct of rat kidney*. Am. J. Physiol, 1989. **256** (Renal Fluid Electrolyte Physiol. **25**): p. F179-F186.
10. Hébert, R., et al., *Functional and molecular aspects of prostaglandin E receptors in the cortical collecting duct*. Can. J. Physiol. Pharmacol., 1995. **73**: p. 172-179.
11. Tomita, K., J.J. Pisano, and M.A. Knepper, *Control of sodium and potassium transport in the cortical collecting duct of the rat. Effects of bradykinin, vasopressin, and deoxycorticosterone*. J. Clin. Invest, 1985. **76**: p. 132-136.
12. Li, L. and J. Schafer, *Dopamine inhibits vasopressin-dependent cAMP production in the rat cortical collecting duct*. Am. J. Physiol., 1998. **275**: p. F62-F67.
13. Blaze, C.A., et al., *Peptide YY receptor distribution and subtype in the kidney: effect on renal hemodynamics and function in rats*. Am J Physiol, 1997. **273**: p. F545-F553.
14. Bischoff, A. and M. Michel, *Renal effects of neuropeptide Y*. Pflugers Arch., 1998. **435**: p. 443-453.
15. Smyth, D.D. and S.B. Penner, *Renal I<sub>1</sub>-imidazoline receptor-selective compounds mediate natriuresis in the rat*. J. Cardiovasc. Pharmacol, 1995. **26**: p. S63-S67.

16. Smyth, D.D., F.K. Darkwa, and S.B. Penner, *Imidazoline receptors and sodium excretion in the rat kidney*. *Annal. N.Y. Acad. Sci*, 1995. **763**: p. 340-352.
17. Star, R.A., et al., *Calcium and cyclic adenosine monophosphate as second messengers for vasopressin in the rat inner medullary collecting duct*. *J. Clin. Invest*, 1988. **81**: p. 1879-1888.
18. Snyder, H.M., T.D. Noland, and M.D. Breyer, *cAMP-dependent protein kinase mediates hydrosmotic effect of vasopressin in collecting duct*. *Am. J. Physiol*, 1992. (**Cell Physiol. 32**): p. C147-C153.
19. Krothapalli, R.K., et al., *Modulation of the hydro-osmotic effect of vasopressin on the rabbit cortical collecting tubule by adrenergic agents*. *J. Clin. Invest*, 1983. **72**: p. 287-294.
20. Krothapalli, R.K. and W.N. Suki, *Functional characterization of the alpha adrenergic receptor modulating the hydroosmotic effect of vasopressin on the rabbit cortical collecting tubule*. *J. Clin. Invest*, 1984. **73**: p. 740-749.
21. Ernsberger, P., et al., *Clonidine binds to imidazole binding sites as well as A2-adrenoceptors in the ventrolateral medulla*. *Eur. J. Pharm.*, 1987. **134**: p. 1-13.
22. Ernsberger, P., et al., *Characterization and visualization of clonidine-sensitive imidazole sites in rat kidney which recognize clonidine-displacing substance*. *Am. J. Hypertens*, 1990. **3**: p. 90-97.
23. Grenney, H., et al., *Coupling of II imidazoline receptors to the cAMP pathway: Studies with a highly selective ligand, benazoline*. *Molecular Pharmacology*, 2000. **57**(6): p. 1142-1151.
24. Ernsberger, P., J.E. Friedman, and R.J. Koletsky, *The II-imidazoline receptor: from binding site to therapeutic target in cardiovascular disease*. *J. of Hypertension*, 1997. **15**: p. S9-23.
25. Smyth, D.D., et al., *Effects of central and peripheral neuropeptide Y on sodium and water excretion in the rat*. *Physiol Behav*, 1989. **46**: p. 9-11.
26. Dillingham, M.A. and R.J. Anderson, *Mechanism of neuropeptide Y inhibition of vasopressin action in rat cortical collecting duct*. *Am. J. Physiol.*, 1989. **256**: p. F408-F413.
27. Gilman, A.G., *Guanine nucleotide-binding regulatory proteins and dual control of adenylate cyclase*. *J. Clin. Invest.*, 1984. **73**: p. 1-4.
28. Takada, K., et al., *The involvement of pertussis toxin-sensitive G proteins in the post receptor mechanism of central II-imidazoline receptors*. *Brit. J. Pharm.*, 1997. **120**: p. 1575-1581.
29. Hawk, C.T., et al., *Inhibition by epinephrine of AVP- and cAMP-stimulated Na<sup>+</sup> and water transport in Dahl rat CCD*. *Am. J. Physiol*, 1993. **265** (**Renal Fluid Electrolyte Physiol. 34**): p. F449-F460.
30. Rouch, A.J. and L.H. Kudo, *Indomethacin and staurosporine reverse  $\alpha$ 2 inhibition of water transport in rat IMCD*. *Kidney International*, 1996. **52**: p. 1351-1358.
31. Bischoff, A., et al., *Neuropeptide Y-enhanced diuresis and natriuresis in anaesthetized rats is independent from renal blood flow reduction*. *Journal of Physiology*, 1996. **495**: p. 525-534.

32. Bischoff, A., et al., *Receptor subtypes Y<sub>1</sub> and Y<sub>5</sub> are involved in the renal effects of neuropeptide Y*. Brit J of Pharmacol, 1997. **120(7)**: p. 1335-1343.
33. el Din, M. and K. Malik, *Neuropeptide Y simulates renal prostaglandin synthesis in the isolated rat kidney: contribution of Ca<sup>++</sup> and calmodulin*. Journal of Pharmacology and Experimental Therapeutics, 1988. **246**: p. 479-484.
34. Ewald, D.A., et al., *Differential G protein-mediated coupling of neurotransmitter receptors to Ca<sup>2+</sup> channels in rat dorsal root ganglion neurons in vitro*. Neuron, 1989. **2**: p. 1185-1193.
35. Michel, M., *Receptors for neuropeptide Y: multiple subtypes and multiple second messengers*. Trends in Physiological Science, 1991. **12**: p. 389-394.
36. Madsen, K.M. and C.C. Tisher, *Structural-functional relationships along the distal nephron*. Am. J. Physiol, 1986. **250**: p. F1-F15.
37. O'Neil, R.G. and R.H. Hayhurst, *Functional differentiation of cell types of the cortical collecting duct*. Am. J. Physiol., 1985. **248**: p. F449-F453.
38. Madsen, K.M. and C.C. Tisher, *Structure-function relationships in H<sup>+</sup>-secreting epithelia*. Federation Proc, 1985. **44**: p. 2704-2709.
39. Schlatter, E. and J.A. Schafer, *Electrophysiological studies in principal cells of rat cortical collecting tubules. ADH increases the apical membrane Na<sup>+</sup>-conductance*. Pflügers Arch, 1987. **409**: p. 81-92.
40. Schafer, J.A. and S.L. Troutman, *cAMP mediates the increase in apical membrane Na conductance produced in rat CCD by vasopressin*. Am. J. Physiol, 1990. **259(Renal Fluid Electrolyte Physiol. 28)**: p. F823-F31.
41. Schafer, J.A., S.L. Troutman, and E. Schlatter, *Vasopressin and mineralocorticoid increase apical membrane driving force for K<sup>+</sup> secretion in rat CCD*. Am J Physiol, 1990. **258 (Renal Fluid Electrolyte Physiol. 27)**: p. F199-F210.
42. Schafer, J.A. and C.T. Hawk, *Regulation of Na<sup>+</sup> channels in the cortical collecting duct by AVP and mineralocorticoids*. Kidney International, 1992. **41**: p. 255-268.
43. Garty, H. and I.S. Edelman, *Amiloride-sensitive trypsinization of apical sodium channels*. J. Gen. Physiol., 1983. **81**: p. 785-803.
44. Oh, Y., et al., *Regulation by phosphorylation of purified epithelial Na<sup>+</sup> channels in planar lipid bilayers*. Am. J. Physiol., 1993. **265**: p. C85-C91.
45. Garty, H. and L.G. Palmer, *Epithelial sodium channels: function, structure, and regulation*. Physiol. Rev., 1997. **77**: p. 359-396.
46. Nielsen, S., et al., *Cellular and subcellular immunolocalization of vasopressin-regulated water channel in rat kidney*. Proc. Natl. Acad. Sci., 1993. **90**: p. 11663-11667.
47. Ausiello, D.A., et al., *Vasopressin signaling in kidney cells*. Kidney Int, 1987. **31**: p. 521-529.
48. Smith, B.L. and P. Agree, *Erythrocyte Mr 28,000 transmembrane protein exists as a multisubunit oligomer similar to channel proteins*. J. Biol. Chem., 1991. **266(10)**: p. 6407-6415.
49. Sabolic, I., et al., *Localization of the CHIP28 water channel in rat kidney*. Am. J. Physiol., 1992. **263**: p. C1225-C1233.

50. Nielsen, S., et al., *CHIP28 water channels are localized in constitutively water-permeable segments of the nephron*. J. Cell Biology, 1993. **120(2)**: p. 371-383.
51. Smith, B.L., et al., *Concurrent expression of erythroid and renal aquaporin CHIP and appearance of water channel activity in perinatal rats*. J. Clin. Invest., 1993. **92**: p. 2035-2041.
52. Nielsen, S., et al., *Aquaporin-1 water channels in short and long loop descending thin limbs and in descending vasa recta in rat kidney*. Am. J. Physiol., 1995. **268**: p. F1023-F1037.
53. Marples, D., et al., *Redistribution of aquaporin-2 water channels induced by vasopressin in rat kidney inner medullary collecting duct*. Am. J. Physiol., 1995. **269**: p. C655-C664.
54. Fushimi, K., et al., *Functional characterization and cell immunolocalization of AQP-CD water channel in kidney collecting duct*. Am. J. Physiol., 1994. **267**: p. F573-582.
55. Harris, H.W., et al., *Characterization of purified endosomes containing the antidiuretic hormone-sensitive water channel from rat renal papilla*. J. Biol. Chem., 1994. **269(16)**: p. 11993-12000.
56. Yamamoto, T., et al., *Vasopressin increases AQP-CD water channel in apical membrane of collecting duct cells in Brattleboro rats*. Am. J. Physiol., 1995. **268**: p. C1546-1551.
57. Hayashi, M., et al., *Role of vasopressin V2 receptor in acute regulation of aquaporin-2*. Kidney Blood Press. Res., 1996. **19**: p. 32-37.
58. Katsura, T., D.A. Ausiello, and D. Brown, *Direct demonstration of aquaporin-2 water channel recycling in stably transfected LLC-PK<sub>1</sub> epithelial cells*. Am. J. Physiol., 1996. **270 (Renal Fluid Electrolyte Physiol. 39)**: p. F548-F553.
59. Saito, T., et al., *Alteration in water channel AQP-2 by removal of AVP stimulation in collecting duct cells of dehydrated rats*. Am. J. Physiol., 1997. **272**: p. F183-F191.
60. Nielsen, S., et al., *Expression of VAMP2-like protein in kidney collecting duct intracellular vesicles*. J. Clin. Invest., 1995. **96**: p. 1834-1844.
61. Jo, I., et al., *Rat kidney papilla contains abundant synaptobrevin protein that participates in the fusion of antidiuretic hormone-regulated water channel-containing endosomes in vitro*. Proc. Natl. Acad. Sci., 1995. **92**: p. 1876-1880.
62. Marples, D., et al., *Dynein and dynactin colocalize with AQP2 water channels in intracellular vesicles from kidney collecting duct*. Am. J. Physiol., 1998. **274**: p. F384-F394.
63. Sands, J.M., H. Nonoguchi, and M.A. Knepper, *Vasopressin effects on urea and H<sub>2</sub>O transport in inner medullary collecting subsegments*. Am. J. Physiol., 1987. **253 (Renal Fluid Electrolyte Physiol. 22)**: p. F823-F832.
64. Wall, S.M., et al., *Kinetics of urea and water permeability activation by vasopressin in rat terminal IMCD*. Am. J. Physiol., 1992. **262**: p. F989-F998.
65. Sasaki, S., K. Ishibashi, and F. Marumo, *Aquaporin-2 and -3: representatives of two subgroups of the aquaporin family colocalized in the kidney collecting duct*. Annu. Rev. Physiol., 1998. **60**: p. 199-220.

66. Ecelbarger, C.A., et al., *Aquaporin-3 water channel localization and regulation in rat kidney*. Am. J. Physiol., 1995. **269 (Renal Fluid Electrolyte Physiol. 38)**: p. F663-F672.
67. Ishibashi, K., et al., *Immunolocalization and effect of dehydration on AQP3, a basolateral water channel of kidney collecting ducts*. Am. J. Physiol., 1997. **272**: p. F235-F241.
68. Ishibashi, K., et al., *Molecular cloning and expression of a member of the aquaporin family with permeability to glycerol and urea in addition to water expressed at the basolateral membrane of kidney collecting duct cells*. Proc. Natl. Acad. Sci., 1994. **91**: p. 6269-6273.
69. Jung, J.S., et al., *Molecular characterization of an aquaporin cDNA from brain: candidate osmoreceptor and regulator of water balance*. Proc. Natl. Acad. Sci., 1994. **91**: p. 13052-13056.
70. Terris, J., et al., *Distribution of aquaporin-4 water channel expression within rat kidney*. Am. J. Physiol., 1995. **269**: p. F775-F785.
71. Hasegawa, H., et al., *Molecular cloning of a mercurial-insensitive water channel expressed in selected water-transporting tissues*. J. Biol. Chem., 1994. **269**: p. 5497-5500.
72. Verbavatz, J.-M., et al., *Tetrameric assembly of CHIP28 water channels in liposomes and cell membranes: a freeze-fracture study*. J. Cell Biol., 1993. **123(3)**: p. 605-618.
73. Jung, J.S., et al., *Molecular structure of the water channel through aquaporin CHIP*. J. Biol. Chem., 1994. **269(20)**: p. 14648-14654.
74. Cheng, A., et al., *Three-dimensional organization of a human water channel*. Nature, 1997. **387**: p. 627-630.
75. Walz, T., et al., *The three-dimensional structure of aquaporin-1*. Nature, 1997. **387**: p. 624-627.
76. Preston, G.M., et al., *Membrane topology of aquaporin CHIP*. J. Biol. Chem., 1994. **269(3)**: p. 1668-1673.
77. Stamer, W.D., R.W. Snyder, and J.W. Regan, *Characterization of the transmembrane orientation of aquaporin-1 using antibodies to recombinant fusion proteins*. Biochemistry, 1996. **35**: p. 16313-16318.
78. Zhang, R., et al., *A point mutation at cysteine 189 blocks the water permeability of rat kidney water channel CHIP28k*. Biochemistry, 1993. **32**: p. 2938-2941.
79. Palmer, L.G. and G. Frindt, *Amiloride-sensitive Na channels from the apical membrane of the rat cortical collecting tubule*. Proc. Natl. Acad. Sci, 1986. **83**: p. 2767-2770.
80. Li, J.H.-Y. and E.J. Cragoe Jr., *Structure-activity relationship of amiloride analogs as blockers of epithelial Na channels: II. Side-chain modifications*. J. Membrane Biol, 1987. **95**: p. 171-185.
81. Garty, H. and D.J. Benos, *Characteristics and regulatory mechanisms of the amiloride-blockable Na<sup>+</sup> channel*. Physiol. Rev, 1988. **68**: p. 309-373.

82. Li, J.H., A. Shaw, and S.T. Kau, *Stereoselective blockade of amphibian epithelial sodium channels by amiloride analogs*. J. Pharmacol. Exp. Ther., 1993. **267**(3): p. 1081-1084.
83. Palmer, L.G. and G. Frindt, *Epithelial sodium channels: characterization by using the patch-clamp technique*. Federation Proc, 1986. **45**(12): p. 2708-2712.
84. Benos, D.J., *The biology of amiloride-sensitive sodium channels*. Hosp Practice, 1989. **24**(4): p. 149-55.
85. Palmer, L.G., *Epithelial Na channels and their kin*. NIPS, 1995. **10**: p. 61-67.
86. Duchatelle, P., et al., *Regulation of renal epithelial sodium channels*. Mol Cell Biochem, 1992. **114**: p. 27-34.
87. Canessa, C.M., et al., *Amiloride-sensitive epithelial Na<sup>+</sup> channel is made of three homologous subunits*. Nature, 1994. **367**: p. 463-467.
88. Canessa, C.M., A.-M. Merillat, and B.C. Rossier, *Membrane topology of the epithelial sodium channel in intact cells*. Am. J. Physiol., 1994. **267**: p. C1682-C1690.
89. Renard, S., et al., *Biochemical analysis of the membrane topology of the amiloride-sensitive Na<sup>+</sup> channel*. J. Biol. Chem., 1994. **269**(7): p. 12981-12986.
90. Snyder, P.M., et al., *Membrane topology of the amiloride-sensitive epithelial sodium channel*. J. Biol. Chem., 1994. **269**(39): p. 24379-24383.
91. Li, X.-J., et al., *Alternatively spliced forms of the  $\alpha$  subunit of the epithelial sodium channel: distinct sites for amiloride binding and channel pore*. Molec. Pharmacol., 1995. **47**: p. 1133-1140.
92. Ismailov, I.I., et al., *Identification of an amiloride binding domain within the  $\alpha$ -subunit of the epithelial Na<sup>+</sup> channel*. J. Biol. Chem., 1997. **272**(34): p. 21075-21083.
93. Duc, C., et al., *Cell-specific expression of epithelial sodium channel  $\alpha$ ,  $\beta$ , and  $\gamma$  subunits in aldosterone-responsive epithelia from the rat: localization by in situ hybridization and immunocytochemistry*. J. Cell Biol., 1994. **127**(6): p. 1907-1921.
94. Giebisch, G. and W. Wang, *Renal tubule potassium channels: function, regulation and structure*. Acta Physiol. Scand., 2000. **170**: p. 153-173.
95. Hebert, S., *An ATP-regulated, inwardly rectifying potassium channel from rat kidney*. Kidney International, 1995. **48**: p. 1010-1016.
96. Giebisch, G., *Renal potassium channels: an overview*. Kidney International, 1995. **48**: p. 1004-1009.
97. Wang, W., H. Sackin, and G. Giebisch, *Renal potassium channels and their regulation*. Annual Review Physiology, 1992. **54**: p. 81-96.
98. Frindt, G. and L.G. Palmer, *Low-conductance K channels in apical membrane of rat cortical collecting tubule*. Am. J. Physiol, 1989. **256** (Renal Fluid Electrolyte Physiol. **25**): p. F143-F151.
99. Wang, W., A. Schwab, and G. Giebisch, *Regulation of small-conductance K<sup>+</sup> channel in apical membrane of rat collecting tubule*. Am. J. Physiol, 1990. **259** (Renal Fluid Electrolyte Physiol. **28**): p. F494-F502.
100. Klaerke, D., *Purification and characterization of epithelial Ca<sup>++</sup>-activated K<sup>+</sup> channels*. Kidney International, 1995. **48**: p. 1047-1056.

101. Hirsch, J. and E. Schlatter, *K<sup>+</sup> channels in the basolateral membrane of rat cortical collecting duct*. *Kidney International*, 1995. **48**: p. 1036-1046.
102. Wald, H., *Regulation of the ROMK potassium channel in the kidney*. *Experimental Nephrology*, 1999. **7**(3): p. 201-206.
103. Hirsch, J., et al., *Regulation and possible physiological role of the Ca<sup>2+</sup>-dependent K<sup>+</sup> channel of the cortical collecting ducts of the rat*. *Pflügers Archives*, 1993. **422**: p. 492-498.
104. Schuster, V., *Function and regulation of collecting duct intercalated cells*. *Annu. Rev. Physiol.*, 1993. **55**: p. 267-288.
105. Sansom, S.C., E.J. Weinman, and R.G. O'Neil, *Microelectrode assessment of chloride-conductive properties of cortical collecting duct*. *Am. J. Physiol.*, 1984. **247** (**Renal Fluid Electrolyte Physiol.** **16**): p. F291-F302.
106. Gross, P., et al., *Ionic conductances of cultured principal cell epithelium of renal collecting duct*. *Pflügers Archives*, 1988. **412**(4): p. 434-441.
107. Uchida, S., *In vivo role of CLC chloride channels in the kidney*. *Am. J. Physiol.*, 2000. **279**: p. F802-F808.
108. Waldegger, S. and T. Jentsch, *From tonus to tonicity: physiology of CLC chloride channels*. *J. Am. Soc. Nephrol.*, 2000. **11**: p. 1331-1339.
109. Schmidt-Rose, T. and T. Jentsch, *Transmembrane topology of a CLC chloride channel*. *Proceedings National Academy of Science*, 1997. **94**: p. 7633-7638.
110. Yoshikawa, M., et al., *Localization of rat CLC-K2 chloride channel mRNA in the kidney*. *Am. J. Physiol.*, 1999. **276**: p. F552-F558.
111. Morales, M., D. Falkenstein, and A. Lopes, *The cystic fibrosis transmembrane regulator (CFTR) in the kidney*. *An. Acad. Bras. Ci.*, 2000. **72**(3): p. 399-404.
112. Todd-Turla, K., et al., *CFTR expression in cortical collecting duct cells*. *Am. J. Physiol.*, 1996. **270**: p. F237-F244.
113. Letz, B. and C. Korbmayer, *cAMP stimulates CFTR-like Cl channels and inhibits amiloride-sensitive Na channels in mouse CCD cells*. *Am. J. Physiol.*, 1997. **272**: p. C657-C666.
114. Kunzelmann, K., R. Schreiber, and A. Boucherot, *Mechanisms of the inhibition of epithelial Na channels by CFTR and purinergic stimulation*. *Kidney Int.*, 2001. **60**: p. 455-461.
115. McNicholas, C., et al., *Sensitivity of a renal K channel (ROMK2) to the inhibitory sulfonylurea compound glibenclamide is enhanced by coexpression with the ATP-binding cassette transporter cystic fibrosis transmembrane regulator*. *Proceedings National Academy of Science*, 1996. **93**: p. 8083-8088.
116. Wang, W., *Regulation of the ROMK channel: interaction of the ROMK with associated proteins*. *Am. J. Physiol.*, 1999. **277**: p. F826-F831.
117. Féraillé, E. and A. Doucet, *Sodium-potassium-adenosinetriphosphatase-dependent sodium transport in the kidney: hormonal control*. *Physiological Reviews*, 2001. **81**(1): p. 345-418.

118. Laski, M., *The renal adenosine triphosphatases: functional integration and clinical significance*. Mineralocorticoid and Electrolyte Metabolism, 1996. **22**(5-6): p. 410-422.
119. Geering, K., et al., *Oligomerization and maturation of Na, K-ATPase: functional interaction of the cytoplasmic NH terminus of the  $\beta$  subunit with the  $\alpha$  subunit*. Journal of Cell Biology, 1996. **133**: p. 1193-1204.
120. Ueno, S., et al., *Significance of the  $\beta$  subunit in the biogenesis of Na/K-ATPase*. Bioscience Reports, 1997. **17**: p. 173-188.
121. Tomita, K., et al., *Effects of vasopressin and bradykinin on anion transport by the rat cortical collecting duct*. J. Clin. Invest, 1986. **77**: p. 136-141.
122. Terada, Y. and M.A. Knepper, *Thiazide-sensitive NaCl absorption in rat cortical collecting duct*. Am. J. Physiol, 1990. **259** (Renal Fluid Electrolyte Physiol. **28**).
123. Schlatter, E., et al., *Regulation of Na/H exchange by diadenosine polyphosphates, angiotensin II, and vasopressin in rat cortical collecting duct*. J. Am. Soc. Nephrol., 1995. **6**: p. 1223-1229.
124. Eiam-Ong, S. and S. Sabatini, *Biochemical mechanisms and regulation of hydrogen transport in renal tubules*. Mineralocorticoid and Electrolyte Metabolism, 1996. **22**: p. 366-381.
125. Depaoli, A., et al., *In situ hybridization of mRNAs and immunolocalization of Na/H exchanger isoform NHE-3 and NHE-4 in rat kidney*. Journal American Society of Nephrology, 1993. **4**: p. 836A.
126. Bookstein, C., et al., *A unique sodium-hydrogen exchange isoform (NHE-4) of the inner medulla of the rat kidney is induced by hyperosmolality*. Journal of Biological Chemistry, 1994. **269**: p. 29704-29709.
127. Krapf, R. and M. Solioz, *Na/H antiporter mRNA expression in single nephron segments of rat kidney cortex*. J. Clin. Invest, 1991. **88**: p. 783-788.
128. Schlatter, E., et al., *Moxonidine inhibits Na<sup>+</sup>/H<sup>+</sup> exchange in proximal tubule cells and cortical collecting duct*. Kidney Int., 1997. **52**: p. 454-459.
129. Livine, A., et al., *increased platelet Na-H exchange rates in essential hypertension: application of a novel test*. Lancet, 1987. **1**(8532): p. 533-536.
130. Noel, J. and J. Pouyssegur, *Hormonal regulation, pharmacology, and membrane sorting of vertebrate Na/H exchanger isoforms*. Am. J. Physiol., 1995. **268**: p. C283-C296.
131. Igarashi, P., et al., *Molecular biology of renal Na-H exchangers*. Kidney Int., 1991. **40**(suppl.33): p. S84-S89.
132. Wakabayashi, S., M. Shigekawa, and J. Pouyssegur, *Molecular physiology of vertebrate Na/H exchangers*. Physiological Reviews, 1997. **77**(1): p. 51-74.
133. Schafer, J.A., L. Chen, and A.J. Rouch, *The role of vasopressin in the regulation of Na<sup>+</sup> and K<sup>+</sup> transport in the cortical collecting duct*. Vasopressin, 1991. **208**: p. 493-501.
134. Katz, A.I., *Renal Na-K-ATPase: its role in tubular sodium and potassium transport*. Am. J. Physiol, 1982. **242**(Renal Fluid Electrolyte Physiol. **11**): p. F207-F219.

135. Sansom, S.C. and R.G. O'Neil, *Mineralocorticoid regulation of apical cell membrane Na<sup>+</sup> and K<sup>+</sup> transport of the cortical collecting duct*. Am. J. Physiol., 1985. **248**(Renal Fluid Electrolyte Physiol. 17): p. F858-F868.
136. O'Neil, R.G. and R.A. Hayhurst, *Sodium-dependent modulation of the renal Na-K-ATPase: Influence of mineralocorticoids on the cortical collecting duct*. J. Membrane Biol, 1985. **85**: p. 169-179.
137. Garty, H., *Mechanisms of aldosterone action in tight epithelia*. J. Membrane Biol, 1990. **90**: p. 193-205.
138. Edelman, I.S., *Receptors and effectors in hormone action on the kidney*. Am. J. Physiol., 1981. **241**: p. F333-F339.
139. Garty, H., *Mechanisms of aldosterone action in tight epithelia*. J. Membrane Biol, 1986. **90**: p. 193-205.
140. Sariban-Sohraby, S., et al., *Methylation increases sodium transport into A6 apical membrane vesicles: Possible mode of aldosterone action*. Science, 1984. **225**: p. 745-746.
141. Grantham, J.J. and M.B. Burg, *Effect of vasopressin and cyclic AMP on permeability of isolated collecting tubules*. Am. J. Physiol, 1966. **211**: p. 255-259.
142. Reif, J.C., S.L. Troutman, and J.A. Schafer, *Sustained response to vasopressin in isolated rat cortical collecting tubule*. Kidney Int, 1984. **26**: p. 725-732.
143. De Sousa, R.C., *Effects of vasopressin on epithelial transport*. J. Cardiovas. Pharmacol., 1986. **8** (7): p. S23-S28.
144. Chen, L., S.K. Williams, and J.A. Schafer, *Differences in synergistic actions of vasopressin and deoxycorticosterone in rat and rabbit CCD*. Am. J. Physiol, 1990. **259** (Renal Fluid Electrolyte Physiol. 28): p. F147-F156.
145. Lester, D.S., C. Asher, and H. Garty, *Characterization of cAMP-induced activation of epithelial sodium channels*. Am. J. Physiol, 1988. **254** (Cell Physiol. 23): p. C802-C808.
146. Li, J.H.Y., et al., *The role of sodium-channel density in the natriuretic response of the toad urinary bladder to an antidiuretic hormone*. J. Membrane Biol, 1982. **64**: p. 77-89.
147. Handler, J.S., *Antidiuretic hormone moves membranes*. Am. J. Physiol, 1988. **255** (Renal Fluid Electrolyte Physiol. 24): p. F375-F382.
148. Kleyman, T.R., E.J. Cragoe, and J.P. Kraehenbuhl, *The cellular pool of Na<sup>+</sup> channels in the amphibian cell line A6 is not altered by mineralocorticoids*. J. Biol. Chem, 1989. **264**: p. 11995-12000.
149. Lewis, D.L., et al., *Intracellular regulation of ion channels in cell membranes*. Mayo Clin. Proc, 1990. **65**: p. 1127-1143.
150. Brown, D. and L. Orci, *Vasopressin stimulates formation of coated pits in rat kidney collecting ducts*. Nature, 1983. **302**: p. 253-255.
151. Wade, J.B., *Role of membrane fusion in hormonal regulation of epithelial transport*. Ann. Rev. Physiol., 1986. **48**: p. 213-223.
152. Wade, J.B., *Dynamics of apical membrane responses to ADH in amphibian bladder*. Am. J. Physiol., 1988. **257**: p. R998-R1003.

153. Shimkets, R.A., R.P. Lifton, and C.M. Canessa, *The activity of the epithelial sodium channel is regulated by clathrin-mediated endocytosis*. J. Biol. Chem., 1997. **272**(41): p. 25537-25541.
154. Wade, J.B., et al., *Long-term regulation of collecting duct water permeability: freeze-fracture analysis of isolated perfused tubules*. Am. J. Physiol., 1994. **266**: p. F723-F730.
155. Knepper, M.A. and T. Inoue, *Regulation of aquaporin-2 water channel trafficking by vasopressin*. Current Opinion in Cell Biology, 1997. **9**: p. 560-564.
156. Zeidel, M.L., et al., *Fate of antidiuretic hormone water channel proteins after retrieval from apical membrane*. Am. J. Physiol., 1993. **265**: p. C822-C833.
157. Besarab, A., et al., *Effect of catecholamines on tubular function in the isolated perfused rat kidney*. Am. J. Physiol., 1977. **233**(1): p. F39-F45.
158. Insel, P.A. and M.D. Snavely, *Catecholamines and the kidney: receptors and renal function*. Ann. Rev. Physiol, 1981. **43**: p. 625-636.
159. Schmitz, J., et al., *Renal  $\alpha 1$  and  $\alpha 2$ -adrenergic receptors. Biochemical and pharmacological correlations*. J. Pharm. Exp. Ther., 1981. **219**: p. 400-408.
160. Umemura, S., et al.,  *$\alpha 2$ -adrenoceptors and cellular cAMP levels in single nephron segments from the rat*. Am. J. Physiol, 1985. **249** (Renal Fluid Electrolyte Physiol. **18**): p. F28-F33.
161. Wilborn, T.W., D. Sun, and J.A. Schafer, *Expression of multiple  $\alpha$ -adrenoceptor isoforms in rat CCD*. Am. J. Physiol., 1998. **275**(44): p. F111-F118.
162. Bains, A., R. Drangnova, and C. Hatcher, *Dopamine production by isolated glomeruli and tubules from rat kidneys*. Can. J. Physiol., 1985. **63**: p. 155-158.
163. Soares-da-silva, P., et al., *Studies on the nature of the antagonistic actions of dopamine and 5-hydroxytryptamine in renal tissues*. Hypertens. Res., 1995. **18**(Suppl. I): p. S47-S51.
164. Soares-da-silva, P., M. Fernandes, and P. Pintodo-O, *Cell inward transport of L-DOPA and 3-O-methyl-L-DOPA in rat renal tubules*. British Journal of Pharmacology, 1994. **112**: p. 611-615.
165. Carey, R., *Renal dopamine system: Paracrine regulator of sodium homeostasis and blood pressure*. Hypertension, 2001. **38**: p. 297-302.
166. Aperia, A., A. Bertorello, and I. Seri, *Dopamine causes inhibition of Na, K-ATPase activity in rat proximal tubule cells*. Am. J. Physiol., 1987. **252**: p. F39-F45.
167. Felder, C., et al., *Dopamine inhibits Na/H exchanger in renal BBMV by stimulation of adenylate cyclase*. Am. J. Physiol., 1990. **259**: p. F297-F303.
168. Sun, D. and J.A. Schafer, *Dopamine inhibits AVP-dependent Na<sup>+</sup> transport and water permeability in rat ccd via a D4-like receptor*. Am. J. Physiol., 1996. **271**: p. f391-400.
169. Edwards, R. and D. Brooks, *Dopamine inhibits vasopressin action in the rat inner medullary collecting duct via  $\alpha 2$ -adrenoceptors*. J. Pharm. Exp. Ther., 2001. **298**: p. 1001-1006.

170. Missale, C., et al., *Dopamine receptors: From structure to function*. Physiological Reviews, 1998. **78**(1): p. 189-225.
171. Sun, D., T. Wilborn, and J. Schafer, *Dopamine D4 receptor isoform mRNA and protein are expressed in the rat cortical collecting duct*. Am. J. Physiol., 1998. **275**: p. F742-F751.
172. Schafer, J., L. Li, and D. Sun, *The collecting duct, dopamine and vasopressin-dependent hypertension*. Acta Physiol. Scand., 2000. **168**: p. 239-244.
173. Stier, C., G. McKendall, and H. Itskovitz, *Serotonin formation in nonblood-perfused rat kidneys*. J. Pharm. Exp. Ther., 1984. **228**(1): p. 53-56.
174. Stier, C. and H. Itskovitz, *Formation of serotonin by rat kidneys in vitro*. PSEBM, 1985. **180**: p. 550-557.
175. Sole, M., A. Madapallimattam, and A. Baines, *An active pathway for serotonin synthesis by renal proximal tubules*. Kidney Int., 1986. **29**: p. 689-694.
176. Itskovitz, H., Y.-H. Chen, and C. Stier, *Reciprocal renal effects of dopamine and 5-hydroxytryptamine formed within the rat kidney*. Clinical Science, 1988. **75**: p. 503-507.
177. Schmidt, A. and S. Peroutka, *5-Hydroxytryptamine receptor "families"*. FASEB, 1989. **3**: p. 2242-2249.
178. Ciaranello, R., G. Tan, and R. Dean, *G-protein-linked serotonin receptors in mouse kidney exhibit identical properties to 5-HT<sub>1B</sub> receptors in brain*. Journal of Pharmacology and Experimental Therapeutics, 1989. **252**(3): p. 1347-1354.
179. Raymond, J., et al., *Immunohistochemical mapping of cellular and subcellular distribution of 5-HT<sub>1A</sub> receptors in rat and human kidneys*. Am. J. Physiol., 1993. **264**: p. F9-F19.
180. Maack, T., et al., *Atrial natriuretic factor: Structure and function*. Kidney Int, 1985. **27**: p. 607-615.
181. Ballermann, B. and B. Brenner, *Role of atrial peptides in body fluid homeostasis*. Circulation Research, 1986. **58**: p. 619-630.
182. Zeidel, M.L., *Renal actions of atrial natriuretic peptide: Regulation of collecting duct sodium and water transport*. Annu. Rev. Physiol, 1990. **52**: p. 747-759.
183. Endlich, K., W.-G. Forssmann, and M. Steinhausen, *Effects of urodilatin in the rat kidney: Comparison with ANF and interaction with vasoactive substances*. Kidney Int., 1995. **47**: p. 1558-1568.
184. Inoue, T., H. Nonoguchi, and K. Tomita, *Physiological effects of vasopressin and atrial natriuretic peptide in the collecting duct*. Cardiovascular Research, 2001. **51**: p. 470-480.
185. Kone, B., *Molecular biology of natriuretic peptides and nitric oxide synthases*. Cardiovascular Research, 2001. **51**: p. 429-441.
186. Nonoguchi, H., J.M. Sands, and M.A. Knepper, *Atrial natriuretic factor inhibits vasopressin-stimulated osmotic water permeability in rat inner medullary collecting duct*. J. Clin. Invest, 1988. **82**: p. 1383-1390.

187. Sands, J.M., H. Nonoguchi, and M.A. Knepper, *Hormone effects on NaCl permeability of rat inner medullary collecting duct*. Am. J. Physiol, 1988. **255 (Renal Fluid Electrolyte Physiol. 24)**: p. F421-F428.
188. Zeidel, M.L., et al., *Atrial natriuretic peptides inhibit conductive sodium uptake by rabbit inner medullary collecting duct cells*. J. Clin. Invest, 1988. **82**: p. 1067-1074.
189. Rocha, A.S. and L.H. Kudo, *Effect of atrial natriuretic factor and cyclic guanosine monophosphate on water and urea transport in the inner medullary collecting duct*. Pflügers Arch, 1990. **417**: p. 84-90.
190. Schulz-Knappe, P., et al., *Endogenous natriuretic peptides: effect on collecting duct function in rat kidney*. Am. J. Physiol., 1990. **259**: p. F415-F418.
191. Light, D.B., et al., *Atrial natriuretic peptide inhibits a cation channel in renal inner medullary collecting duct cells*. Science, 1989. **243**: p. 383-385.
192. Umemura, S., D. Smyth, and W. Pettinger, *Lack of inhibition by atrial natriuretic factor on cyclic AMP levels in single nephron segments and the glomerulus*. Biochem. Biophys. Res. Comm., 1985. **127**: p. 943-949.
193. Nonoguchi, H., M. Knepper, and V. Manganiello, *Effects of atrial natriuretic factor on cyclic guanosine monophosphate and cyclic adenosine monophosphate accumulation in microdissected nephron segments from rats*. Clin. Invest., 1987. **79**: p. 500-507.
194. Dillingham, M. and R. Anderson, *Inhibition of vasopressin action by atrial natriuretic factor*. Science, 1986. **231**: p. 1572-1573.
195. Rouch, A.J., et al., *Na<sup>+</sup> transport in the isolated rat CCD: Effects of bradykinin, ANP, clonidine and hydrochlorothiazide*. Am. J. Physiol, 1991. **260 (Renal Fluid Electrolyte Physiol. 29)**: p. F86-F95.
196. Hawk, C. and J. Schafer, *Clonidine, but not bradykinin or ANP, inhibits Na and water transport in Dahl SS rat kidney*. Kidney Int., 1993. **44**: p. 30-35.
197. Schlatter, E., et al., *cGMP-activating peptides do not regulate electrogenic electrolyte transport in principal cells of rat CCD*. Am. J. Physiol., 1996. **271**: p. F1158-F1165.
198. Forssmann, W.-G., M. Meyer, and K. Forssmann, *The renal urodilatin system: clinical implications*. Cardiovascular Research, 2001. **51**: p. 450-462.
199. Heim, J., et al., *Urodilatin and B-ANF: Binding properties and activation of guanylate cyclase*. Biochem. Biophys. Res. Comm., 1989. **163**: p. 37-41.
200. Stanton, B., *Molecular mechanisms of ANP inhibition of renal sodium transport*. Can. J. Physiol. Pharmacol., 1990. **69**: p. 1546-1552.
201. Cornwell, T. and T. Lincoln, *Regulation of intracellular Ca levels in cultured vascular smooth muscle cells. Reduction of Ca by atriopeptin and 8-bromo-cyclic GMP-dependent protein kinase*. J. Biol. Chem., 1989. **264**: p. 1146-1155.
202. Forssmann, W.-G., *Urodilatin (Ularitide, INN): A renal natriuretic peptide*. Nephron, 1995. **69**: p. 211-222.
203. Meyer, M., R. Richter, and R. Brunkhorst, *Urodilatin is involved in sodium homeostasis and exerts sodium-state dependent natriuretic and diuretic effects*. Am. J. Physiol., 1996. **271**: p. F489-F497.

204. Forssmann, W.-G., R. Richter, and M. Meyer, *The endocrine heart and natriuretic peptides: histochemistry, cell biology, and functional aspects of the renal urodilatin system*. *Histochem. Cell Biol.*, 1998. **110**: p. 335-357.
205. Yanagisawa, M., et al., *A novel vasoconstrictor peptide produced by vascular endothelial cells*. *Nature*, 1988. **332**: p. 411-415.
206. Inoue, A., et al., *The human endothelin family: three structurally and pharmacologically distinct isopeptides predicted by three separate genes*. *Proceedings National Academy of Science*, 1989. **86**: p. 2863-2867.
207. Kohan, D. and E. Padilla, *Endothelin-1 is an autocrine factor in rat inner medullary collecting ducts*. *Am. J. Physiol.*, 1992. **263**: p. F607-F612.
208. Karet, F. and A. Davenport, *Localization of endothelin peptides in human kidney*. *Kidney Int.*, 1996. **49**: p. 382-387.
209. Kedzierski, R. and M. Yanagisawa, *Endothelin system: The double-edged sword in health and disease*. *Annu. Rev. Pharmacol. Toxicol.*, 2001. **41**: p. 851-876.
210. Douglas, S. and E. Ohlstein, *Signal transduction mechanisms mediating vascular actions of endothelin*. *J. Vasc. Res.*, 1997. **34**: p. 152-164.
211. Terada, Y., et al., *Different localization of two types of endothelin receptor mRNA in microdissected rat nephron segments using reverse transcription and polymerase chain reaction assay*. *J. Clin. Invest.*, 1992. **90**: p. 107-112.
212. Chow, L., et al., *Endothelin receptor mRNA expression in renal medulla identified by in situ RT-PCR*. *Am. J. Physiol.*, 1995. **269**: p. F449-F457.
213. Tomita, K., H. Nonoguchi, and F. Marumo, *Effects of endothelin on peptide-dependent cyclic adenosine monophosphate accumulation along the nephron segments of the rat*. *J. Clin. Invest.*, 1990. **85**: p. 2014-2018.
214. Nadler, S.P., J.A. Zimpelmann, and R.L. Hébert, *Endothelin inhibits vasopressin-stimulated water permeability in rat terminal inner medullary collecting duct*. *J. Clin. Invest.*, 1992. **90**: p. 1458-1466.
215. Edwards, R.M., et al., *Endothelin inhibits vasopressin action in rat inner medullary collecting duct via the ET<sub>B</sub> receptor*. *J. Pharmacol. Exp. Ther.*, 1993. **267**: p. 1028-1033.
216. Gariepy, C., et al., *Salt-sensitive hypertension in endothelin-B receptor-deficient rats*. *J. Clin. Invest.*, 2000. **105**: p. 925-933.
217. Pollock, D., et al., *Upregulation of endothelin B receptors in kidneys of DOCA-salt hypertensive rats*. *Am. J. Physiol.*, 2000. **278**: p. F279-F286.
218. Birnbaumer, M., et al., *Molecular cloning of the receptor for human antidiuretic hormone*. *Nature*, 1992. **357**: p. 333-335.
219. Lolait, S.J., et al., *Cloning and characterization of a vasopressin V<sub>2</sub> receptor and possible link to nephrogenic diabetes insipidus*. *Nature*, 1992. **357**: p. 336-339.
220. Morel, A., et al., *Molecular cloning and expression of a rat V<sub>1a</sub> arginine vasopressin receptor*. *Nature*, 1992. **356**: p. 523-526.
221. Phillips, P.A., et al., *Localization of vasopressin binding sites in rat tissues using specific V<sub>1</sub> and V<sub>2</sub> selective ligands*. *Endocrinology*, 1990. **126**(3): p. 1478-1484.

222. Ostrowski, N.L., et al., *Distribution of V1a and V2 vasopressin receptor messenger ribonucleic acids in rat liver, kidney, pituitary and brain*. *Endocrinology*, 1992. **131**: p. 533-535.
223. Takeuchi, K., et al., *Different cellular mechanisms of vasopressin receptor V1 and V2 subtype in vasopressin-induced adenosine 3', 5'-monophosphate formation in an immortalized renal tubule cell line, TKC2*. *Biochem. Biophys. Res. Comm.*, 1994. **202**(2): p. 680-687.
224. Russell, W.E. and L.R. Bucher, *Vasopressin modulates liver regeneration in the Brattleboro rat*. *Am. J. Physiol.*, 1983. **245**: p. G321-G324.
225. Burnatowska-Hledin, M.A. and W. Speilman, *Vasopressin increases cytosolic free calcium in LLC-PK1 cells through a V1 receptor*. *Am. J. Physiol.*, 1987. **253**: p. F328.
226. Serradeil-Le Gal, C., et al., *Autoradiographic localization of vasopressin V1a receptors in the rat kidney using [<sup>3</sup>H]-SR 49059*. *Kidney International*, 1996. **50**: p. 499-505.
227. Park, F., et al., *Localization of the vasopressin V1a and V2 receptors within the renal cortical and medullary circulation*. *Am. J. Physiol.*, 1997. **273**: p. R243-R251.
228. Antoni, F.A., *Novel ligand specificity of pituitary vasopressin receptors in the rat*. *Neuroendocrinology*, 1984. **39**: p. 186-188.
229. Schafer, J.A. and S.L. Troutman, *Effect of ADH on rubidium transport in isolated perfused rat cortical collecting tubules*. *Am. J. Physiol.*, 1986. **250 (Renal Fluid Electrolyte Physiol. 19)**: p. F1063-F1072.
230. Kojro, E., et al., *Direct identification of an extracellular agonist binding site in the renal V2 vasopressin receptor*. *Biochemistry*, 1993. **32**: p. 13537-13544.
231. Lands, A.M., F.P. Luduena, and H.J. Buzzo, *Differentiation of receptors responsive to isoproterenol*. *Life Sci.*, 1967. **6**: p. 2241-2249.
232. Lomasney, J.W., et al., *Molecular biology of  $\alpha$ -adrenergic receptors: implications for receptor classification and for structure-function relationships*. *Biochim. Biophys. Acta*, 1991. **1095**: p. 127-139.
233. Bylund, D.B., C. Ray-Prenger, and T.J. Murphy, *Alpha-2A- and alpha-2B-adrenergic receptor subtypes: antagonist binding in tissues and cell lines containing only one subtype*. *J Pharmacol Exp Ther*, 1988. **245**: p. 600-607.
234. Lanier, S.M., et al., *Identification of structurally distinct  $\alpha_2$ -adrenergic receptors*. *J. Biol. Chem*, 1988. **263**: p. 14491-14496.
235. Minneman, K.P.,  *$\alpha_1$ -adrenergic receptor subtypes, inositol phosphates, and sources of cell  $Ca^{++}$* . *Pharmacol Rev*, 1988. **40**: p. 87-119.
236. Lorenz, W., et al., *Expression of three  $\alpha_2$ -receptor subtypes in rat tissues: Implications for  $\alpha_2$ -receptor classification*. *Mol. Pharmacol.*, 1990. **38**: p. 599.
237. Uhlén, S. and J.E.S. Wikberg, *Delineation of three pharmacological subtypes of  $\alpha_2$ -adrenoceptor in the rat kidney*. *Br. J. Pharmacol*, 1991. **104**: p. 657-664.
238. Ruffolo, R.R.J., et al., *Structure and function of  $\alpha$ -adrenoceptors*. *Pharmacol. Rev*, 1991. **43**: p. 475-505.

239. Bylund, D.B., *Subtypes of  $\alpha_1$ - and  $\alpha_2$ -adrenergic receptors*. FASEB J, 1992. **6**: p. 832-839.
240. Bylund, D.B., et al., *Pharmacological characteristics of  $\alpha_2$ -adrenergic receptors: comparison of pharmacologically defined subtypes with subtypes identified by molecular cloning*. Mol. Pharmacol, 1992. **42**: p. 1-5.
241. Ruffolo, R.R.J., J.M. Stadel, and J.P. Hieble,  *$\alpha$ -Adrenoceptors: recent developments*. Med. Res. Rev, 1994. **14**: p. 229-270.
242. Blaxall, H.S., et al., *Characterization of the alpha-2C adrenergic receptor subtype in opossum kidney and in the OK cell line*. J. Pharmacol. Exp. Ther, 1991. **259**: p. 323-329.
243. Simonneaux, V., M. Ebada, and D.B. Bylund, *Identification and characterization of  $\alpha_{2D}$ -adrenergic receptors in bovine pineal gland*. Mol. Pharmacol, 1991. **40**: p. 235-241.
244. Timmermans, P.B.M.W.M., et al., *Characterization of  $\alpha$ -adrenoceptors participating in the central hypotensive and sedative effects of clonidine using yohimbine, rauwolscine and corynanthine*. Eur J Pharmacol, 1981. **70**: p. 7-15.
245. Coupry, I., et al., *Evidence for imidazoline binding sites in basolateral membranes from rabbit kidney*. Biochem. Biophys. Res. Commun, 1987. **147**: p. 1055-1060.
246. Michel, M.C., et al., *[ $^3$ H] idazoxan and some other  $\alpha_2$ -adrenergic drugs also bind with high affinity to a nonadrenergic site*. Mol. Pharmacol, 1989. **35**: p. 324-330.
247. Bousquet, P., et al., *New concepts on the central regulation of blood pressure. Alpha 2-adrenoceptors and "imidazoline receptors"*. Am J Med, 1989. **87**(3C): p. 10S-13S.
248. Bousquet, P., et al., *Imidazoline receptors. A new concept in central regulation of the arterial blood pressure*. Am J Hypertens, 1992. **5**(4 Pt 2): p. 47S-50S.
249. Penner, S.B. and D.D. Smyth, *Natriuresis following central and peripheral administration of agmatine in the rat*. Pharm., 1996. **53**: p. 160-169.
250. Angel, I., et al., *[ $^3$ H]Cirazoline as a tool for the characterization of imidazoline sites*. Ann. N.Y. Acad. Sci., 1995. **763**: p. 112-124.
251. Bousquet, P., *Imidazoline receptors: from basic concepts to recent developments*. J. Cardiovasc. Pharmacol, 1995. **26**(Suppl. 2): p. S1-S6.
252. Ernsberger, P.R., et al., *A second generation of centrally acting antihypertensive agents act on putative  $I_1$ -imidazoline receptors*. J. Cardiovasc. Pharmacol, 1992. **20**: p. S1-S10.
253. Hamilton, C.A., *The role of imidazoline receptors in blood pressure regulation*. Pharmacol. Ther, 1992. **54**: p. 231-248.
254. Molderings, G.J., et al., *Binding of [ $^3$ H] clonidine to  $I_1$ -imidazoline sites in bovine adrenal medullary membranes*. Naunyn-Schmiedeberg's Arch Pharmacol, 1993. **348**: p. 70-76.
255. Hamilton, C.A., *Imidazoline receptors, subclassification, and drug-induced regulation*. Annal. N.Y. Acad. Sci, 1995. **763**: p. 57-65.
256. Grenney, H., et al., *Heterogeneity of imidazoline binding sites revealed by a cirazoline derivative*. Eur. J. Pharm., 1994. **271**: p. 533-536.

257. Escribá, P.V., et al., *Molecular characterization and isolation of a 45-kilodalton imidazoline receptor protein from the rat brain*. Mol. Brain. Res, 1995. **32**: p. 187-196.
258. Olmos, G., R. Alemany, and J.A. Garcia-Sevilla, *Pharmacological and molecular discrimination of brain I2-imidazoline receptor subtypes*. Naunyn-Schmiedeberg's Arch Pharmacol, 1996. **354**: p. 709-716.
259. Tesson, F., et al., *Localization of I2-imidazoline binding sites on monoamine oxidases*. J. Biol. Chem., 1995. **270**: p. 9856-9861.
260. Atlas, D. and Y. Burnstein, *Isolation and partial purification of a clonidine-displacing endogenous brain substance*. Eur. J. Biochem., 1984. **144**: p. 287-293.
261. Li, G., et al., *Agmatine: an endogenous clonidine-displacing substance in the brain*. Science, 1994. **263**: p. 966-969.
262. Reis, D.J., G. Li, and S. Regunathan, *Endogenous ligands of imidazoline receptors: classic immunoreactive clonidine-displacing substance and agmatine*. Annal. N.Y. Acad. Sci, 1995. **763**: p. 295-313.
263. Piletz, J.E., D.N. Chikkala, and P. Ernsberger, *Comparison of the properties of agmatine and endogenous clonidine-displacing substance at imidazoline and alpha-2 adrenergic receptors*. J Pharmacol Exp Ther, 1995. **272**(2): p. 581-587.
264. Piletz, J.E., H. Zhu, and D.N. Chikkala, *Comparison of ligand binding affinities at human I1-imidazoline binding sites and the high affinity state of the alpha-2 adrenoceptor subtypes*. J Pharmacol Exp Ther, 1996. **279**(2): p. 694-702.
265. Feng, Y., A.E. Halaris, and J.E. Piletz, *Determination of agmatine in brain and plasma using high-performance liquid chromatography with fluorescence detection*. J Chromatogr B Biomed Appl, 1997. **691**(2): p. 277-286.
266. Reis, D., *Agmatine containing axon terminals in rat hippocampus form synapses on pyramidal cells*. Neuroscience Letters, 1999. **250**: p. 185-188.
267. Reis, D. and S. Regunathan, *Is agmatine a novel neurotransmitter in brain?* Trends in Physiological Science, 2000. **21**: p. 187-193.
268. Sastre, M., *Uptake of agmatine into rat brain synaptosomes: possible role of cation channels*. J. Neurochem., 1997. **69**: p. 2421-2426.
269. Lortie, M.J., et al., *Agmatine, a bioactive metabolite of arginine*. J. Clin. Invest, 1996. **97**: p. 413-420.
270. Regunathan, S.D. and D.J. Reis, *Imidazoline receptors and their endogenous ligands*. Annu Rev Pharmacol Toxicol, 1996. **36**: p. 511-544.
271. Loring, R.H., *Agmatine acts as an antagonist of neuronal nicotinic receptors*. Br J Pharmacol, 1990. **99**(1): p. 207-211.
272. Sener, A., et al., *Stimulus-secretion coupling of arginine-induced insulin release*. Biochemical Pharm., 1989. **38**: p. 327-330.
273. Taylor, I.L., *Pancreatic polypeptide family: pancreatic polypeptide, neuropeptide Y, and peptide YY*, in *Handbook of Physiology-The Gastrointestinal System*. 1989, Am. Physiol. Soc.: Bethesda. p. 475-543.
274. Ekblad, E., et al., *Neuropeptide Y co-exists and co-operates with noradrenaline in perivascular nerve fibers*. Regul. Peptides, 1984. **8**: p. 225-235.

275. Wahlestedt, C., et al., *Neuropeptide Y potentiates noradrenaline-evoked vasoconstriction: mode of action*. J Exp Pharmacol Exper Therapeut, 1985. **234 (3)**: p. 735-741.
276. Wahlestedt, C., et al., *Norepinephrine and neuropeptide Y: vasoconstrictor cooperation in vivo and in vitro*. Am J Physiol, 1990. **258**: p. R736-R742.
277. Ohtomo, Y., et al., *Coexisting NPY and NE synergistically regulate renal tubular Na<sup>+</sup>, K<sup>+</sup>-ATPase activity*. Kidney International, 1994. **45**: p. 1606-1613.
278. Ohtomo, Y., et al., *Neuropeptide Y regulates rat renal tubular Na, K-ATPase through several signalling pathways*. Acta Physiol Scand, 1996. **158**: p. 97-105.
279. Edvinsson, L., et al., *Neuropeptide Y potentiates the effect of various vasoconstrictor agents on rabbit blood vessels*. Br J Pharmacol, 1984. **83(2)**: p. 519-525.
280. Hill, F.L., et al., *Peptide YY, a new gut hormone*. Steroids, 1991. **56 (2)**(Feb): p. 77-82.
281. Sheikh, S.O., *Neuropeptide Y and peptide YY: major modulators of gastrointestinal blood flow and function*. Am. J. Physiol., 1991. **261**: p. G701-G715.
282. Pernow, J. and J.M. Lundberg, *Modulation of noradrenaline and neuropeptide Y (NPY) release in the pig kidney in vivo: involvement of alpha<sub>2</sub>, NPY and angiotensinII receptors*. Naunyn-Schmiedeberg's Arch Pharmacol, 1989. **340**: p. 379-385.
283. Dumont, Y., et al., *Neuropeptide Y and neuropeptide Y receptor subtypes in brain and peripheral tissues*. Prog. Neurobiol., 1992. **38**: p. 125-167.
284. Michel, M.C., et al., *XVI. International union of pharmacology recommendations for the nomenclature of neuropeptide Y, peptide YY, and pancreatic polypeptide receptors*. Pharmacol. Rev., 1998. **50(1)**: p. 143-150.
285. Walker, M.W. and R.J. Miller, *<sup>125</sup>I-neuropeptide Y and <sup>125</sup>I-peptide YY bind to multiple receptor sites in rat brain*. Mol. Pharmacol., 1988. **34**: p. 779-792.
286. Dumont, Y., et al., *Evaluation of truncated neuropeptide Y analogues with modifications of the tyrosine residue in position 1 on Y1, Y2 and Y3 receptor subtypes*. Eur J Pharmacol, 1993. **238(1)**(Jul 6): p. 37-45.
287. Jacques, D., et al., *Characterization of neuropeptide Y receptor subtypes in the normal human brain, including the hypothalamus*. Neuroscience, 1997. **79 (1)**: p. 129-148.
288. Dumont, Y., et al., *Comparitive characterization and autoradiographic distribution of neuropeptide Y receptor subtypes in the rat brain*. J Neurosci, 1993. **13(1)**(Jan 13): p. 73-86.
289. Gerald, C., et al., *A receptor subtype involved in neuropeptide-Y-induced food intake*. Nature, 1996. **382**: p. 168-171.
290. Gimpl, G., J. Wahl, and R.E. Lang, *Identification of a receptor protein for neuropeptide Y in rabbit kidney*. FEBS, 1991. **279 (2)**: p. 219-222.
291. Ausiello, D.A., et al., *Cell Signaling, in The Kidney: Physiology and Pathophysiology*, D.W. Seldin and G. Giebisch, Editors. 1992, Raven Press: New York. p. 645-706.
292. Northup, J.K., et al., *The subunits of the stimulatory regulatory component of adenylate cyclase*. J. Biol. Chem, 1983. **258**: p. 11369-11376.

293. Neer, E.J. and D.E. Clapham, *Roles of G protein subunits in transmembrane signalling*. Nature, 1988. **333**: p. 129-134.
294. Miller, R.T., *Transmembrane signalling through G proteins*. Kidney International, 1991. **39**: p. 421-429.
295. Masters, S.B., et al., *Carboxyl terminal domain of  $G_{s\alpha}$  specifies coupling of receptors to stimulation of adenylyl cyclase*. Science, 1988. **241**: p. 448-451.
296. Grady, E.F., S.K. Bohm, and N.W. Bunnett, *Turning off the signal: mechanisms that attenuate signaling by G protein-coupled receptors*. Am. J. Physiol., 1997. **273**: p. G586-G601.
297. Birnbaumer, L., J. Abramowitz, and A.M. Brown, *Receptor-effector coupling by G proteins*. Biochimica et Biophysica Acta, 1990. **1031**: p. 163-224.
298. Jans, D.A. and B.A. Hemmings, *cAMP-dependent protein kinase activation affects vasopressin  $V_2$ -receptor number and internalization in LLC-PK<sub>1</sub> renal epithelial cells*. FEBS Letters, 1991. **281**(1,2): p. 267-271.
299. Pratt, A.G., D.A. Ausiello, and H.F. Cantiello, *Vasopressin and protein kinase A activate G protein-sensitive epithelial Na<sup>+</sup> channels*. Am. J. Physiol., 1993. **265**: p. C218-C223.
300. Edwards, R.M. and M. Gellai, *Inhibition of vasopressin-stimulated cyclic AMP accumulation by alpha-2 adrenoceptor agonists in isolated papillary collecting ducts*. J. Pharm. Exp. Ther., 1988. **244**: p. 526-530.
301. Lankford, S.P., et al., *Regulation of collecting duct water permeability independent of cAMP-mediated AVP response*. Am. J. Physiol., 1991. **261**: p. F554-F566.
302. Breyer, M.D., *Regulation of water and salt transport in collecting duct through calcium-dependent signaling mechanisms*. Am. J. Physiol, 1991. **260 (Renal Fluid Electrolyte Physiol. 29)**: p. F1-F11.
303. Yanase, M. and J.S. Handler, *Activators of protein kinase C inhibit sodium transport in A6 epithelia*. Am. J. Physiol, 1986. **250 (Cell Physiol. 19)**: p. C517-C522.
304. Mohrmann, M., H.F. Cantiello, and D.A. Ausiello, *Inhibition of epithelial Na<sup>+</sup> transport by atriopeptin, protein kinase c, and pertussis toxin*. Am. J. of Physiol, 1987. **253 (Renal Fluid Electrolyte Physiol. 22)**: p. F372-F376.
305. Torikai, S. and K. Kurokawa, *Effect of PGE<sub>2</sub> on vasopressin-dependent cell cAMP in isolated single nephron segments*. Am. J. Physiol, 1983. **245 (Renal Fluid Electrolyte Physiol. 14)**: p. F58-F66.
306. Hébert, R.L., H.R. Jacobson, and M.D. Breyer, *PGE<sub>2</sub> inhibits AVP-induced water flow in cortical collecting ducts by protein kinase C activation*. Am. J. Physiol, 1990. **259 (Renal Fluid Electrolyte Physiol. 28)**: p. F318-F325.
307. Nadler, S.P., J.A. Zimpelmann, and R.L. Hébert, *PGE<sub>2</sub> inhibits water permeability at a post-cAMP site in rat terminal inner medullary collecting duct*. Am. J. Physiol, 1992. **262 (Renal Fluid Electrolyte Physiol. 31)**: p. F229-F235.
308. Kokko, K.E., et al., *Effects of prostaglandin E<sub>2</sub> on amiloride-blockable Na<sup>+</sup> channels in a distal nephron cell line (A6)*. Am. J. Physiol., 1994. **267**: p. C1414-C1425.
309. Simonds, W., *G protein regulation of adenylate cyclase*. Trends in Physiological Science, 1999. **20**: p. 66-72.

310. Sunahara, R., C. Dessauer, and A. Gilman, *Complexity and diversity of mammalian adenylyl cyclases*. Annual Review Pharmacology and Toxicology, 1996. **36**: p. 461-480.
311. Krupinski, J., et al., *Adenylyl cyclase amino acid sequence: possible channel- or transporter-like structure*. Science, 1989. **244**: p. 1558-1564.
312. Gao, B. and A. Gilman, *Cloning and expression of a widely distributed (type IV) adenylyl cyclase*. Proceedings National Academy of Science, 1991. **88**: p. 10178-10182.
313. Katsushika, S., et al., *Cloning and characterization of a sixth adenylyl cyclase isoform: types V and VI constitute a subgroup within the mammalian adenylyl cyclase family*. Proceedings National Academy of Science, 1992. **89**: p. 8774-8778.
314. Cali, J., et al., *Type VIII adenylyl cyclase*. Journal of Biological Chemistry, 1994. **269**: p. 12190-12195.
315. Watson, P., et al., *Molecular cloning and characterization of the type VII isoform of mammalian adenylyl cyclase expressed widely in mouse tissues and in S49 mouse lymphoma cells*. Journal of Biological Chemistry, 1994. **269**: p. 28893-28898.
316. Taussig, R., et al., *Distinct patterns of bidirectional regulation of mammalian adenylyl cyclases*. Journal of Biological Chemistry, 1994. **269**(8): p. 6093-6100.
317. Wittpoth, C., et al., *Regions on adenylyl cyclase that are necessary for inhibition of activity by  $\beta\gamma$  and  $G_{i\alpha}$  subunits of heterotrimeric G proteins*. Proceedings National Academy of Science, 1999. **96**: p. 9551-9556.
318. Hélices-Toussaint, C., et al., *Cellular localization of type 5 and type 6 ACs in collecting duct and regulation of cAMP synthesis*. Am. J. Physiol., 2000. **279**: p. F185-F194.
319. Ishikawa, Y. and C. Homcy, *The adenylyl cyclases as integrators of transmembrane signal transduction*. Circulation Research, 1997. **80**: p. 297-304.
320. Razani, B., C. Rubin, and M. Lisante, *Regulation of cAMP-mediated signal transduction via interaction of caveolins with the catalytic subunit of protein kinase A*. Journal of Biological Chemistry, 1999. **274**(37): p. 26353-26360.
321. Fraser, I., et al., *A novel lipid-anchored A-kinase anchoring protein facilitates cAMP-responsive membrane events*. EMBO Journal, 1998. **17**(8): p. 2261-2272.
322. Edwards, A. and J. Scott, *A-kinase anchoring proteins: protein kinase A and beyond*. Current Opinion in Cell Biology, 2000. **12**: p. 217-221.
323. Klussmann, E., et al., *Protein kinase A anchoring proteins are required for vasopressin-mediated translocation of aquaporin-2 into cell membranes of renal principal cells*. Journal of Biological Chemistry, 1998. **274**(8): p. 4934-4938.
324. Nishizuka, Y., *Protein kinase C and lipid signaling for sustained cellular responses*. FASEB J, 1995. **9**: p. 484-496.
325. Alvarez, J., M. Montero, and J. Garcia-Sancho, *Subcellular  $Ca^{++}$  dynamics*. News in Physiological Science, 1999. **14**: p. 161-168.
326. Pfaff, I., H.-J. Wagner, and V. Vallon, *Immunolocalization of protein kinase C isoenzymes  $\alpha$ ,  $\beta I$  and  $\beta II$  in rat kidney*. Journal American Society of Nephrology, 1999. **10**: p. 1861-1873.

327. Mochly-Rosen, D., H. Khaner, and J. Lopez, *Identification of intracellular receptor proteins for activated protein kinase C*. Proceedings National Academy of Science, 1991. **88**: p. 3997-4000.
328. Mochly-Rosen, D. and A. Gordon, *Anchoring proteins for protein kinase C: a means for isozyme selectivity*. FASEB, 1998. **12**: p. 35-42.
329. Bonvalet, J., P. Pradelles, and N. Farman, *Segmental synthesis and actions of prostaglandins along the nephron*. Am. J. Physiol., 1987. **253**: p. F377-F387.
330. Chabardès, D., et al., *Effect of PGE<sub>2</sub> and  $\alpha$ -adrenergic agonists on AVP-dependent cAMP levels in rabbit and rat CCT*. Am. J. Physiol, 1988. **255 (Renal Fluid Electrolyte Physiol. 24)**: p. F43-F48.
331. Stokes, J.B., *Modulation of vasopressin-induced water permeability of the cortical collecting tubule by endogenous and exogenous prostaglandins*. Mineral Electrolyte Metab, 1985. **11**: p. 240-248.
332. Blandford, D.E. and D.D. Smyth, *Potentiation of the natriuretic effect of clonidine following indomethacin in the rat*. Can. J. Physiol. Pharmacol, 1991. **69**: p. 1196-1203.
333. Breyer, M.D., H.R. Jacobson, and R.L. Hebert, *Cellular mechanisms of prostaglandin E<sub>2</sub> and vasopressin interactions in the collecting duct*. Kidney Int, 1990. **38**: p. 618-624.
334. Abramov, M., R. Beauwens, and E. Cogan, *Cellular events in vasopressin action*. Kidney Int., 1987. **32**: p. 56-66.
335. Ishikawa, S., K. Okada, and T. Saito, *Arginine vasopressin increases cellular free calcium concentration and adenosine 3',5'-monophosphate production in rat renal papillary collecting tubule cells in culture*. Endocrinology, 1988. **123**: p. 1376-1384.
336. Naruse, M., *Arginine vasopressin increases intracellular calcium ion concentration in isolated mouse collecting tubule cells: Distinct mechanism of action through V2 receptor, but independent of adenylate cyclase activation*. Japanese Journal of Nephrology, 1991. **34(4)**: p. 337-347.
337. Champigneulle, A., et al., *V2-like vasopressin receptor mobilizes intracellular Ca<sup>2+</sup> in rat medullary collecting tubules*. Am. J. Physiol., 1993. **265**: p. F35-F45.
338. Ecelbarger, C.A., et al., *Evidence for dual signaling pathways for V2 vasopressin receptor inn rat inner medullary collecting duct*. Am. J. Physiol., 1996. **270**: p. F623-633.
339. Dillingham, M.A., B.S. Dixon, and R.J. Anderson, *Calcium modulates vasopressin effect in rabbit cortical collecting tubule*. Am. J. Physiol., 1987. **252**: p. F115-121.
340. Jones, S.M., G. Frindt, and W. E.E., *Effect of peritubular [Ca] or ionomycin on hydrosmotic response of CCTs to ADH or cAMP*. Am. J. Physiol, 1988. **254(Renal Fluid Electrolyte Physiol. 23)**: p. F240-F253.
341. Teitelbaum, I. and T. Berl, *Increased cytosolic Ca<sup>2+</sup> inhibits AVP-stimulated adenylate cyclase activity in rat imct cells by activation of PKC*. Am. J. Physiol., 1994. **266**: p. F486-490.
342. Ridderstrale, Y., et al., *Morphological heterogeneity of the rabbit collecting duct*. Kidney International, 1987. **34**: p. 655-670.

343. Du Bois, R., A. Verniory, and M. Abramow, *Computation of the osmotic water permeability of perfused tubule segments*. *Kidney Int*, 1976. **10**: p. 478-479.
344. Hawk, C., L. Li, and J. Schafer, *AVP and aldosterone at physiological concentrations have synergistic effects on Na<sup>+</sup> transport in rat CCD*. *Kidney Int.*, 1996. **57**: p. S35-S41.
345. Benjamin, B.A., P.J. Mannon, and C.M. Breen, *Peptide YY inhibits vasopressin-stimulated chloride current in mIMCD-K2 cells*. *FASEB J.*, 1997. **11**: p. A9.
346. Helman, S.I., J.J. Grantham, and M.B. Burg, *Effect of vasopressin on electrical resistance of renal cortical collecting tubules*. *Am. J. Physiol.*, 1971. **220**: p. 1825-1832.
347. Frindt, G., H. Sackin, and L.G. Palmer, *Whole-cell currents in rat cortical collecting tubule: low-Na diet increases amiloride-sensitive conductance*. *Am. J. Physiol.*, 1990. **258 (Renal Fluid Electrolyte Physiol. 27)**: p. F562-F567.
348. Dawson-Saunders, B. and R. Trapp, *Basic and Clinical Biostatistics*. 1994: Appleton and Lange.
349. Glantz, S. and B. Slinker, *Primer of Applied Regression and Analysis of Variance*. 1990, New York: McGraw-Hill, Inc.
350. Dunn, O. and V. Clark, *Basic Statistics: A Primer for the Biomedical Sciences*. 3rd ed. Wiley series in probability and statistics, ed. N. Cressie. 2001, New York: John Wiley & Sons, Inc.
351. Payton, M., A. Miller, and W. Raun, *Testing statistical hypotheses using standard error bars and confidence intervals*. *Commun. Soil Sci. Plant Anal.*, 2000. **31(5,6)**: p. 547-551.
352. Hébert, R.L., H.R. Jacobson, and M.D. Breyer, *Prostaglandin E<sub>2</sub> inhibits sodium transport in rabbit cortical collecting duct by increasing intracellular calcium*. *J. Clin. Invest*, 1991. **87**: p. 1992-1998.
353. Gesek, F.A., *Alpha2-adrenergic receptors activate phospholipase C in renal epithelial cells*. *Molecular Pharmacology*, 1996. **50**: p. 407-414.
354. Rouch, A.J. and L.H. Kudo, *Role of PGE<sub>2</sub> in  $\alpha_2$ -induced inhibition of AVP-stimulated H<sub>2</sub>O, Na<sup>+</sup>, and urea transport in the IMCD*. *Am. J. Physiol.*, 1996. **279(2)**: p. F294-F304.
355. Ando, Y., H.R. Jacobson, and M.D. Breyer, *Phorbol ester and A23187 have additive but mechanistically separate effects on vasopressin action in rabbit collecting tubule*. *J. Clin. Invest*, 1988. **81**: p. 1578-1584.
356. Ishikawa, S.-E., K. Okada, and T. Saito, *Modulation by intracellular calcium pool of arginine vasopressin induced cellular cyclic AMP production in rat renal papillary collecting tubule cells in culture*. *Journal of Pharmacology and Experimental Therapeutics*, 1992. **263**: p. 1050-1055.
357. Maeda, Y., et al., *Vasopressin and oxytocin receptors coupled to Ca<sup>2+</sup> mobilization in rat inner medullary collecting duct*. *Am. J. Physiol.*, 1993. **265**: p. F15-25.
358. Champigneulle, A., et al., *Relationship between extra- and intracellular calcium in distal segments of the renal tubule. Role of the Ca<sup>2+</sup> receptor RaKCaR*. *J. Membrane Biol.*, 1997. **156**: p. 117-129.

359. Hoenderop, J., et al., *Hormone-stimulated  $Ca^{++}$  reabsorption in rabbit kidney cortical collecting system is cAMP-independent and involves a phorbol ester-insensitive PKC isotype.* *Kidney Int.*, 1999. **55**: p. 225-233.
360. Ankorina-Stark, L., S. Haxelmans, and E. Schlatter, *Functional evidence for the regulation of cytosolic  $Ca^{2+}$  activity via  $V1A$ -receptors and  $B$ -adrenoceptors in rat CCD.* *Cell Calcium*, 1997. **21**: p. 163-171.
361. Sands, J.M., et al., *Apical extracellular calcium/polyvalent cation-sensing receptor regulates vasopressin-elicited water permeability in rat kidney inner medullary collecting duct.* *J. Clin Invest.*, 1997. **99**: p. 1399-1405.
362. Riccardi, D., et al., *Localization of the extracellular  $Ca^{2+}$ -sensing receptor and PTH/PTHrP receptor in rat kidney.* *Am. J. Physiol.*, 1996. **271**: p. F951-956.
363. Kusano, E., et al., *Effects of calcium on the vasopressin-sensitive cAMP metabolism in medullary tubules.* *Am. J. Physiol.*, 1985. **249**: p. F956-F966.
364. Rouch, A.J., et al., *Intracellular  $Ca^{2+}$  and PKC activation do not inhibit  $Na^{+}$  and water transport in rat CCD.* *Am. J. Physiol.*, 1993. **265 (Renal Fluid Electrolyte Physiol. 34)**: p. F569-F577.
365. Ando, Y., H.R. Jacobson, and M.D. Breyer, *Phorbol myristate acetate, dioctanoylglycerol, and phosphatidic acid inhibit the hydroosmotic effect of vasopressin on rabbit cortical collecting tubule.* *J. Clin. Invest.*, 1987. **80**: p. 590-593.
366. Holt, W.F. and C. Lechene, *ADH-PGE<sub>2</sub> interactions in cortical collecting tubule. I. Depression of sodium transport.* *Am. J. Physiol.*, 1981. **241 (Renal Fluid Electrolyte Physiol. 10)**: p. F452-F460.
367. Schlatter, E., *Antidiuretic hormone regulation of electrolyte transport in the distal nephron.* *Renal Physiol. Biochem.*, 1989. **12**: p. 65-84.
368. Schafer, J. and L. Chen, *Low  $Na^{+}$  diet inhibits  $Na^{+}$  and water transport response to vasopressin in the rat cortical collecting duct.* *Kidney Int.*, 1998. **54**: p. 180-187.
369. Helman, S.I., *Determination of electrical resistance of the isolated cortical collecting tubule and its possible anatomical location.* *Yale J. Bio and Med*, 1972. **45**: p. 339-345.
370. Naruse, M., et al., *Electrophysiological study of luminal and basolateral vasopressin in rabbit cortical collecting duct.* *Am. J. Physiol.*, 1995. **268**: p. F20-F29.
371. Frindt, G., et al., *Potential role of cytoplasmic calcium ions in the regulation of sodium transport in renal tubules.* *Mineral Electrolyte Metab*, 1988. **14**: p. 40-47.
372. Frindt, G. and E.E. Windhager,  *$Ca^{2+}$  - dependent inhibition of sodium transport in rabbit cortical collecting tubules.* *Am. J. Physiol.*, 1990. **258 (Renal Fluid Electrolyte Physiol. 27)**: p. F568-F582.
373. Uhlén, S., et al., *Comparison of the binding activities of some drugs on  $\alpha_{2A}$ ,  $\alpha_{2B}$  and  $\alpha_{2C}$ -adrenoceptors and non-adrenergic imidazoline sites in the guinea pig.* *Pharmacol. Toxicol.*, 1995. **76**: p. 353-364.
374. Blandford, D.E. and D.D. Smyth, *Enhanced natriuretic potency of intravenous clonidine: Extrarenal site of action?* *Eur. J. Pharmacol.*, 1989. **174**: p. 181-188.

375. Smyth, D.D., et al., *Opposite rank order of potency for alpha-2 adrenoceptor agonists on water and solute excretion in the rat: two sites and/or receptors?* J. Pharmacol. Exp. Ther, 1992. **261**: p. 1080-1086.
376. Chabardés, D., et al., *Inhibition of  $\alpha_2$ -adrenergic agonists on AVP-induced cAMP accumulation in isolated collecting tubule of the rat kidney.* Mol. Cell Endocrinol, 1984. **37**: p. 263-275.
377. Ling, B.N., et al., *Regulation of the amiloride-blockable sodium channel from epithelial tissue.* Mol. Cell. Biochem, 1990. **99**: p. 141-150.
378. Wilborn, T.W., et al., *Multiple  $\alpha_1$  and  $\alpha_2$  isoforms are expressed in the rat proximal straight tubule and cortical collecting duct.* FASEB J, 1996. **10**: (abstract) A404.
379. Bousquet, P., J. Feldman, and J. Schwartz, *Central cardiovascular effects of Alpha adrenergic drugs: differences between catecholemines and imidazolines.* J. of Pharm. and Exp. Therapeutics, 1984. **230**: p. 232-236.
380. Allan, D.R., S.B. Penner, and D.D. Smyth, *Renal imidazoline preferring sites and solute excretion in the rat.* Br. J. Pharmacol, 1993. **108**: p. 870-875.
381. Michel, M.C. and P. Ernsberger, *Keeping an eye on the I site: imidazoline-preferring receptors.* TIPS, 1992. **13**: p. 369-370.
382. Callado, L.F., A.M. Gabilondo, and J.J. Meana, *[<sup>3</sup>H]RX821002 (2-methoxyidazoxan) binds to  $\alpha_2$ -adrenoceptor subtypes and a non-adrenoceptor imidazoline binding site in rat kidney.* Eur. J. Pharmacol, 1996. **316**: p. 359-368.
383. Blandford, D.E. and D.D. Smyth, *Dose-selective dissociation of water and solute excretion after renal alpha<sub>2</sub>- adrenoceptor stimulation.* J. Pharmacol. Exp. Ther, 1988. **247**: p. 1181-1186.
384. Nutt, D., et al., *Functional studies of specific imidazoline-2 receptor ligands.* Annals New York Academy of Science, 1995. **12**(763): p. 125-139.
385. Morrissey, M.R., Ishidoya S, Klahr S, *Partial cloning and characterization of an arginine decarboxylase in the kidney.* Kidney Int., 1995. **47**: p. 1458-1461.
386. Schwartz, D., et al., *Agmatine affects glomerular filtration via a nitric oxide synthase-dependent mechanism.* Am. J. Physiol., 1997. **272**(41): p. F597-F601.
387. Bousquet, P., et al., *From the alpha 2-adrenoceptors to the imidazoline preferring receptors.* Fundam Clin Pharmacol, 1992. **6**(Suppl 1): p. 15S-21S.
388. Piletz, J.E. and K. Sletten, *Nonadrenergic imidazoline binding sites on human platelets.* J. Pharmacol. Exp. Ther, 1993. **267**: p. 1493--1502.
389. Alemany, R., G. Olmos, and J. Garcia-Sevilla, *The effects of phenelzine and other monoamine oxidase inhibitor antidepressants on brain and liver I<sub>2</sub> imidazoline-preferring receptors.* British Journal of Pharmacology, 1995. **114**: p. 837-845.
390. Bidet, M., P. Poujeol, and A. Parini, *The imidazoline-guanidinium receptor site, a target for some alpha-2 adrenergic agonists, is involved in inhibition of Na<sup>+</sup>-H<sup>+</sup> exchange in renal proximal tubule cells.* J. Hypertens, 1991. **9**: p. S216-S217.
391. Carpené, C., et al., *Inhibition of amine oxidase activity by derivatives that recognize imidazoline I<sub>2</sub> sites.* Journal of Pharmacology and Experimental Therapeutics, 1995. **272**(2): p. 681-688.

392. Pignini, M., et al., *Imidazoline receptors: qualitative structure-activity relationships and discovery of racizoline and benazoline. Two ligands with high affinity and unprecedented selectivity.* Bioorganic and Medicinal Chem., 1997. **5**: p. 833-841.
393. Flamaz, A., et al., *Pharmacological characterization of I<sub>1</sub> and I<sub>2</sub> imidazoline receptors in human striatum.* Neurochemistry International, 1997. **30**(1): p. 25-29.
394. Bricca, G., et al., *Human brain imidazoline receptors: further characterization with [<sup>3</sup>H]clonidine.* Eur. J. Pharmacol, 1994. **266**: p. 25-33.
395. Pinthong, D., et al., *Agmatine recognizes  $\alpha_2$ -adrenoceptor binding sites but neither activates nor inhibits  $\alpha_2$ -adrenoceptors.* Naunyn-Schmiedeberg's Arch. Pharmacol., 1995. **351**: p. 10-16.
396. Molderings, G., et al., *Dual interaction of agmatine with the rat  $\alpha_{2D}$ -adrenoceptor: competitive antagonism and allosteric activation.* British Journal of Pharmacology, 2000. **130**: p. 1706-1712.
397. Perney, T. and R. Miller, *Two different G proteins mediate neuropeptide Y and bradykinin-stimulated phospholipid breakdown in cultured rat sensory neurons.* Journal of Biological Chemistry, 1989. **264**: p. 7371-7327.
398. Michel, M., et al., *Further characterization of neuropeptide Y receptor subtypes using centrally truncated analogs of neuropeptide Y: evidence for subtype-differentiating effects on affinity and intrinsic efficacy.* Molecular Pharmacology, 1992. **42**: p. 642-648.
399. Sheikh, P., M. Sheikh, and T. Schwartz, *Y<sub>2</sub>-type receptors for peptide YY on renal proximal tubular cells in the rabbit.* Am. J. Physiol., 1989. **257**: p. F978-F984.
400. Leys, K., M. Schachter, and P. Sever, *Autoradiographic localisation of NPY receptors in rabbit kidney: comparison with rat, guinea-pig and human.* European Journal of Pharmacology, 1987. **134**: p. 233-237.
401. Price, J., et al., *Neuropeptide Y (NPY) metabolism by endopeptidase-2 hinders characterization of NPY receptors in rat kidney.* British Journal of Pharmacology, 1991. **104**: p. 321-326.
402. Wahlestedt, C., N. Yanaihara, and R. Hakanson, *Evidence for different pre- and post-junctional receptors for neuropeptide Y and related peptides.* Regulatory Peptides, 1986. **13**: p. 307-318.
403. Savage, A., et al., *Is raised plasma peptide YY after intestinal resection in the rat responsible for the trophic response?* Gut, 1985. **26**: p. 1353-1358.
404. Voisin, T., C. Rouyer-Fessard, and M. Laburthe, *Distribution of common peptide YY-neuropeptide Y receptor along rat intestinal villus-crypt axis.* Am. J. Physiol., 1990. **258**: p. G753-G759.
405. Playford, R., et al., *Effect of peptide YY on human renal function.* Am. J. Physiol., 1995. **268**: p. F754-F759.
406. Illes, P. and J. Regenold, *Interaction between neuropeptide Y and noradrenaline on central catecholamine neurons.* Nature, 1990. **344**: p. 62-63.
407. Selbie, L., et al., *Synergistic interaction of Y<sub>1</sub>-neuropeptide Y and  $\alpha_1$ -adrenergic receptors in the regulation of phospholipase C, protein kinase C, and arachidonic acid production.* Journal of Biological Chemistry, 1995. **270**(20): p. 11789-11796.

408. Harfstrand, A. and K. Fluxé, *Simultaneous central administration of adrenaline and neuropeptide Y leads to antagonistic interactions in vasodepressor responses in awake male rats*. Acta Physiol. Scand., 1987. **130**: p. 529-531.

## Appendix A - $\alpha$ -Adrenergic and Imidazoline Receptor Agonists and Antagonists

### Agonists:

Agmatine	IR, $\alpha_2$ -AR	$I_1 \gg I_2 \gg \alpha_{2A}$
AGN192403	IR <sub>1</sub>	
2 BFI	IR <sub>2</sub>	$I_2 > I_1 \gg \alpha_{2A}$
BHT920	$\alpha_{2A}$ -AR, IR	
Cirazoline	$\alpha_2$ -AR, IR	$I_2 > I_1 > \alpha_{2A}$
Cimetidine	IR <sub>1</sub>	
Clonidine	$\alpha_2$ -AR, IR <sub>1</sub>	$\alpha_{2A} > I_1 \gg I_2$
p-Aminoclonidine	$\alpha_2$ -AR, IR	
Dexmedetomidine	$\alpha_2$ -AR, IR	
Epinephrine	$\alpha_1$ -AR, $\alpha_2$ -AR	
Guanabenz	$\alpha_2$ -AR, IR <sub>2</sub>	$\alpha_{2A} > I_2 \gg I_1$
Guanfacine (GOB)	$\alpha_{2A}$ -AR	
Methoxamine	$\alpha_1$ -AR	
Moxonidine	IR <sub>1</sub>	$I_1 > \alpha_{2A} \gg I_2$
Naphazoline	$\alpha_2$ -AR, IR	$\alpha_{2A} > I_1 \gg I_2$
Oxymetazoline	$\alpha_{2A}$ -AR	$\alpha_{2A} = I_1 > \alpha_{2C} \gg \alpha_{2B} \gg I_2$
Phenylephrine	$\alpha_1$ -AR	
Rilmenidine	$\alpha_2$ -AR, IR <sub>1</sub>	$\alpha_{2A} = I_1$
UK14304	$\alpha_2$ -AR, IR	

### Antagonists:

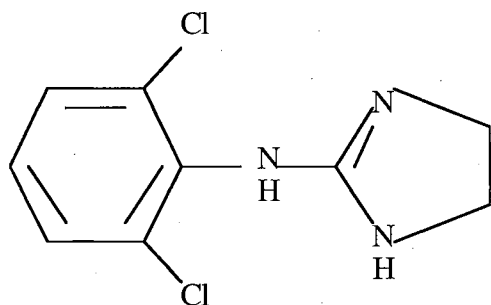
Arc239	$\alpha_{2B}$ -AR	
Atipamizole	$\alpha_2$ -AR, IR	
Benextramine	$\alpha_2$ -AR	
BRL44408	$\alpha_{2A}$ -AR	
BU224, 226, 239	IR <sub>2</sub>	
Corynanthine	$\alpha_1$ -AR	
Efaroxan	$\alpha_2$ -AR, IR <sub>1</sub>	$\alpha_{2A} > I_1 \gg I_2$
Idazoxan	$\alpha_2$ -AR, IR <sub>2</sub>	$I_2 > \alpha_{2A} \gg I_1$
Indoramin	$\alpha_1$ -AR	
Phentolamine	$\alpha_1$ -AR, $\alpha_2$ -AR, IR	$I_1 > \alpha_{2A} \gg I_2$
Prazosin	$\alpha_1$ -AR, $\alpha_{2B}$ -AR	
Rauwolscine	$\alpha_2$ -AR	
RX821002	$\alpha_2$ -AR	
SK&F104078	$\alpha_2$ -AR	
SK&F86466	$\alpha_2$ -AR	
Tolazoline	$\alpha_1$ -AR, $\alpha_2$ -AR, IR	
WB4101	$\alpha_1$ -AR, $\alpha_{2C}$ -AR	$\alpha_{2C} > \alpha_{2A} > \alpha_{2B}$
Yohimbine	$\alpha_2$ -AR	

### NOTES:

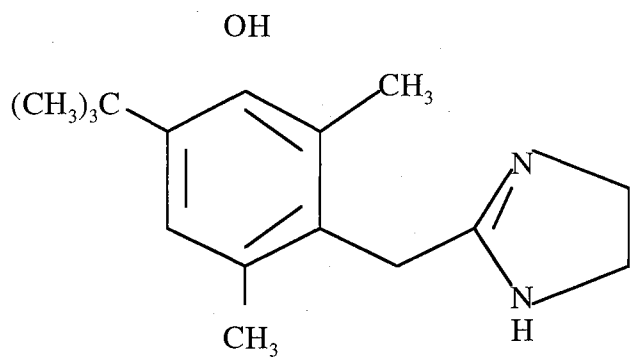
I<sub>1</sub> - clonidine preference, plasma membrane bound and G protein mediated

I<sub>2</sub> - cirazoline and idazoxan preference, mitochondrial bound and MAO mediated

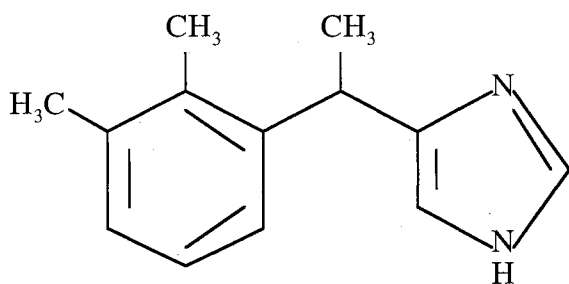
Appendix B - Chemical Structures



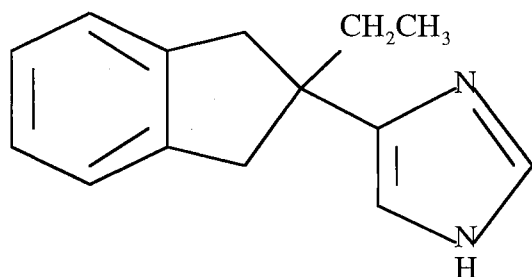
Clonidine



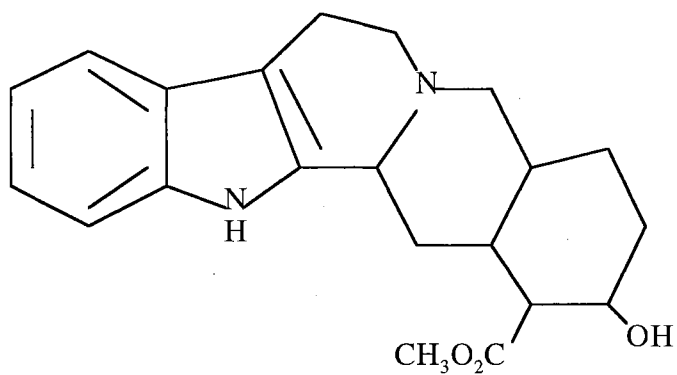
Oxymetazoline



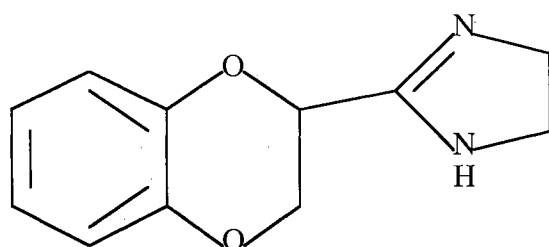
Dexmedetomidine



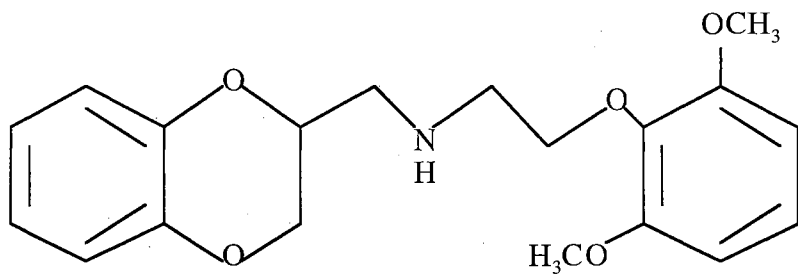
Atipamezole



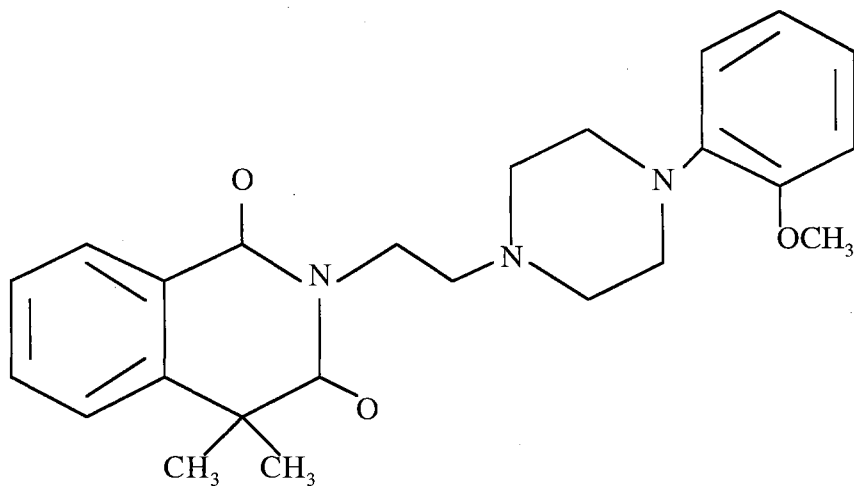
Yohimbine



Idazoxan



WB4101



ARC-239

### Appendix C - Experimental Drugs

Agmatine (Agm) Use 1 $\mu$ l in 10 mls bath for 1 $\mu$ M	Stock solution	2.28 mg Agm per ml water
Amiloride (Amil) May need to sonicate to dissolve Filter before using	0.27 mg in 100 mls control bath solution	
Arginine Vasopressin (AVP) Use 1 $\mu$ l per ml bath for 220 pM Make new stock solution every 2 weeks	Stock solution:	100 $\mu$ l AVP in 9.89 mls water
Atipamizole (Ati) Use 1 $\mu$ l in 100 mls bath for 100 nM Use 1 $\mu$ l in 10 mls bath for 1 $\mu$ M	Stock solution:	3.1 mg Ati per ml water
cAMP (8-CPT-cAMP) Use 750 $\mu$ l in 150 mls bath for 100 $\mu$ M Aliquot and freeze with dessicant	Stock solution: water	100 mg cAMP in 10 mls
Dexmedetomidine (Dex) Use 1 $\mu$ l in 100 mls bath for 100 nM Use 1 $\mu$ l in 10 mls bath for 1 $\mu$ M	Stock solution:	2.95 mg Dex per ml water
Idazoxan (Ida) Use 12 $\mu$ l in 50 mls bath	Stock solution:	1 mg Ida per ml water
Indomethacin (Indo) Use 1 $\mu$ l per ml bath for 5 $\mu$ M	Stock solution:	1.8 mg Indo per ml water
Oxymetazoline (Oxy) Use 1 $\mu$ l in 10 mls bath for 1 $\mu$ M	Stock solution:	2.97 mg Oxy per ml water
Peptide YY <sub>3-36</sub> (PYY <sub>3-36</sub> ) Aliquot and freeze 92 $\mu$ l per vial Use 1 vial per 50 mls bath for 100 nM	Stock solution:	2.5 mls water in 0.5 mg vial
Staurosporine (ST) Aliquot and freeze 100 $\mu$ l per vial Use 1 vial per 200 mls bath for 1 $\mu$ M	Stock solution:	100 mg SSP in 1 ml water
WB 4101 (WB) Aliquot and freeze 5 $\mu$ l per vial Use 5 $\mu$ l in 100 mls bath for 1 $\mu$ M	Stock solution:	50 mg WB in 6.58 mls water
Yohimbine (Yoh) HCl Aliquot and freeze 100 $\mu$ l per vial Use 1 vial per 100 mls bath for 1 $\mu$ M	Stock solution:	9.8 mg Yoh in 25 mls water

## Appendix D - Data Tables and Statistics

### Chapter IV - Figure 1A

#### Raw Data:

Experiment	#1	#2	#3	#4
Control	3.0000	4.0000	5.0000	4.0000
AVP	176.00	272.00	177.00	568.00
AVP2	133.00	143.00	78.000	488.00
AVP3	173.00	115.00	82.000	462.00

#### Descriptive Statistics:

	Count	Mean	Std. Dev.	Std. Error
Control	4	4.000	.816	.408
AVP	4	298.250	185.383	92.692
AVP2	4	210.500	187.194	93.597
AVP3	4	208.000	173.461	86.730

#### ANOVA:

##### Type III Sums of Squares

Source	df	Sum of Squares	Mean Square	F-Value	P-Value	G-G	H-F
Subject	3	218976.688	72992.229				
condition	3	186692.688	62230.896	7.043	.0098	.0643	.0477
condition * Subject	9	79517.063	8835.229				

Dependent: conditions

#### Contrasts:

	Vs.	Diff.	Std. Error	t-Test	P-Value
Control	AVP	-294.250	66.465	-4.427	.0017
	AVP2	-206.500	66.465	-3.107	.0126
	AVP3	-204.000	66.465	-3.069	.0134
AVP	AVP2	87.750	66.465	1.320	.2193
	AVP3	90.250	66.465	1.358	.2076
AVP2	AVP3	2.500	66.465	.038	.9708

Chapter IV - Figure 1B

Raw Data:

Experiment	#1	#2	#3	#4
Control	0.0000	0.0000	2.0000	2.0000
AVP	326.00	236.00	202.00	315.00
LC AVP	171.00	148.00	267.00	332.00
AVP2	183.00	208.00	290.00	316.00
Control	13.000	0.0000	29.000	4.0000

Descriptive Statistics:

	Count	Mean	Std. Dev.	Std. Error
Control	4	1.000	1.155	.577
AVP	4	269.750	60.390	30.195
LC AVP	4	229.500	85.590	42.795
AVP2	4	249.250	63.788	31.894
Control2	4	11.500	12.871	6.436

ANOVA:

Type III Sums of Squares

Source	df	Sum of Squares	Mean Square	F-Value	P-Value	G-G	H-F
Subject	3	15458.000	5152.667				
conditions	4	287479.700	71869.925	28.588	.0001	.0019	.0001
conditions * Subject	12	30167.500	2513.958				

Dependent: Compact Variable 1

Contrasts:

	Vs.	Diff.	Std. Error	t-Test	P-Value
Control	AVP	-268.750	35.454	-7.580	.0001
	LC AVP	-228.500	35.454	-6.445	.0001
	AVP2	-248.250	35.454	-7.002	.0001
	Control2	-10.500	35.454	-.296	.7722
AVP	LC AVP	40.250	35.454	1.135	.2784
	AVP2	20.500	35.454	.578	.5738
	Control2	258.250	35.454	7.284	.0001
LC AVP	AVP2	-19.750	35.454	-.557	.5877
	Control2	218.000	35.454	6.149	.0001
AVP2	Control2	237.750	35.454	6.706	.0001

Chapter IV - Figure 2A

Raw Data:

Experiment	#1	#2	#3	#4
Control	10.000	4.0000	2.0000	35.000
AVP	557.00	571.00	417.00	747.00
AVP+Dex	38.000	120.00	131.00	246.00
AVP+Dex+Ati	451.00	597.00	326.00	633.00

Descriptive Statistics:

	Count	Mean	Std. Dev.	Std. Error
Control	4	12.750	15.218	7.609
AVP	4	573.000	135.243	67.621
AVP+Dex	4	133.750	85.566	42.783
AVP+Dex+Ati	4	501.750	141.141	70.571

ANOVA:

Type III Sums of Squares

Source	df	Sum of Squares	Mean Square	F-Value	P-Value	G-G	H-F
Subject	3	86222.688	28740.896				
condition	3	901083.188	300361.063	52.931	.0001	.0003	.0001
condition * Subject	9	51071.563	5674.618				

Dependent: conditions

Contrasts:

	Vs.	Diff.	Std. Error	t-Test	P-Value
Control	AVP	-560.250	53.266	-10.518	.0001
	AVP+Dex	-121.000	53.266	-2.272	.0492
	AVP+Dex+Ati	-489.000	53.266	-9.180	.0001
AVP	AVP+Dex	439.250	53.266	8.246	.0001
	AVP+Dex+Ati	71.250	53.266	1.338	.2138
AVP+Dex	AVP+Dex+Ati	-368.000	53.266	-6.909	.0001

Chapter IV - Figure 2B

Raw Data:

Experiment	#1	#2	#3	#4	#5
Control	3.000	0.000	3.000	2.000	2.000
AVP	465.0	406.0	228.0	713.0	707.0
LC AVP+Dex	466.0	296.0	74.00	114.0	149.0
AVP	595.0	351.0	157.0	715.0	337.0

Descriptive Statistics:

	Count	Mean	Std. Dev.	Std. Error
control	5	2.000	1.225	.548
avp	5	503.800	207.479	92.788
LC avp+dex	5	219.800	161.156	72.071
avp2	5	431.000	222.410	99.465

ANOVA:

Type III Sums of Squares

Source	df	Sum of Squares	Mean Square	F-Value	P-Value	G-G	H-F
Subject	4	195859.300	48964.825				
condition	3	767302.950	255767.650	11.037	.0009	.0038	.0009
condition * Subject	12	278086.300	23173.858				

Dependent: conditions

Contrasts:

	Vs.	Diff.	Std. Error	t-Test	P-Value
control	avp	-501.800	96.278	-5.212	.0002
	LC avp+dex	-217.800	96.278	-2.262	.0430
	avp2	-429.000	96.278	-4.456	.0008
avp	LC avp+dex	284.000	96.278	2.950	.0121
	avp2	72.800	96.278	.756	.4642
LC avp+dex	avp2	-211.200	96.278	-2.194	.0487

Chapter IV - Figure 1D

Raw Data:

Experiment	#1	#2	#3
Control	1.0000	2.0000	1.0000
AVP	234.00	536.00	202.00
LC AVP+Q2AM	31.000	-87.000	50.000
AVP	17.000	-205.00	-299.00

Descriptive Statistics:

	Count	Mean	Std. Dev.	Std. Error
control	3	1.333	.577	.333
avp	3	324.000	184.293	106.402
q2am	3	-2.000	74.223	42.852
avp2	3	-162.333	162.263	93.683

ANOVA:

Type III Sums of Squares

Source	df	Sum of Squares	Mean Square	F-Value	P-Value	G-G	H-F
Subject	2	16239.500	8119.750				
condition	3	374560.917	124853.639	6.493	.0259	.0690	.0259
condition * Subject	6	115365.833	19227.639				

Dependent: conditions conditions

Contrasts:

	Vs.	Diff.	Std. Error	t-Test	P-Value
control	avp	-322.667	113.218	-2.850	.0292
	q2am	3.333	113.218	.029	.9775
	avp2	163.667	113.218	1.446	.1984
avp	q2am	326.000	113.218	2.879	.0281
	avp2	486.333	113.218	4.296	.0051
q2am	avp2	160.333	113.218	1.416	.2065

Chapter IV - Figure 3A

Raw Data:

Experiment	#1	#2	#3	#4
Control	2.0000	1.0000	0.0000	4.0000
AVP	585.00	417.00	583.00	288.00
AVP+Dex	31.000	157.00	328.00	104.00
AVP+Dex+I+S	231.00	276.00	555.00	257.00
AVP+Dex	0.0000	167.00	362.00	200.00

Descriptive Statistics:

	Count	Mean	Std. Dev.	Std. Error
Control	4	1.750	1.708	.854
AVP	4	468.250	143.660	71.830
AVP+Dex	4	155.000	126.372	63.186
AVP+dex+I+S	4	334.750	149.243	74.622
AVP+Dex2	4	182.250	148.406	74.203

ANOVA:

Type III Sums of Squares

Source	df	Sum of Squares	Mean Square	F-Value	P-Value	G-G	H-F
Subject	3	130156.400	43385.467				
condition	4	510903.800	127725.950	13.616	.0002	.0094	.0003
condition * Subject	12	112570.600	9380.883				

Dependent: conditions

Contrasts:

	Vs.	Diff.	Std. Error	t-Test	P-Value
Control	AVP	-466.500	68.487	-6.812	.0001
	AVP+Dex	-153.250	68.487	-2.238	.0450
	AVP+dex+I+S	-333.000	68.487	-4.862	.0004
	AVP+Dex2	-180.500	68.487	-2.636	.0218
AVP	AVP+Dex	313.250	68.487	4.574	.0006
	AVP+dex+I+S	133.500	68.487	1.949	.0750
	AVP+Dex2	286.000	68.487	4.176	.0013
AVP+Dex	AVP+dex+I+S	-179.750	68.487	-2.625	.0222
	AVP+Dex2	-27.250	68.487	-.398	.6977
AVP+dex+I+S	AVP+Dex2	152.500	68.487	2.227	.0459

Chapter IV - Figure 3B

Raw Data:

Experiment	#1	#2	#3	#4	#5
Control	3.0000	7.0000	6.0000	2.0000	7.0000
AVP	494.00	306.00	382.00	546.00	546.00
AVP+Dex	28.000	132.00	109.00	281.00	271.00
AVP+Dex+I	46.000	47.000	0.0000	159.00	182.00
AVP+Dex	20.000	0.0000	0.0000	299.00	205.00

Descriptive Statistics:

	Count	Mean	Std. Dev.	Std. Error
control	4	3.000	2.944	1.472
avp	4	543.750	38.871	19.435
avp+dex	4	191.000	117.073	58.536
avp+dex+indo	4	126.500	59.646	29.823
avp+dex2	4	174.250	115.906	57.953

ANOVA:

Type III Sums of Squares

Source	df	Sum of Squares	Mean Square	F-Value	P-Value	G-G	H-F
Subject	3	58493.400	19497.800				
condition	4	651291.700	162822.925	51.203	.0001	.0019	.0003
condition * Subject	12	38159.100	3179.925				

Dependent: conditions

Contrasts:

	Vs.	Diff.	Std. Error	t-Test	P-Value
control	avp	-540.750	39.874	-13.561	.0001
	avp+dex	-188.000	39.874	-4.715	.0005
	avp+dex+indo	-123.500	39.874	-3.097	.0092
	avp+dex2	-171.250	39.874	-4.295	.0010
avp	avp+dex	352.750	39.874	8.847	.0001
	avp+dex+indo	417.250	39.874	10.464	.0001
	avp+dex2	369.500	39.874	9.267	.0001
avp+dex	avp+dex+indo	64.500	39.874	1.618	.1317
	avp+dex2	16.750	39.874	.420	.6819
avp+dex+indo	avp+dex2	-47.750	39.874	-1.198	.2542

Chapter IV - Figure 3C

Raw Data:

Experiment	#1	#2	#3	#4
Control	0.0000	6.0000	12.000	18.000
AVP	564.00	444.00	261.00	279.00
AVP+Dex	294.00	78.000	54.000	29.000
AVP+Dex+S	273.00	155.00	174.00	0.0000

Descriptive Statistics:

	Count	Mean	Std. Dev.	Std. Error
control	4	9.000	7.746	3.873
avp	4	387.000	143.896	71.948
avp+dex	4	113.750	121.821	60.910
avp+dex+st	4	150.500	112.885	56.442

ANOVA:

Type III Sums of Squares

Source	df	Sum of Squares	Mean Square	F-Value	P-Value	G-G	H-F
Subject	3	89801.688	29933.896				
conditions	3	305827.188	101942.396	16.607	.0005	.0046	.0005
conditions * Subject	9	55246.063	6138.451				

Dependent: condition

Contrasts:

	Vs.	Diff.	Std. Error	t-Test	P-Value
control	avp	-378.000	55.401	-6.823	.0001
	avp+dex	-104.750	55.401	-1.891	.0912
	avp+dex+st	-141.500	55.401	-2.554	.0310
avp	avp+dex	273.250	55.401	4.932	.0008
	avp+dex+st	236.500	55.401	4.269	.0021
avp+dex	avp+dex+st	-36.750	55.401	-.663	.5237

Chapter IV - Figure 3D

Raw Data:

Experiment	#1	#2	#3	#4	#5
Control	5.0000	1.0000	1.0000	12.000	6.0000
AVP	292.00	195.00	200.00	261.00	325.00
AVP+Dex	125.00	90.000	62.000	54.000	78.000
AVP+Dex+S	167.00	188.00	112.00	174.00	155.00

Descriptive Statistics:

	Count	Mean	Std. Dev.	Std. Error
control	5	5.000	4.528	2.025
avp	5	254.600	56.853	25.426
avp+dex	5	81.800	27.896	12.476
avp+dex+st	5	159.200	28.960	12.951

ANOVA:

Type III Sums of Squares

Source	df	Sum of Squares	Mean Square	F-Value	P-Value	G-G	H-F
Subject	4	7079.300	1769.825				
conditions	3	171159.750	57053.250	55.215	.0001	.0001	.0001
conditions * Subject	12	12399.500	1033.292				

Dependent: condition

Contrasts:

	Vs.	Diff.	Std. Error	t-Test	P-Value
control	avp	-249.600	20.330	-12.277	.0001
	avp+dex	-76.800	20.330	-3.778	.0026
	avp+dex+st	-154.200	20.330	-7.585	.0001
avp	avp+dex	172.800	20.330	8.500	.0001
	avp+dex+st	95.400	20.330	4.693	.0005
avp+dex	avp+dex+st	-77.400	20.330	-3.807	.0025

Chapter IV - Figure 4A

Raw Data:

Experiment	#1	#2	#3	#4	#5
Control	1.00	0.00	0.00	-1.00	-3.00
AVP	0.00	-1.00	-1.00	-4.00	-4.00
LC AVP	0.50	-1.50	-1.00	-5.00	-2.00
AVP	0.00	-1.00	-1.00	-2.00	-3.00

Descriptive Statistics:

	Count	Mean	Std. Dev.	Std. Error
Control	5	-.600	1.517	.678
AVP	5	-2.000	1.871	.837
LC AVP	5	-.700	1.151	.515
AVP2	5	-1.400	1.140	.510

ANOVA:

Type III Sums of Squares

Source	df	Sum of Squares	Mean Square	F-Value	P-Value	G-G	H-F
Subject	4	24.825	6.206				
condition	3	6.438	2.146	2.901	.0787	.1553	.1466
condition * Subject	12	8.875	.740				

Dependent: conditions

Chapter IV - Figure 4B

Raw Data:

Experiment	#1	#2	#3	#4	#5
Control	162.0	125.0	118.0	77.00	155.0
AVP	155.0	86.00	116.0	70.00	128.0
LC AVP	158.0	98.00	116.0	65.00	111.0
AVP	155.0	88.00	126.0	56.00	100.0

Descriptive Statistics:

	Count	Mean	Std. Dev.	Std. Error
Control	5	127.400	33.887	15.155
AVP	5	111.000	33.749	15.093
LC AVP	5	109.600	33.575	15.015
AVP2	5	105.000	37.603	16.817

ANOVA:

Type III Sums of Squares

Source	df	Sum of Squares	Mean Square	F-Value	P-Value	G-G	H-F
Subject	4	17725.000	4431.250				
condition	3	1433.350	477.783	3.607	.0459	.1014	.0724
condition * Subject	12	1589.400	132.450				

Dependent: conditions

Contrasts:

	Vs.	Diff.	Std. Error	t-Test	P-Value
Control	AVP	16.400	7.279	2.253	.0437
	LC AVP	17.800	7.279	2.445	.0308
	AVP2	22.400	7.279	3.077	.0096
AVP	LC AVP	1.400	7.279	.192	.8507
	AVP2	6.000	7.279	.824	.4258
LC AVP	AVP2	4.600	7.279	.632	.5393

Chapter IV - Figure 5A

Raw Data:

Experiment	#1	#2	#3	#4	#5
Control	0.00	2.00	2.00	0.00	0.00
AVP	-11.0	1.00	-5.00	-10.0	-5.00
AVP+Dex	-6.00	2.00	-2.00	-7.00	-3.00
AVP+Dex+I+S	-6.00	1.80	-2.00	-6.00	-4.00
AVP+Dex	-4.00	2.10	-2.00	-4.00	-3.00

Descriptive Statistics:

	Count	Mean	Std. Dev.	Std. Error
Control	5	.800	1.095	.490
AVP	5	-6.000	4.796	2.145
AVP+Dex	5	-3.200	3.564	1.594
AVP+Dex+I+St	5	-3.240	3.269	1.462
AVP+Dex2	5	-2.180	2.532	1.132

ANOVA;

Type III Sums of Squares

Source	df	Sum of Squares	Mean Square	F-Value	P-Value	G-G	H-F
Subject	4	177.650	44.412				
conditions	4	119.658	29.914	12.480	.0001	.0165	.0107
conditions * Subject	16	38.350	2.397				

Dependent: condition

Contrasts:

	Vs.	Diff.	Std. Error	t-Test	P-Value
Control	AVP	6.800	.979	6.945	.0001
	AVP+Dex	4.000	.979	4.085	.0009
	AVP+Dex+I+St	4.040	.979	4.126	.0008
	AVP+Dex2	2.980	.979	3.043	.0077
AVP	AVP+Dex	-2.800	.979	-2.860	.0114
	AVP+Dex+I+St	-2.760	.979	-2.819	.0124
	AVP+Dex2	-3.820	.979	-3.901	.0013
AVP+Dex	AVP+Dex+I+St	.040	.979	.041	.9679
AVP+Dex	AVP+Dex2	-1.020	.979	-1.042	.3130
	AVP+Dex+I+St	-1.060	.979	-1.083	.2951

Chapter IV - Figure 5B

Raw Data:

Experiment	#1	#2	#3	#4	#5
Control	50.60	16.80	34.80	25.30	18.20
AVP	42.10	12.40	30.20	20.30	16.00
AVP+Dex	48.10	25.10	33.30	25.60	17.60
AVP+Dex+I+S	48.10	19.80	32.00	25.20	16.80
AVP+Dex2	53.70	28.90	34.10	29.40	19.80

Descriptive Statistics:

	Count	Mean	Std. Dev.	Std. Error
Control	5	29.140	13.958	6.242
AVP	5	24.200	12.022	5.376
AVP+Dex	5	29.940	11.572	5.175
AVP+Dex+I+S	5	28.380	12.448	5.567
AVP+Dex2	5	33.180	12.585	5.628

ANOVA:

Type III Sums of Squares

Source	df	Sum of Squares	Mean Square	F-Value	P-Value	G-G	H-F
Subject	4	3047.638	761.910				
conditions	4	208.974	52.244	8.469	.0007	.0252	.0127
conditions * Subject	16	98.702	6.169				

Dependent: Compact Variable 1

Contrasts:

	Vs.	Diff.	Std. Error	t-Test	P-Value
Control	AVP	4.940	1.571	3.145	.0063
	AVP+Dex	-.800	1.571	-.509	.6175
	AVP+Dex+I+S	.760	1.571	.484	.6351
	AVP+Dex2	-4.040	1.571	-2.572	.0205
AVP	AVP+Dex	-5.740	1.571	-3.654	.0021
	AVP+Dex+I+S	-4.180	1.571	-2.661	.0171
	AVP+Dex2	-8.980	1.571	-5.717	.0001
AVP+Dex	AVP+Dex+I+S	1.560	1.571	.993	.3354
	AVP+Dex2	-3.240	1.571	-2.063	.0558
AVP+Dex+I+S	AVP+Dex2	-4.800	1.571	-3.056	.0075

Chapter IV - Figure 6

Raw Data:

Experiment	#1	#2	#3	#4	#5	#6	#7	#8
AVP+D	187.0	211.0	193.0	155.0	354.0	374.0	202.0	320.0
AVP+D+I	328.0	313.0	354.0	183.0	250.0	291.0	124.0	365.0
AVP+D+I+S	21.00	219.0	345.0	320.0	229.0	73.00	37.00	159.0
AVP+D+I	28.00	105.0	388.0	226.0	165.0	73.00	11.00	159.0

Descriptive Statistics:

	Count	Mean	Std. Dev.	Std. Error
AVP+Dex	8	249.500	85.489	30.225
+Indo	8	276.000	85.132	30.099
+Stauro	8	175.375	124.324	43.955
-Stauro	8	144.375	122.260	43.225

ANOVA:

Type III Sums of Squares

Source	df	Sum of Squares	Mean Square	F-Value	P-Value	G-G	H-F
Subject	7	135271.375	19324.482				
condition	3	91319.125	30439.708	3.562	.0316	.0699	.0545
condition * Subject	21	179446.375	8545.065				

Dependent: Conditions

Contrasts:

	Vs.	Diff.	Std. Error	t-Test	P-Value
AVP+Dex	+Indo	-26.500	46.220	-.573	.5725
	+Stauro	74.125	46.220	1.604	.1237
	-Stauro	105.125	46.220	2.274	.0335
+Indo	+Stauro	100.625	46.220	2.177	.0410
	-Stauro	131.625	46.220	2.848	.0096
+Stauro	-Stauro	31.000	46.220	.671	.5097

Chapter V -Figure 7A

Raw Data:

Experiment	#1	#2	#3	#4	#5
Control	7.0000	2.0000	2.0000	0.0000	5.0000
AVP	750.00	584.00	820.00	484.00	734.00
AVP+Oxy	295.00	239.00	258.00	223.00	27.000
AVP+Oxy+Ati	1140.0	1280.0	1010.0	408.00	674.00

Experiment:	#6	#7	#8	#9	#10
Control	15.0000	1.0000	14.0000	7.0000	1.0000
AVP	339.00	727.00	962.00	1073.0	304.00
AVP+Oxy	306.00	206.00	284.00	0.0000	101.00
AVP+Oxy+Ati	489.00	574.00	604.00	782.00	426.00

Descriptive Statistics:

	Count	Mean	Std. Dev.	Std. Error
Control	10	5.400	5.400	1.707
AVP	10	677.700	251.404	79.501
AVP+Oxy	10	193.900	111.617	35.296
AVP+Oxy+Ati	10	738.700	307.043	97.095

ANOVA:

Type III Sums of Squares

Source	df	Sum of Squares	Mean Square	F-Value	P-Value	G-G	H-F
Subject	9	510994.525	56777.169				
condition	3	3899597.275	1299865.758	34.452	.0001	.0001	.0001
condition * Subject	27	1018702.975	37729.740				

Dependent: conditions

Contrasts:

	Vs.	Diff.	Std. Error	t-Test	P-Value
Control	AVP	-672.300	86.867	-7.739	.0001
	AVP+Oxy	-188.500	86.867	-2.170	.0390
	AVP+Oxy+Ati	-733.300	86.867	-8.442	.0001
AVP	AVP+Oxy	483.800	86.867	5.569	.0001
	AVP+Oxy+Ati	-61.000	86.867	-.702	.4886
AVP+Oxy	AVP+Oxy+Ati	-544.800	86.867	-6.272	.0001

Chapter V -Figure 7B

Raw Data:

Experiment	#1	#2	#3	#4
Control	24.00	3.000	9.000	6.000
Oxy	9.000	65.00	0.000	128.0
Oxy+AVP+Ati	683.0	633.0	287.0	423.0
Oxy+AVP	166.0	474.0	44.00	358.0

Descriptive Statistics:

	Count	Mean	Std. Dev.	Std. Error
Control	4	10.500	9.327	4.664
Oxy	4	50.500	59.130	29.565
Oxy+AVP+Ati	4	506.500	184.668	92.334
Oxy+AVP	4	260.500	192.259	96.130

ANOVA:

Type III Sums of Squares

Source	df	Sum of Squares	Mean Square	F-Value	P-Value	G-G	H-F
Subject	3	92259.500	30753.167				
condition	3	622668.000	207556.000	14.185	.0009	.0051	.0009
condition * Subject	9	131688.500	14632.056				

Dependent: conditions

Contrasts:

	Vs.	Diff.	Std. Error	t-Test	P-Value
Control	Oxy	-40.000	85.534	-.468	.6512
	Oxy+AVP+Ati	-496.000	85.534	-5.799	.0003
	Oxy+AVP	-250.000	85.534	-2.923	.0170
Oxy	Oxy+AVP+Ati	-456.000	85.534	-5.331	.0005
	Oxy+AVP	-210.000	85.534	-2.455	.0364
Oxy+AVP+Ati	Oxy+AVP	246.000	85.534	2.876	.0183

Chapter V -Figure 7C

Raw Data:

Experiment	#1	#2	#3	#4	#5
Control	0.000	1.000	3.000	17.00	11.00
cAMP	409.0	628.0	509.0	469.0	161.0
cAMP+Oxy	418.0	515.0	595.0	328.0	183.0
cAMP+Oxy+Ati	507.0	527.0	578.0	307.0	218.0

Descriptive Statistics:

	Count	Mean	Std. Dev.	Std. Error
Control	5	6.400	7.335	3.280
cAMP	5	435.200	172.940	77.341
cAMP+Oxy	5	407.800	160.890	71.952
cAMP+Oxy+Ati	5	427.400	155.950	69.743

ANOVA:

Type III Sums of Squares

Source	df	Sum of Squares	Mean Square	F-Value	P-Value	G-G	H-F
Subject	4	211225.200	52806.300				
condition	3	654285.200	218095.067	23.912	.0001	.0008	.0001
condition * Subject	12	109446.800	9120.567				

Dependent: conditions

Contrasts:

	Vs.	Diff.	Std. Error	t-Test	P-Value
Control	cAMP	-428.800	60.401	-7.099	.0001
	cAMP+Oxy	-401.400	60.401	-6.646	.0001
	cAMP+Oxy+Ati	-421.000	60.401	-6.970	.0001
cAMP	cAMP+Oxy	27.400	60.401	.454	.6582
	cAMP+Oxy+Ati	7.800	60.401	.129	.8994
cAMP+Oxy	cAMP+Oxy+Ati	-19.600	60.401	-.325	.7511

Chapter V -Figure 8A

Raw Data:

Experiment	#1	#2	#3	#4
Control	-6.000	-5.500	-7.000	-5.000
AVP	-12.00	-7.000	-10.00	-7.000
AVP+Oxy	-8.00	-6.000	-9.000	-6.000
AVP	-11.00	-7.000	-10.00	-7.000

Descriptive Statistics:

	Count	Mean	Std. Dev.	Std. Error
control	4	-5.875	.854	.427
avp	4	-9.000	2.449	1.225
avp+oxy	4	-7.250	1.500	.750
avp2	4	-8.750	2.062	1.031

ANOVA:

Type III Sums of Squares

Source	df	Sum of Squares	Mean Square	F-Value	P-Value	G-G	H-F
Subject	3	31.797	10.599				
condition	3	25.297	8.432	9.618	.0036	.0456	.0354
condition * Subject	9	7.891	.877				

Dependent: conditions

Contrasts:

	Vs.	Diff.	Std. Error	t-Test	P-Value
control	avp	3.125	.662	4.720	.0011
	avp+oxy	1.375	.662	2.077	.0676
	avp2	2.875	.662	4.342	.0019
avp	avp+oxy	-1.750	.662	-2.643	.0268
	avp2	-.250	.662	-.378	.7145
avp+oxy	avp2	1.500	.662	2.266	.0497

Chapter V -Figure 8B

Raw Data:

Experiment	#1	#2	#3	#4
Control	62.00	49.40	30.00	29.50
AVP	51.00	43.10	25.30	22.30
AVP+Oxy	59.00	44.20	27.60	31.30
AVP	59.00	40.40	25.30	24.90

Descriptive Statistics:

	Count	Mean	Std. Dev.	Std. Error
control	4	42.725	15.842	7.921
avp	4	35.425	13.860	6.930
avp+oxy	4	40.525	14.224	7.112
avp2	4	37.400	16.106	8.053

ANOVA:

Type III Sums of Squares

Source	df	Sum of Squares	Mean Square	F-Value	P-Value	G-G	H-F
Subject	3	2664.757	888.252				
condition	3	126.162	42.054	7.627	.0077	.0269	.0077
condition * Subject	9	49.626	5.514				

Dependent: conditions

Contrasts:

	Vs.	Diff.	Std. Error	t-Test	P-Value
control	avp	7.300	1.660	4.396	.0017
	avp+oxy	2.200	1.660	1.325	.2178
	avp2	5.325	1.660	3.207	.0107
avp	avp+oxy	-5.100	1.660	-3.072	.0133
	avp2	-1.975	1.660	-1.189	.2647
avp+oxy	avp2	3.125	1.660	1.882	.0925

Chapter V -Figure 8C

Raw Data:

Experiment	#1	#2	#3	#4	#5	#6
Control	-9.00	3.00	-7.00	-2.00	-8.00	-4.00
AVP	-16.0	-1.00	-11.0	-7.00	-12.0	-9.00
AVP+Oxy	-15.0	0.00	-10.0	-4.00	-10.0	-7.00
AVP2	-16.0	-1.00	-6.00	-6.00	-11.0	-8.00

Descriptive Statistics:

	Count	Mean	Std. Dev.	Std. Error
Control	6	-4.500	4.506	1.839
AVP	6	-9.333	5.086	2.076
AVP+Oxy	6	-7.667	5.241	2.140
AVP2	6	-8.000	5.099	2.082

ANOVA:

Type III Sums of Squares

Source	df	Sum of Squares	Mean Square	F-Value	P-Value	G-G	H-F
Subject	5	474.375	94.875				
condition	3	75.458	25.153	15.858	.0001	.0022	.0004
condition * Subject	15	23.792	1.586				

Dependent: Conditions

Contrasts:

	Vs.	Diff.	Std. Error	t-Test	P-Value
Control	AVP	4.833	.727	6.647	.0001
	AVP+Oxy	3.167	.727	4.355	.0006
	AVP2	3.500	.727	4.814	.0002
AVP	AVP+Oxy	-1.667	.727	-2.292	.0368
	AVP2	-1.333	.727	-1.834	.0866
AVP+Oxy	AVP2	.333	.727	.458	.6532

Chapter V -Figure 8D

Raw Data:

Experiment	#1	#2	#3	#4	#5	#6	#7	#8
Control	41.0	62.0	51.0	52.0	23.0	62.0	52.0	31.0
AVP	32.0	58.0	40.0	13.0	19.0	51.0	47.0	19.0
AVP+Oxy	33.0	60.0	45.0	55.0	23.0	59.0	55.0	17.0
AVP	22.0	51.0	44.0	29.0	19.0	59.0	55.0	16.0

Descriptive Statistics:

	Count	Mean	Std. Dev.	Std. Error
Control	8	46.750	14.059	4.970
AVP	8	34.875	16.728	5.914
AVP+Oxy	8	43.375	16.953	5.994
AVP2	8	36.875	17.349	6.134

ANOVA:

Type III Sums of Squares

Source	df	Sum of Squares	Mean Square	F-Value	P-Value	G-G	H-F
Subject	7	6426.219	918.031				
condition	3	736.844	245.615	4.984	.0091	.0313	.0199
condition * Subject	21	1034.906	49.281				

Dependent: Conditions

Contrasts:

	Vs.	Diff.	Std. Error	t-Test	P-Value
Control	AVP	11.875	3.510	3.383	.0028
	AVP+Oxy	3.375	3.510	.962	.3472
	AVP2	9.875	3.510	2.813	.0104
AVP	AVP+Oxy	-8.500	3.510	-2.422	.0246
	AVP2	-2.000	3.510	-.570	.5749
AVP+Oxy	AVP2	6.500	3.510	1.852	.0782

Chapter V -Figure 8E

Raw Data:

Experiment	#1	#2	#3	#4
AVP	-82.00	-87.00	-87.00	-88.00
AVP+Oxy	-84.00	-90.00	-87.50	-90.00
AVP	-84.00	-87.00	-87.00	-88.50

Descriptive Statistics:

	Count	Mean	Std. Dev.	Std. Error
ADH	4	-86.000	2.708	1.354
Oxy	4	-87.875	2.839	1.420
ADH2	4	-86.125	2.839	1.420

ANOVA:

Type III Sums of Squares

Source	df	Sum of Squares	Mean Square	F-Value	P-Value	G-G	H-F
Subject	3	68.167	22.722				
condition	2	8.792	4.396	11.943	.0081	.0352	# #
condition * Subject	6	2.208	.368				

Dependent: conditions

Contrasts:

	Vs.	Diff.	Std. Error	t-Test	P-Value
ADH	Oxy	1.875	.429	4.371	.0047
	ADH2	.125	.429	.291	.7806
Oxy	ADH2	-1.750	.429	-4.079	.0065

Chapter V -Figure 8F

Raw Data:

Experiment	#1	#2	#3	#4	#5
AVP	0.950	0.900	0.870	0.950	0.890
AVP+Oxy	0.950	0.940	0.900	0.970	0.900
AVP	0.940	0.920	0.900	0.960	0.870

Descriptive Statistics:

	Count	Mean	Std. Dev.	Std. Error
ADH	5	.912	.036	.016
Oxy	5	.932	.031	.014
ADH2	5	.914	.036	.016

ANOVA:

Type III Sums of Squares

Source	df	Sum of Squares	Mean Square	F-Value	P-Value	G-G	H-F
Subject	4	.013	.003				
condition	2	.001	.001	4.090	.0598	.0643	.0598
condition * Subject	8	.001	1.483E-4				

Dependent: conditions

Chapter V -Figure 8G

Raw Data:

Experiment	#1	#2	#3	#4	#5
Control	-3.00	-7.00	-4.00	-4.00	-5.00
AVP	-6.00	-10.0	-6.00	-7.00	-12.0
AVP+Oxy	-4.00	-7.00	-4.00	-6.00	-8.00
AVP2	-5.00	-9.00	-6.00	-7.00	-9.00

Descriptive Statistics:

	Count	Mean	Std. Dev.	Std. Error
Control	5	-4.600	1.517	.678
AVP	5	-8.200	2.683	1.200
AVP+Oxy	5	-5.800	1.789	.800
AVP2	5	-7.200	1.789	.800

ANOVA:

Type III Sums of Squares

Source	df	Sum of Squares	Mean Square	F-Value	P-Value	G-G	H-F
Subject	4	54.200	13.550				
condition	3	37.350	12.450	15.894	.0002	.0062	.0018
condition * Subject	12	9.400	.783				

Dependent: Conditions

Contrasts:

	Vs.	Diff.	Std. Error	t-Test	P-Value
Control	AVP	3.600	.560	6.431	.0001
	AVP+Oxy	1.200	.560	2.144	.0532
	AVP2	2.600	.560	4.645	.0006
AVP	AVP+Oxy	-2.400	.560	-4.288	.0011
	AVP2	-1.000	.560	-1.786	.0993
AVP+Oxy	AVP2	1.400	.560	2.501	.0279

Chapter V -Figure 8H

Raw Data:

Experiment	#1	#2	#3	#4
Control	14.10	10.30	52.60	37.20
AVP	12.10	9.200	46.90	37.10
AVP+Oxy	13.90	10.30	52.60	38.50
AVP	12.80	9.700	52.60	37.40

Descriptive Statistics:

	Count	Mean	Std. Dev.	Std. Error
Control	4	28.550	19.959	9.980
AVP	4	26.325	18.575	9.287
AVP+Oxy	4	28.825	20.206	10.103
AVP2	4	28.125	20.489	10.244

ANOVA:

Type III Sums of Squares

Source	df	Sum of Squares	Mean Square	F-Value	P-Value	G-G	H-F
Subject	3	4700.367	1566.789				
condition	3	15.187	5.062	3.267	.0732	.1586	.1435
condition * Subject	9	13.946	1.550				

Dependent: Conditions

Chapter V -Figure 9A

Raw Data:

Experiment	#1	#2	#3	#4
Control	4.000	20.00	6.000	4.000
AVP	434.0	233.0	198.0	312.0
AVP+Dex	214.0	56.00	115.0	226.0
AVP+Dex+ARC	315.0	139.0	152.0	316.0

Decriptive Statistics:

	Count	Mean	Std. Dev.	Std. Error
control	4	7.750	6.238	3.119
avp	4	320.250	79.693	39.846
dex	4	157.000	74.900	37.450
arc239	4	258.000	97.717	48.859

ANOVA:

**Type III Sums of Squares**

Source	df	Sum of Squares	Mean Square	F-Value	P-Value	G-G	H-F
Subject	3	39297.500	13099.167				
conditions	3	223283.500	74427.833	26.426	.0001	.0020	.0001
conditions * Subject	9	25348.000	2816.444				

Dependent: conditions

Contrasts:

	Vs.	Diff.	Std. Error	t-Test	P-Value
control	avp	-312.500	37.526	-8.327	.0001
	dex	-149.250	37.526	-3.977	.0032
	arc239	-250.250	37.526	-6.669	.0001
avp	dex	163.250	37.526	4.350	.0018
	arc239	62.250	37.526	1.659	.1315
dex	arc239	-101.000	37.526	-2.691	.0247

Chapter V -Figure 9B

Raw Data:

Experiment	#1	#2	#3	#4
Control	4.0000	2.0000	10.000	12.000
AVP	715.00	440.00	636.00	486.00
AVP+Dex+ARC	571.00	308.00	458.00	418.00
AVP+Dex	263.00	93.000	105.00	405.00

Descriptive Statistics:

	Count	Mean	Std. Dev.	Std. Error
control	4	7.000	4.761	2.380
avp	4	569.250	128.238	64.119
arc239	4	438.750	108.607	54.304
dex	4	216.500	147.625	73.812

ANOVA::

Type III Sums of Squares

Source	df	Sum of Squares	Mean Square	F-Value	P-Value	G-G	H-F
Subject	3	65702.750	21900.917				
cond.	3	737281.250	245760.417	26.186	.0001	.0030	.0001
cond. * Subject	9	84465.750	9385.083				

Dependent: condition

Contrasts:

	Vs.	Diff.	Std. Error	t-Test	P-Value
control	avp	-562.250	68.502	-8.208	.0001
	arc239	-431.750	68.502	-6.303	.0001
	dex	-209.500	68.502	-3.058	.0136
avp	arc239	130.500	68.502	1.905	.0892
	dex	352.750	68.502	5.149	.0006
arc239	dex	222.250	68.502	3.244	.0101

Chapter V -Figure 10A

Raw Data:

Experiment	#1	#2	#3	#4	#5
Control	4.0000	2.0000	16.000	4.0000	21.000
AVP	545.00	513.00	464.00	448.00	682.00
AVP+Dex	5.0000	381.00	18.000	147.00	111.00
AVP+Dex+WB4101	392.00	407.00	256.00	342.00	522.00

Descriptive Statistics:

	Count	Mean	Std. Dev.	Std. Error
control	5	9.400	8.532	3.816
AVP	5	530.400	93.136	41.652
AVP+Dex	5	132.400	151.485	67.746
AVP+dex+WB4101	5	383.800	97.192	43.465

ANOVA:

Type III Sums of Squares

Source	df	Sum of Squares	Mean Square	F-Value	P-Value	G-G	H-F
Subject	4	63984.500	15996.125				
condition	3	837303.600	279101.200	33.299	.0001	.0007	.0001
condition * Subject	12	100579.900	8381.658				

Dependent: conditions

Contrasts:

	Vs.	Diff.	Std. Error	t-Test	P-Value
control	AVP	-521.000	57.902	-8.998	.0001
	AVP+Dex	-123.000	57.902	-2.124	.0551
	AVP+dex+WB4101	-374.400	57.902	-6.466	.0001
AVP	AVP+Dex	398.000	57.902	6.874	.0001
	AVP+dex+WB4101	146.600	57.902	2.532	.0263
AVP+Dex	AVP+dex+WB4101	-251.400	57.902	-4.342	.0010

Chapter V -Figure 10B

Raw Data:

Experiment	#1	#2	#3	#4
Control	15.000	7.0000	9.0000	3.0000
AVP	571.00	632.00	621.00	627.00
AVP+Dex+WB4101	269.00	383.00	326.00	470.00
AVP+Dex	46.000	135.00	78.000	252.00

Descriptive Statistics:

	Count	Mean	Std. Dev.	Std. Error
control	4	8.500	5.000	2.500
AVP	4	612.750	28.194	14.097
AVP+Dex+WB	4	362.000	85.732	42.866
AVP+Dex	4	127.750	90.644	45.322

ANOVA:

Type III Sums of Squares

Source	df	Sum of Squares	Mean Square	F-Value	P-Value	G-G	H-F
Subject	3	27556.500	9185.500				
condition	3	857274.500	285758.167	119.055	.0001	.0010	.0004
condition * Subject	9	21602.000	2400.222				

Dependent: conditions

Contrasts:

	Vs.	Diff.	Std. Error	t-Test	P-Value
control	AVP	-604.250	34.643	-17.442	.0001
	AVP+Dex+WB	-353.500	34.643	-10.204	.0001
	AVP+Dex	-119.250	34.643	-3.442	.0074
AVP	AVP+Dex+WB	250.750	34.643	7.238	.0001
	AVP+Dex	485.000	34.643	14.000	.0001
AVP+Dex+WB	AVP+Dex	234.250	34.643	6.762	.0001

Chapter VI -Figure 11A

Raw Data:

Experiment	#1	#2	#3	#4	#5	#6	#7
Control	25.00	3.000	3.000	14.00	9.000	15.00	35.00
AVP	394.0	346.0	627.0	444.0	495.0	705.0	548.0
AVP+Dex	1.000	55.00	97.00	221.0	19.00	251.0	0.000
AVP+Dex+Ida	267.0	99.00	170.0	282.0	460.0	348.0	140.0

Descriptive Statistics:

	Count	Mean	Std. Dev.	Std. Error
control	7	14.857	11.725	4.432
avp	7	508.429	127.850	48.323
avp+dex	7	92.000	104.395	39.458
avp+dex+ida	7	252.286	126.676	47.879

ANOVA:

Type III Sums of Squares

Source	df	Sum of Squares	Mean Square	F-Value	P-Value	G-G	H-F
Subject	6	103281.429	17213.571				
condition	3	998636.679	332878.893	38.094	.0001	.0001	.0001
condition * Subject	18	157288.571	8738.254				

Dependent: conditions

Contrasts:

	Vs.	Diff.	Std. Error	t-Test	P-Value
control	avp	-493.571	49.966	-9.878	.0001
	avp+dex	-77.143	49.966	-1.544	.1400
	avp+dex+ida	-237.429	49.966	-4.752	.0002
avp	avp+dex	416.429	49.966	8.334	.0001
	avp+dex+ida	256.143	49.966	5.126	.0001
avp+dex	avp+dex+ida	-160.286	49.966	-3.208	.0049

Chapter VI -Figure 11B

Raw Data:

Experiment	#1	#2	#3	#4
Control	2.0000	0.0000	7.0000	0.0000
AVP	362.00	313.00	457.00	319.00
AVP+Agm	84.000	171.00	71.000	217.00
AVP	151.00	276.00	222.00	290.00

Descriptive Statistics:

	Count	Mean	Std. Dev.	Std. Error
Control	4	2.250	3.304	1.652
AVP	4	362.750	66.515	33.258
AVP+Agm	4	135.750	70.035	35.018
AVP2	4	234.750	63.063	31.531

ANOVA:

Type III Sums of Squares

Source	df	Sum of Squares	Mean Square	F-Value	P-Value	G-G	H-F
Subject	3	6971.250	2323.750				
condition	3	279552.750	93184.250	25.429	.0001	.0089	.0035
condition * Subject	9	32979.750	3664.417				

Dependent: conditions

Contrasts:

	Vs.	Diff.	Std. Error	t-Test	P-Value
Control	AVP	-360.500	42.804	-8.422	.0001
	AVP+Agm	-133.500	42.804	-3.119	.0123
	AVP2	-232.500	42.804	-5.432	.0004
AVP	AVP+Agm	227.000	42.804	5.303	.0005
	AVP2	128.000	42.804	2.990	.0152
AVP+Agm	AVP2	-99.000	42.804	-2.313	.0460

Chapter VI -Figure 11C

Raw Data:

Experiment	#1	#2	#3	#4
Control	7.0000	0.0000	12.000	0.0000
AVP	399.00	333.00	268.00	260.00
AVP+Agm	212.00	0.0000	206.00	76.000
AVP+Agm+Yoh	256.00	22.000	199.00	0.0000

Descriptive Statistics:

	Count	Mean	Std. Dev.	Std. Error
control	4	4.750	5.852	2.926
avp	4	315.000	64.843	32.422
avp+agm	4	123.500	103.517	51.758
avp+agm+yoh	4	119.250	127.461	63.730

ANOVA:

Type III Sums of Squares

Source	df	Sum of Squares	Mean Square	F-Value	P-Value	G-G	H-F
Subject	3	51599.250	17199.750				
condition	3	198475.250	66158.417	14.176	.0009	.0109	.0009
condition * Subject	9	42003.250	4667.028				

Dependent: Compact Variable 1

Contrasts:

	Vs.	Diff.	Std. Error	t-Test	P-Value
control	avp	-310.250	48.306	-6.423	.0001
	avp+agm	-118.750	48.306	-2.458	.0363
	avp+agm+yoh	-114.500	48.306	-2.370	.0419
avp	avp+agm	191.500	48.306	3.964	.0033
	avp+agm+yoh	195.750	48.306	4.052	.0029
avp+agm	avp+agm+yoh	4.250	48.306	.088	.9318

Chapter VI -Figure 11D

Raw Data:

Experiment	#1	#2	#3	#4	#5	#6
Control	6.000	3.000	4.000	3.000	2.000	2.000
cAMP	227.0	458.0	430.0	361.0	212.0	235.0
cAMP+Agm	286.0	288.0	211.0	270.0	0.000	184.0
cAMP+Agm+Ida	272.0	144.0	275.0	205.0	31.00	70.00

Descriptive Statistics:

	Count	Mean	Std. Dev.	Std. Error
control	6	3.333	1.506	.615
cAMP	6	320.500	109.874	44.856
Agm	6	206.500	109.694	44.782
Ida	6	166.167	102.531	41.858

ANOVA:

**Type III Sums of Squares**

Source	df	Sum of Squares	Mean Square	F-Value	P-V...	G-G	H-F
Subject	5	90970.875	18194.175				
conditions	3	310241.458	103413.819	18.888	.0001	# #	.0001
conditions * Subject	15	82128.292	5475.219				

Dependent: conditions

Contrasts:

	Vs.	Diff.	Std. Error	t-Test	P-Value
control	cAMP	-317.167	42.721	-7.424	.0001
	Agm	-203.167	42.721	-4.756	.0003
	Ida	-162.833	42.721	-3.812	.0017
cAMP	Agm	114.000	42.721	2.668	.0175
	Ida	154.333	42.721	3.613	.0026
Agm	Ida	40.333	42.721	.944	.3601

Chapter VII -Figure 12A

Raw Data:

Experiment	#1	#2	#3	#4
Control	1.0000	3.0000	7.0000	6.0000
AVP	532.00	559.00	580.00	323.00
AVP+PYY	508.00	376.00	473.00	211.00
AVP	646.00	376.00	558.00	323.00

Descriptive Statistics:

	Count	Mean	Std. Dev.	Std. Error
control	4	4.250	2.754	1.377
avp	4	498.500	118.638	59.319
avp+pyy	4	392.000	132.959	66.479
avp2	4	475.750	151.693	75.847

ANOVA:

**Type III Sums of Squares**

Source	df	Sum of Squares	Mean Squa...	F-Value	P-Value
condition	3	635819.250	211939.75	15.478	.0002
Residual	12	164314.500	13692.875		

Dependent: conditions

Contrasts:

	Vs.	Diff.	Std. Error	t-Test	P-Value
control	avp	-494.250	82.743	-5.973	.0001
	avp+pyy	-387.750	82.743	-4.686	.0005
	avp2	-471.500	82.743	-5.698	.0001
avp	avp+pyy	106.500	82.743	1.287	.2223
	avp2	22.750	82.743	.275	.7880
avp+pyy	avp2	-83.750	82.743	-1.012	.3314

Chapter VII -Figure 12B

Raw Data:

Experiment	#1	#2	#3	#4	#5
Control	0.0000	0.0000	2.0000	2.0000	4.0000
AVP	563.00	279.00	360.00	352.00	421.00
AVP+PYY	253.00	158.00	139.00	52.000	271.00
AVP	364.00	196.00	164.00	245.00	236.00

Descriptive Statistics:

	Count	Mean	Std. Dev.	Std. Error
Control	5	1.600	1.673	.748
AVP	5	395.000	106.572	47.660
AVP+PYY	5	174.600	89.461	40.008
AVP2	5	241.000	76.033	34.003

ANOVA:

**Type III Sums of Squares**

Source	df	Sum of Squares	Mean Square	F-Value	P-Value
Conditions	3	398382.550	132794.183	21.125	.0001
Residual	16	100578.400	6286.150		

Dependent: Condition

Contrasts:

	Vs.	Diff.	Std. Error	t-Test	P-Value
Control	AVP	-393.400	50.144	-7.845	.0001
	AVP+PYY	-173.000	50.144	-3.450	.0033
	AVP2	-239.400	50.144	-4.774	.0002
AVP	AVP+PYY	220.400	50.144	4.395	.0005
	AVP2	154.000	50.144	3.071	.0073
AVP+PYY	AVP2	-66.400	50.144	-1.324	.2041

Chapter VII -Figure 12C

Raw Data:

Experiment	#1	#2	#3	#4	#5
Control	6.0000	11.000	2.0000	2.0000	13.000
AVP	463.00	461.00	489.00	348.00	659.00
AVP+PYY	301.00	324.00	323.00	236.00	371.00
AVP+PYY+Yoh	129.00	313.00	43.000	87.000	76.000

Descriptive Statistics:

	Count	Mean	Std. Dev.	Std. Error
Control	5	6.800	5.070	2.267
AVP	5	484.000	111.933	50.058
AVP+PYY	5	311.000	49.087	21.952
AVP+PYY+Yoh	5	129.600	107.032	47.866

ANOVA:

**Type III Sums of Squares**

Source	df	Sum of Squares	Mean Square	F-Value	P-Value	G-G	H-F
Subject	4	35022.800	8755.700				
Condition	3	654714.550	218238.183	37.064	.0001	.0008	# #
Condition * Subject	12	70657.200	5888.100				

Dependent: conditions Conditions

Contrasts:

	Vs.	Diff.	Std. Error	t-Test	P-Value
Control	AVP	-477.200	48.531	-9.833	.0001
	AVP+PYY	-304.200	48.531	-6.268	.0001
	AVP+PYY+Yoh	-122.800	48.531	-2.530	.0264
AVP	AVP+PYY	173.000	48.531	3.565	.0039
	AVP+PYY+Yoh	354.400	48.531	7.303	.0001
AVP+PYY	AVP+PYY+Yoh	181.400	48.531	3.738	.0028

Chapter VII -Figure 13A

Raw Data:

Experiment	#1	#2	#3	#4	#5	#6	#7	#8
Control	-5.00	-1.00	2.00	1.00	-6.00	-5.00	-5.00	-5.00
AVP	-8.00	-8.00	-4.00	-5.00	-7.00	-7.00	-11.0	-7.00
AVP+PYY	-7.00	-4.00	-4.00	-3.00	-6.00	-5.00	-9.00	-6.00
AVP	-8.00	-6.00	-6.00	-6.00	-7.00	-7.00	-10.0	-8.00
Control	-7.00	-3.00	-4.00	0.00	-7.00	-4.00	-8.00	-7.00

Descriptive Statistics:

	Count	Mean	Std. Dev.	Std. Error
control	8	-3.000	3.162	1.118
avp	8	-7.125	2.100	.743
avp+pyy	8	-5.500	1.927	.681
avp2	8	-7.250	1.389	.491
control2	8	-5.000	2.726	.964

ANOVA:

Type III Sums of Squares

Source	df	Sum of Squares	Mean Square	F-Value	P-Value	G-G	H-F
Subject	7	145.775	20.825				
condition	4	97.400	24.350	14.631	.0001	.0002	.0001
condition * Subject	28	46.600	1.664				

Dependent: conditions

Contrasts:

	Vs.	Diff.	Std. Error	t-Test	P-Value
control	avp	4.125	.645	6.395	.0001
	avp+pyy	2.500	.645	3.876	.0006
	avp2	4.250	.645	6.589	.0001
	control2	2.000	.645	3.101	.0044
avp	avp+pyy	-1.625	.645	-2.519	.0177
	avp2	.125	.645	.194	.8477
	control2	-2.125	.645	-3.294	.0027
avp+pyy	avp2	1.750	.645	2.713	.0113
	control2	-.500	.645	-.775	.4447
avp2	control2	-2.250	.645	-3.488	.0016

Chapter VII -Figure 13A

Raw Data:

Experiment	#1	#2	#3	#4	#5	#6	#7	#8
Control	349.0	204.0	222.0	55.00	88.00	142.0	149.0	125.0
AVP	231.0	136.0	165.0	50.00	82.00	129.0	146.0	100.0
AVP+PYY	240.0	154.0	170.0	53.00	103.0	154.0	145.0	113.0
AVP	222.0	138.0	175.0	47.00	105.0	137.0	130.0	113.0

Descriptive Statistics:

	Count	Mean	Std. Dev.	Std. Error
Control	8	166.750	91.819	32.463
AVP	8	129.875	55.192	19.513
AVP+PYY	8	141.500	54.728	19.349
AVP2	8	133.375	51.149	18.084
Control2	8	142.375	54.555	19.288

ANOVA:

Type III Sums of Squares

Source	df	Sum of Squares	Mean Square	F-Value	P-Value	G-G	H-F
Subject	7	128017.375	18288.196				
Condition	4	6650.850	1662.712	3.744	.0146	.0808	.0740
Condition * Subject	28	12434.750	444.098				

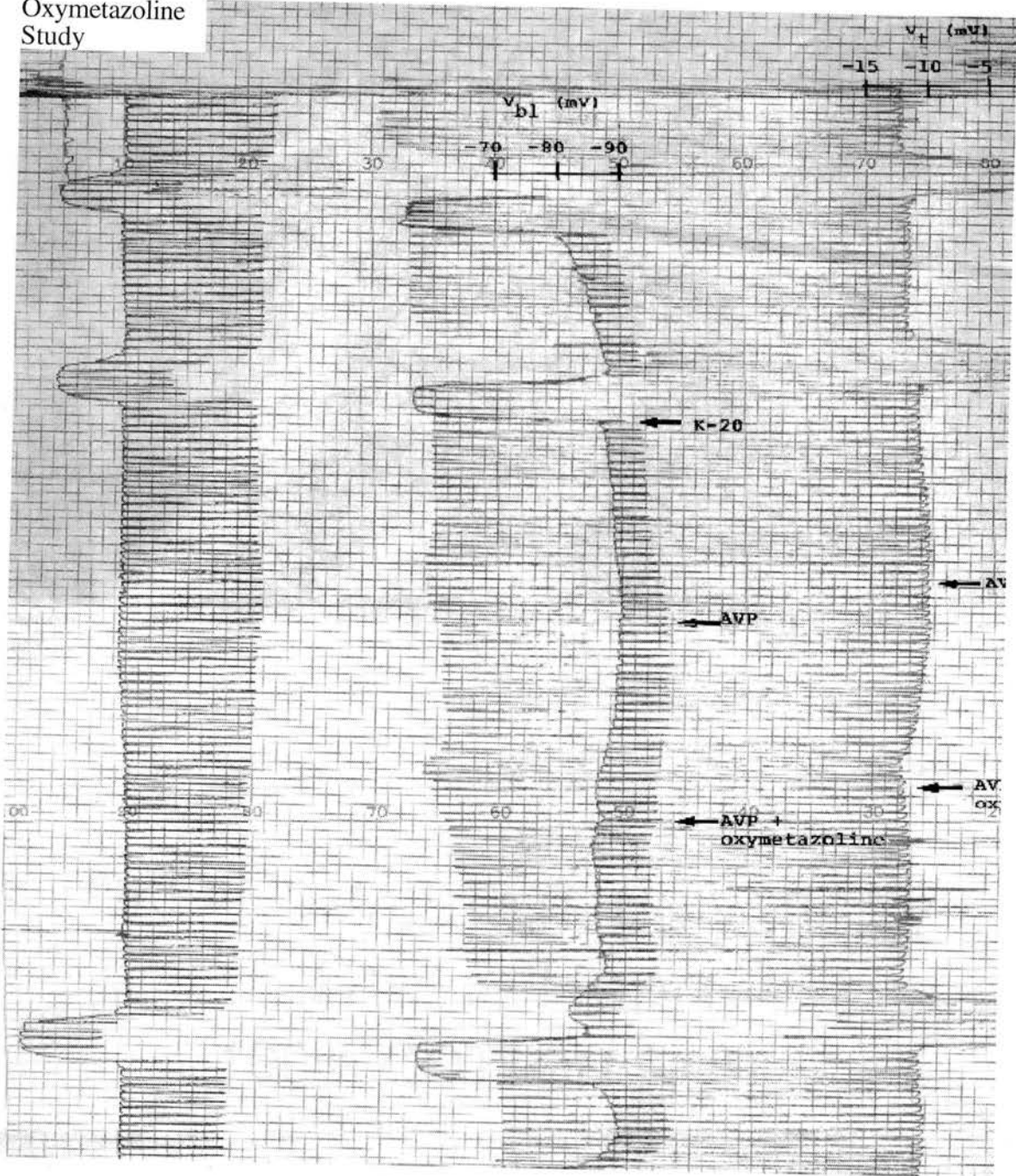
Dependent: Conditions

Contrasts:

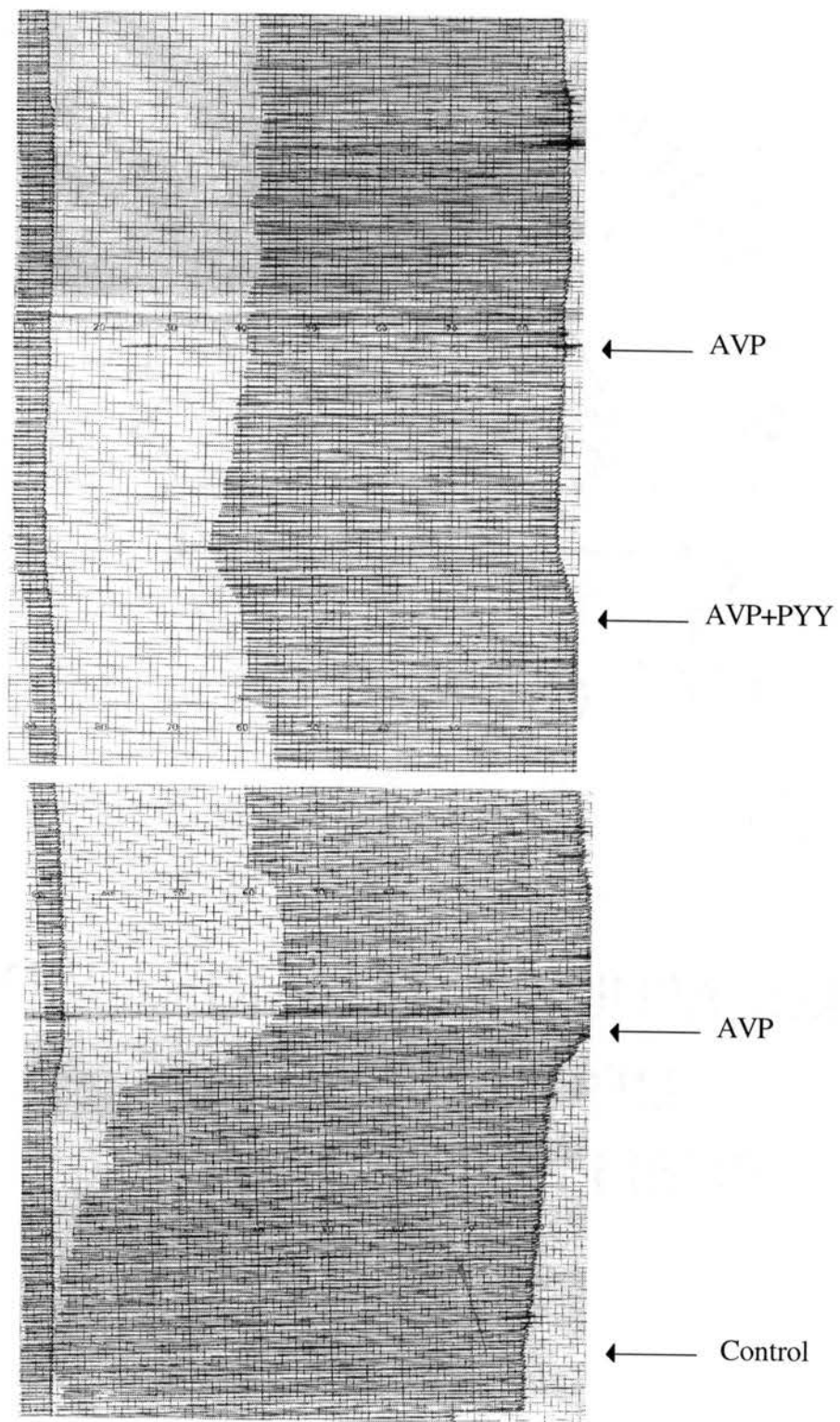
	Vs.	Diff.	Std. Error	t-Test	P-Value
Control	AVP	36.875	10.537	3.500	.0016
	AVP+PYY	25.250	10.537	2.396	.0235
	AVP2	33.375	10.537	3.167	.0037
	Control2	24.375	10.537	2.313	.0283
AVP	AVP+PYY	-11.625	10.537	-1.103	.2793
	AVP2	-3.500	10.537	-.332	.7422
	Control2	-12.500	10.537	-1.186	.2455
AVP+PYY	AVP2	8.125	10.537	.771	.4471
	Control2	-.875	10.537	-.083	.9344
AVP2	Control2	-9.000	10.537	-.854	.4003

Appendix E - Stripchart Recordings from Electrophysiology Studies

Oxymetazoline  
Study



Peptide YY  
Study



## VITA

Connie Hébert <sup>2</sup>

Candidate for the Degree of

Doctor of Philosophy

Thesis: FUNCTIONAL CHARACTERIZATION OF ALPHA-2 ADRENERGIC  
INHIBITION OF AVP-STIMULATED SALT AND WATER TRANSPORT IN  
THE RAT CORTICAL COLLECTING DUCT

Major Field: Biomedical Sciences

Biographical:

Personal Data: Born in Altus, Oklahoma, on August 15, 1960, the youngest daughter of Col. John Bradford and Christina Dakos Bradford. Wife of Thomas Glenn Hébert and mother of three children, Christina Ashley, Emily Irene, and Austin Thomas.

Education: Graduated from Southwest High School, Fort Worth, Texas in December 1977; received Bachelor of Science degree in Biology from Sam Houston State University, Huntsville, Texas in December 1983; received Master of Science degree in Physiology from the University of Tulsa, Tulsa, Oklahoma in December 1995. Completed the requirements for the Doctor of Philosophy degree in Biomedical Science at Oklahoma State University in May 2002.

Experience: Employed as a research technician for the W.K. Warren Medical Research Institute / University of Oklahoma -TMC from October 1987 to October 1991; laboratory supervisor for Cancer Treatment Center of Tulsa from October 1991 to December 1992; research assistant for the University of Tulsa from August 1993 to May 1994; research technician for Oklahoma State University College of Osteopathic Medicine from September 1995 to September 1998.

Professional Memberships: American Physiological Society, Oklahoma Academy of Science, Oklahoma Society of Physiologists, Sigma Xi, Society of Experimental Biology and Medicine.

Professional Appointments: Institutional Review Board (IRB) for Cancer Treatment Center of Tulsa 1998-2000 and served as vice-chair 2000-2002.